

11-17-2017

Folding of Bovine Pancreatic Trypsin Inhibitor (BPTI) is Faster using Aromatic Thiols and their Corresponding Disulfides

Ram Prasad Marahatta

Florida International University, rmara011@fiu.edu

DOI: 10.25148/etd.FIDC004036

Follow this and additional works at: <https://digitalcommons.fiu.edu/etd>

 Part of the [Analytical Chemistry Commons](#), [Biological and Chemical Physics Commons](#), [Medicinal-Pharmaceutical Chemistry Commons](#), and the [Organic Chemistry Commons](#)

Recommended Citation

Marahatta, Ram Prasad, "Folding of Bovine Pancreatic Trypsin Inhibitor (BPTI) is Faster using Aromatic Thiols and their Corresponding Disulfides" (2017). *FIU Electronic Theses and Dissertations*. 3530.
<https://digitalcommons.fiu.edu/etd/3530>

This work is brought to you for free and open access by the University Graduate School at FIU Digital Commons. It has been accepted for inclusion in FIU Electronic Theses and Dissertations by an authorized administrator of FIU Digital Commons. For more information, please contact dcc@fiu.edu.

FLORIDA INTERNATIONAL UNIVERSITY

Miami, Florida

FOLDING OF BOVINE PANCREATIC TRYPSIN INHIBITOR (BPTI) IS FASTER
USING AROMATIC THIOLS AND THEIR CORRESPONDING DISULFIDES

A dissertation submitted in partial fulfillment of

the requirements for the degree of

DOCTOR OF PHILOSOPHY

in

CHEMISTRY

by

Ram Prasad Marahatta

2017

To: Dean Michael R. Heithaus
College of Arts, Sciences and Education

This dissertation, written by Ram Prasad Marahatta, and entitled Folding of Bovine Pancreatic Trypsin Inhibitor (BPTI) is Faster using Aromatic Thiols and their Corresponding Disulfides, having been approved in respect to style and intellectual content, is referred to you for judgment.

We have read this dissertation and recommend that it be approved.

Kevin O'Shea

Prem P. Chapagain

Francisco Alberto Fernandez Lima

Xiaotang Wang

Watson J. Lees, Major Professor

Date of Defense: November 17, 2017

The dissertation of Ram Prasad Marahatta is approved.

Dean Michael R. Heithaus
College of Arts, Sciences and Education

Andrés G. Gil
Vice President for Research and Economic Development
and Dean of the University Graduate School

Florida International University, 2017

© Copyright 2017 by Ram Prasad Marahatta

All rights reserved.

DEDICATION

I would like to dedicate this humble work to my loving wife, cute daughter, loving mother, my siblings, and whole Marahatta family for their encouragement and patience during my doctoral studies. I would like to remember my late father Tara Nidhi Marahatta, who had an aim to teach me to this higher level of education and without his blessing from heaven, I could not do anything. I would also like to thank my relatives and friends who always supported me during my graduate study.

ACKNOWLEDGMENTS

I would like to deeply appreciate to my committee chair Dr. Watson J. Lees for providing me an opportunity to work with him. I would not be able to complete my dissertation without his guidance and persistent help. I would also like to thank my committee member Dr. Prem P. Chapagain for encouraging and supporting me to complete simulation works. I am also very thankful to my other committee members Dr. Kevin O'Shea, Dr. Francisco Fernandez-Lima, and Dr. Xiaotang Wang for their suggestions which were very helpful to me to complete my dissertation work.

I would like to thank all members of Dr. Lees' group whom I met during my research period. I am also very thankful to my friend Rudra Mani Pokhrel for his help during my works for Chapter 5. Likewise, I acknowledge faculty members of Department of Chemistry and Biochemistry at Florida International University for their help and encouragement. Finally, I appreciate to Department of Chemistry and Biochemistry and lab coordinators as well for letting me work as a teaching assistant for five years of my study, and many thanks to graduate secretary Magali Autie for her help regarding other aspects of graduate life.

ABSTRACT OF THE DISSERTATION
FOLDING OF BOVINE PANCREATIC TRYPSIN INHIBITOR (BPTI) IS FASTER
USING AROMATIC THIOLS AND THEIR CORRESPONDING DISULFIDES

by

Ram Prasad Marahatta

Florida International University, 2017

Miami, Florida

Professor Watson J. Lees, Major Professor

Improvement in the *in vitro* oxidative folding of disulfide containing proteins, such as extracellular and pharmaceutically important proteins, is required. Traditional folding methods using small molecule aliphatic thiol and disulfide, such as glutathione (GSH) and glutathione disulfide (GSSG) are slow and low yielding. Small molecule aromatic thiols and disulfides show great potentiality because aromatic thiols have low pKa values, close to the thiol pKa of protein disulfide isomerase (PDI), higher nucleophilicity and good leaving group ability. Our studies showed that thiols with positively charged group, quaternary ammonium salts (QAS), are better than thiols with negatively charged groups such as phosphonic acid and sulfonic acid for the folding of bovine pancreatic trypsin inhibitor (BPTI). An enhanced folding rate of BPTI was observed when the protein was folded with a redox buffer composed of a QAS thiol and its corresponding disulfide.

Quaternary ammonium salt (QAS) thiols and their corresponding disulfides with longer alkyl side chains were synthesized. These QAS thiols and their

corresponding disulfides are promising small molecule thiols and disulfides to fold reduced BPTI efficiently because these thiols are more hydrophobic and can enter the core of the protein.

Conformational changes of disulfide containing proteins during oxidative folding influence the folding pathway greatly. We performed the folding of BPTI using targeted molecular dynamics (TMD) simulation and investigated conformational changes along with the folding pathway. Applying a bias force to all atoms versus to only alpha carbons and the sulfur of cysteines showed different folding pathways. The formation of kinetic traps N' and N* were not observed during our simulation applying bias force to all atoms of the starting structure. The final native conformation was obtained once the correct antiparallel β -sheets and subsequent Cys14-Cys38 distance was decreased to a bond distance level. When bias force was applied to only alpha carbons and the sulfur of cysteines, the distance between Cys14-Cys38 increased and decreased multiple times, structure similar to the conformation of N*, N^{SH} were formed and native protein was ultimately obtained. We concluded that there could be multiple pathways of conformational folding which influence oxidative folding.

TABLE OF CONTENTS

CHAPTER	PAGE
1 Introduction.....	1
1.1 Structure and folding of protein	1
1.1.1 Protein structure	1
1.1.2 <i>In vitro</i> protein folding	2
1.1.2.1 Process of <i>in vitro</i> protein production	2
1.1.2.2 Importance of protein folding	6
1.1.3 Folding of disulfide containing proteins	8
1.1.4 Folding with Protein Disulfide Isomerase (PDI).....	8
1.1.4.1 General information.....	8
1.1.4.2 Oxidative protein folding with PDI	10
1.1.4.2.1 Oxidative <i>in vivo</i> protein folding with PDI	10
1.1.4.3 Oxidative <i>in vitro</i> protein folding with PDI.....	11
1.1.4.4 Folding with small molecules.....	12
1.2 Folding of bovine pancreatic trypsin inhibitor (BPTI).....	16
1.2.1 Introduction of BPTI.....	16
1.2.2 Traditional <i>in vitro</i> oxidative folding of BPTI	20
1.2.3 Updated folding pathway of BPTI	24
1.3 Folding of BPTI with aromatic thiols and their corresponding disulfides	26
1.3.1 Introduction.....	26
1.3.2 Construction of the structure of small molecule aromatic thiols	27
1.4 Molecular dynamics (MD) simulation study of BPTI.....	29
1.4.1 Importance of MD simulation.....	29
1.4.2 Protein folding and MD simulation.....	29
1.4.3 Molecular dynamics (MD) simulation of BPTI	30
2 Objectives.....	32
2.1 Synthesis of different aromatic thiols and their corresponding disulfides for the study of folding of reduced BPTI	32
2.2 Folding of reduced BPTI faster using different aromatic thiols and their corresponding disulfides.....	32
2.3 Molecular dynamics (MD) simulation study of BPTI intermediates to understand the folding of BPTI at a molecular level.....	32
3 Synthesis of aromatic thiols and corresponding disulfides.....	33
3.1 Abstract	33
3.2 Introduction.....	34
3.3 Results and discussion.....	37
3.3.1 Synthesis of quaternary ammonium salt thiol 1.....	37
3.3.2 Synthesis of quaternary ammonium salt thiol 2.....	37
3.3.3 Synthesis of quaternary ammonium salt thiol 3.....	40
3.3.4 Synthesis of quaternary ammonium salt thiol 4.....	40

3.3.5 Synthesis of sulfonic acid thiol 9	41
3.4 Experimental section	42
3.4.1 Synthesis of 1-(4-(mercaptophenyl)- <i>N,N,N</i> -trimethylmethanaminium bromide (1)	42
3.4.1.1 Synthesis of <i>S-p</i> -tolyl benzothiophenol (13).....	42
3.4.1.2 Synthesis of <i>S</i> -4-(bromomethyl)phenyl benzothiophenol (14)	43
3.4.1.3 Synthesis of 1-(4-(benzoylthio)phenyl)- <i>N,N,N</i> -trimethylmethanaminium bromide (15).....	43
3.4.1.4 Synthesis of 1-(4-(mercaptophenyl)- <i>N,N,N</i> -trimethylmethanaminium bromide (1).....	44
3.4.2 Synthesis of 2- <i>S</i> -(4-mercapto)benzyl)- <i>N,N,N</i> -trimethylethanaminium bromide [extended QAS thiol] (2)	44
3.4.2.1 Synthesis of 2- <i>S</i> -(4-(benzothio)benzyl)ethanol (16).....	44
3.4.2.2 Synthesis of 2- <i>S</i> -(4-(benzoylthio)benzyl)-1-bromoethane (17)	45
3.4.2.3 Synthesis of 2- <i>S</i> -(4-(benzoylthio)benzyl)- <i>N,N,N</i> -trimethylethanaminium bromide (18).....	45
3.4.2.4 Synthesis of 2- <i>S</i> -(4-mercapto)benzyl)- <i>N,N,N</i> -trimethylethanaminium bromide (2).....	46
3.4.2.5 Synthesis of 1,1'-(4,4'-disulfanediylbis(1,4-phenylene)bis(2- <i>S</i> - <i>N,N,N</i> -trimethylethanaminium) bromide [Disulfide of extended QAS thiol] (6)....	46
3.4.3 Synthesis of hexyl QAS thiol	46
3.4.3.1 Synthesis of 1-(4-(benzoylthio)phenyl)- <i>N,N</i> -dimethyl- <i>N</i> -hexylmethanaminium bromide (20)	46
3.4.3.2 Synthesis of 1-(4-mercaptophenyl)- <i>N,N</i> -dimethyl- <i>N</i> -hexylmethanaminium bromide (3).....	47
3.4.4 Synthesis of octyl QAS thiol	47
3.4.4.1 Synthesis of 1-(4-(benzoylthio)phenyl)- <i>N,N</i> -dimethyl- <i>N</i> -octylmethanaminium bromide (22)	47
3.4.4.2 Synthesis of 1-(4-mercaptophenyl)- <i>N,N</i> -dimethyl- <i>N</i> -octylmethanaminium bromide (4)	48
3.4.5 Synthesis of 4-mercaptobenzene sulfonic acid (9).....	49
3.4.5.1 Preparation of sodium-4,4'-dithiobis(benzenesulfonate) (26).....	49
3.4.5.2 Synthesis of 4-mercaptobenzene sulfonic acid (9).....	50
3.5 Conclusion.....	50
4 Dramatic increase in the folding rate of Bovine Pancreatic Trypsin Inhibitor (BPTI) with the buffer composed of positively charged aromatic thiol and its corresponding disulfide	52
4.1 Abstract	52
4.2 Introduction.....	53
4.3 Results	57
4.3.1 Folding with negatively charged aromatic thiols and their corresponding disulfides.....	59
4.3.2 Folding with positively charged aromatic thiol 1 and its corresponding disulfide 5	61

4.4 Discussion	71
4.5 Experimental section	76
4.5.1 Materials	76
4.5.2 Preparation of reduced BPTI	77
4.5.3 Oxidative folding of reduced BPTI	78
4.6 Conclusion.....	79
5 Targeted Molecular Dynamics (TMD) simulation study of conformational folding from [5-55] like conformation to native conformation of BPTI	81
5.1 Abstract	81
5.2 Introduction.....	82
5.3 Methods.....	85
5.3.1 Molecular dynamics (MD) setup for equilibrium and TMD	85
5.4 Results and discussion.....	86
5.4.1 TMD using all atoms.....	87
5.4.1.1 Change in structural configuration of BPTI during TMD	87
5.4.1.2 Distance between CYS residues of the native disulfide bonds	89
5.4.1.3 Root mean square deviation during TMD.....	90
5.4.1.4 Analysis of intermediates with the change in radius of gyration	91
5.4.1.5 Analysis of folding trajectories	93
5.4.2 TMD using C _α and sulfur of cysteines (SG) only	94
5.4.2.1 Change in structural conformation during simulation	94
5.4.2.2 Root mean square deviation analysis	95
5.4.2.3 Distance analysis of native disulfide bonds.....	96
5.4.2.4 Analysis of intermediates with the change in radius of gyration	98
5.4.2.5 Analysis of trajectories	99
5.5 Conclusion.....	101
6 Conclusion.....	102
7 Future works.....	104
References	105
VITA.....	116

LIST OF FIGURES

FIGURE	PAGE
1.1 Four levels of protein structure	2
1.2 Thiol-disulfide interchange reaction during renaturation of protein	5
1.3 Mechanism of aggregation of amyloid fibrils	7
1.4 Structure of human PDI	10
1.5 Open and closed CXXC motif of PDI	10
1.6 Proposed mechanism of thiol-disulfide exchange between Ero1p and a thioredoxin-like domain of PDI	11
1.7 Oxidative protein folding mechanism in vivo	12
1.8 Some traditional small molecule thiols and disulfides	14
1.9 Generic structures of aromatic thiol and disulfide	16
1.10 Structure of BPTI	18
1.11 Thermal denaturation of BPTI at pH 2.1	18
1.12 The BPTI folding pathway proposed by Creighton	22
1.13 The folding pathway of BPTI proposed by Kim	23
1.14 Updated oxidation-rearrangement BPTI folding pathway	26
3.1 Quaternary ammonium salt (QAS) thiols 1-4 and their corresponding disulfides 5-8	36
3.2 Sulfonic acid thiol 9 and its disulfide 10	36
3.3 Side products of the first step in the preparation of compound 16	39
3.4 Tosylation of 16	40
4.1 Mechanism of PDI	55
4.2 Different aromatic thiols and their corresponding disulfides	58

4.3 Folding of reduced BPTI with 0.09 mM disulfide 10 and different concentrations of thiol 9	60
4.4 Total area of protein in different folding conditions with thiol 9 and disulfide 10	61
4.5 Folding of reduced BPTI with 0.09 mM disulfide 5 and different concentrations of thiol 1	62
4.6 Folding of reduced BPTI with 0.25 mM disulfide 5 and different concentrations of thiol 1	63
4.7 Total area of protein in different folding conditions with thiol 1 and disulfide 5.....	63
4.8 Oxidation of thiol 1 in different folding conditions with thiol 1 and disulfide 5.....	64
4.9 Prominent intermediate during folding of reduced BPTI with 0.25 mM disulfide 5 and thiol 1 at 38 min	64
4.10 Prominent intermediate during folding of reduced BPTI with 0.25 mM disulfide 5 and thiol 1 at 42 min	65
4.11 Different quenching conditions	65
4.12 Folding of reduced BPTI with 0.25 mM disulfide 5 and different concentrations of thiol 1	66
4.13 Analysis of total protein area with different storage methods.....	67
4.14 Total protein area in new HPLC method	68
4.15 Folding of reduced BPTI with 0.25 mM disulfide 5 and different concentrations of thiol 1	68
4.16 Chromatogram showing native protein and intermediates with 0.25 mM disulfide 5 and 10 mM thiol 1.....	69
4.17 Chromatogram showing native protein and intermediates with 0.25 mM disulfide 5 and 1 mM thiol 1.....	69
4.18 Chromatogram showing native protein and intermediates with 0.25 mM disulfide 5 and 2 mM thiol 1.....	70

4.19 Chromatogram showing native protein and intermediates with 0.25 mM disulfide 5 and 5 mM thiol 1	70
4.20 Folding of reduced BPTI with 10 mM thiol 1 and different concentrations of disulfide 5	71
4.21 Comparison of folding of reduced BPTI with our optimal condition (10 mM thiol 1 and 0.25 mM disulfide 5) with optimal condition of traditional buffer (5 mM GSH and 5 mM GSSG).....	71
4.22 Effect of negatively and positively charged thiols on net charge of BPTI	74
5.1 Native structure of BPTI showing α -helices (in red), β -strands (in green), disulfide bonds (in yellow), and loops and turns (in blue).....	87
5.2 The folding secondary structure of BPTI with its three disulfide bonds.....	88
5.3 Snapshots of conformations formed at different stages of conformational changes during conformational folding of BPTI using TMD simulation. Sulfur atoms of cysteines are shown in yellow balls	88
5.4 Evolution of secondary structure from TMD simulations of BPTI [(5-55) to N].....	89
5.5 Distance between sulfur atoms in native disulfide bonds	90
5.6 Change in RMSD during TMD of BPTI	91
5.7 Folding trajectories demonstrating the BPTI folding pathway from [5-55] conformation to folded native state	93
5.8 Snapshots of different conformations formed during TMD simulation of [5-55] like conformation of BPTI to native like BPTI	94
5.9 Snapshots of conformations formed at different stages of conformational changes during conformational folding of BPTI using TMD simulation	95
5.10 Change in RMSD during TMD	96
5.11 Distance between sulfur atoms in native disulfide bonds	97
5.12 Formation of native and non-native disulfide bonds.....	98

5.13 Folding trajectories demonstrating the BPTI folding pathway from [5-55] conformation to folded native state	100
5.14 Snapshots of different conformations formed during TMD simulation of [5-55] like conformation of BPTI to native like BPTI	101

LIST OF SCHEMES

SCHEME	PAGE
1.1 Nucleophilic substitution in thiol-disulfide interchange reaction	28
1.2 Rearrangement of protein disulfide with aromatic thiolate ion.....	28
1.3 Formation of protein disulfide with aromatic disulfide.....	29
3.1 Synthesis of quaternary ammonium thiol 1	38
3.2 Synthesis of elongated quaternary ammonium thiol 2	39
3.3 Synthesis of hexyl QAS thiol 3	40
3.4 Synthesis of octyl QAS thiol 4	41
3.5 Synthesis of sulfonic acid thiol 9	41
4.1 Intra- and intermolecular formation of disulfide bonds	54
4.2 Reactions of aromatic thiol as a nucleophile and/or central thiol in a redox buffer	73

LIST OF ABBREVIATIONS AND ACRONYMS

ATP	Adenosine triphosphate
BMC	(±) Trans-1,2-bis(mercaptoacetamido)cyclohexane
BME	Beta mercaptoethanol
BPTI	Bovine pancreatic trypsin inhibitor
CHARMM	Chemistry at Harvard Macromolecular Mechanics
CTD	C-terminal domain
Cu ²⁺	Copper ion
C α	Alpha carbon
DIPEA	Diisopropylethylamine
DMF	Dimethylformamide
DTT	Dithiothreitol
DTT ^{ox}	Oxidized dithiothreitol
DTT ^{red}	Reduced dithiothreitol
EDTA	Ethylenediaminetetraacetic acid
ER	Endoplasmic reticulum
Ero1p	Endoplasmic reticulum oxidoreductase protein 1
FAD	Flavin adenine dinucleotide
GSH	Glutathione
GSSG	Glutathione disulfide
GUI	Graphical user interface
Gdn-HCl	Guanidinium chloride
HCl	Hydrochloric acid

HPLC	High performance liquid chromatography
kDa	Kilodalton
KCl	Potassium chloride
MD	Molecular dynamics
NAMD	Nanoscale molecular dynamics
NMA	N-methylmercaptoacetamide
NMR	Nuclear magnetic resonance
PA	Phosphonic acid
PCDs	Protein conformational disorders
PDB	Protein data bank
PDI	Protein disulfide isomerase
QAS	Quaternary ammonium salt
R_g	Radius of gyration
RMSD	Root mean square deviation
RP	Reverse phase
SA	Sulfonic acid
SG	Sulfur of cysteine
S_N2	Substitution nucleophilic bimolecular reaction
TFA	Trifluoroacetic acid
TMD	Targeted molecular dynamics
UV-vis	Ultraviolet-visible
VMD	Visual molecular dynamics

CHAPTER 1

Introduction

1.1 Structure and folding of protein

1.1.1 Protein structure

Gerhardus Johannes Mulder, a Dutch chemist, first described and coined the name 'protein' in 1838 meaning 'the first quality'.¹ Proteins are polymers of amino acids and are composed of nitrogen, carbon, hydrogen, oxygen and sulfur. In humans, protein consists of 15.1 percent of a person's dry weight.² Proteins are enzymes, hormones, antibodies, and major components of tissues such as hair and muscles. Proteins play a primary role in most biological processes such as building, repairing and replacing tissues.

Protein structure is described in four levels - primary, secondary, tertiary, and quaternary (Figure 1.1). The primary structure of a protein is the actual sequence of amino acids in that protein which is set by DNA. The primary bonds of any protein are the peptide bonds between amino acids. Biosynthesis of a protein's primary structure occurs on the ribosome with information provided by messenger RNA in a process called translation.³ The secondary structure of a protein is a local structural conformation, which is determined by H-bonds within the backbone. There are mainly two types of secondary structure in proteins: the α -helix and the β -sheet. The tertiary structure of a protein is the overall three-dimensional structure of a single protein molecule which is described by distant interactions between groups. These interactions include H-bonding, Vander Waals interactions, hydrophobic packing, and disulfide bonding. The quaternary

structure of a protein is formed by interactions between individual protein subunits. These four levels of a protein structure are crucial to the stability of the folded native conformation of a protein.

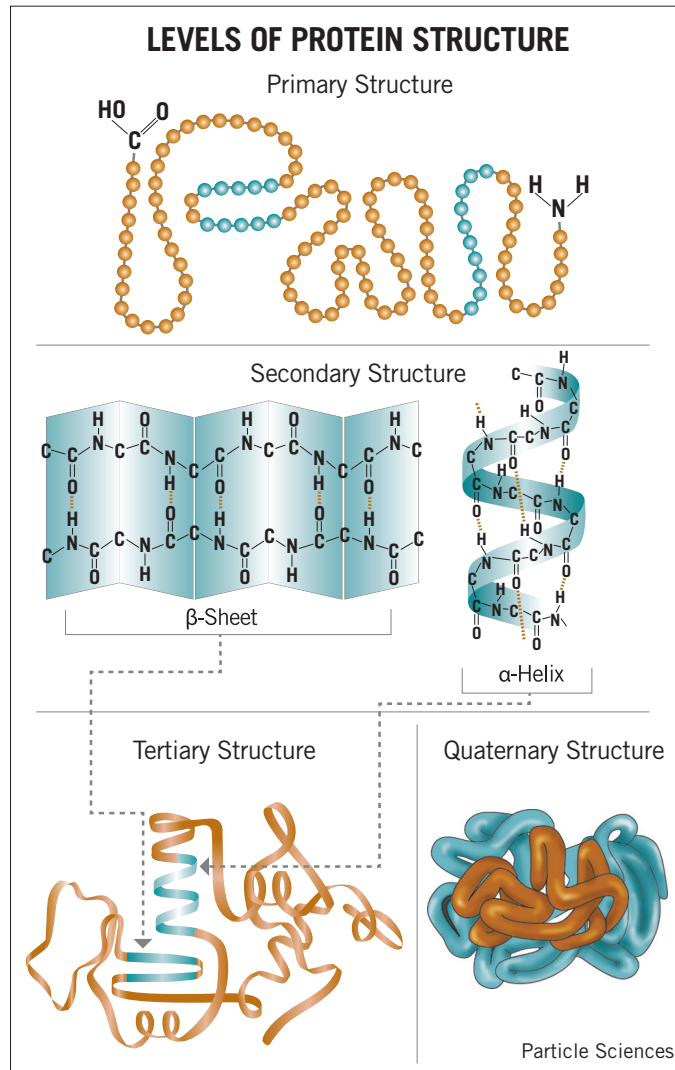


Figure 1.1. Four levels of protein structure (From reference 4).⁴

1.1.2 *In vitro* protein folding

1.1.2.1 Process of *in vitro* protein production

The advancement in recombinant DNA technology has allowed the production of therapeutic proteins⁵ in microbial hosts; *Escherichia coli* is the most

common organism used. In many cases, the protein of interest misfolds and forms insoluble aggregates known as inclusion bodies.⁶ The major desirable factor associated with the production of inclusion bodies either in the cytoplasm or in the periplasm of *E. coli* is the rapid formation of the desired protein.⁷ Additional advantages associated with the overexpression include issues related to toxicity of desired protein to the host cell are eliminated by the production of that particular protein via inclusion bodies formation,⁸ the large quantity of inclusion bodies expressed is highly enriched with a particular protein, and inclusion bodies are protected from proteolytic degradation.⁸ But, there are still some disadvantages of the expression of the protein as inclusion bodies such as; the of inactivity and insolubility of the protein within the inclusion bodies, posing a difficulty in solubility for further steps of protein production.⁶ Inclusion body formation is particularly important in the case of disulfide containing proteins, as the disulfide bond formation requires an oxidative environment which is not found in the cytosol of bacteria.⁹ The result is the aggregation of protein. However, the challenge remains with the regeneration of active and soluble proteins from these misfolded aggregates.^{5,9} The recent advancement in the restoration process has made it possible to produce large quantities of therapeutic proteins from highly dense inclusion bodies which reach to 90% at optimal conditions.⁵

Formation of active protein from inclusion bodies involves several steps. The first step is the isolation and purification of the inclusion bodies. Isolation is done using one of two procedures. The most common method is cell lysis followed by centrifugation of the resulting suspension at modest rotor speed.¹⁰

The other method of isolation is the separation of inclusion bodies from soluble proteins by filtration.⁸ The isolated inclusion bodies are contaminated mainly with membrane associated proteins. The membrane associated proteins and other contaminants are washed away with a mixture containing EDTA and a low concentration of denaturant or detergent such as deoxycholate, octylglucoside, or Triton X-100.^{8,11} The next step is the solubilization of the purified inclusion bodies which is commonly accomplished by using strong denaturants such as urea or guanidinium chloride (Gdn-HCl). During the solubilization of the inclusion bodies the protein is either completely unfolded or partially unfolded as the intramolecular and intermolecular interactions are disrupted. In the case of disulfide-containing proteins, proteins within the inclusion bodies contain both non-native inter- and intra-molecular disulfide bonds, which diminishes the solubility. Therefore, the addition of thiol containing reagents such as β -mercaptoethanol, dithiothreitol (DTT), dithioerythritol, cystamine, glutathione (GSH), or cysteine along with the denaturants mentioned above at alkaline pH is required.¹² These reagents are necessary to break disulfide bonds via thiol-disulfide interchange reactions forming reduced protein which is more soluble than protein with mismatched or intermolecular disulfide bonds. The last step in the *in vitro* protein production via the formation of inclusion bodies is the renaturation of the solubilized inclusion proteins. The excess of denaturants and thiol reagents are first removed using different methods such as dilution, dialysis, gel-filtration chromatography, immobilization on a solid support, etc. followed by the exposure of reduced protein to oxidizing conditions. The refolding process is

highly dependent on pH, temperature, and ionic strength of the protein; therefore, these factors must be carefully considered during the optimization of the renaturation step.⁵

The renaturation of disulfide containing proteins must be performed in a redox buffer containing an oxidizing agent and in the case of monothiols a reducing agent.^{5,9} For example, glutathione (GSH), the reduced form, and glutathione disulfide (GSSG), the oxidized form, mixed in the proper molar ratio can be utilized to increase the rate and yield of the formation of an active protein by facilitating thiol-disulfide interchange reactions. Other redox systems which can be used are pairs like DTT/GSSG, cysteine/cystine, cysteamine/cystamine.⁸ A small amount of EDTA is added during the preparation of the redox buffer to prevent the oxidation of the protein thiols and redox buffer by air in the presence of metal ions such as Cu^{2+} .

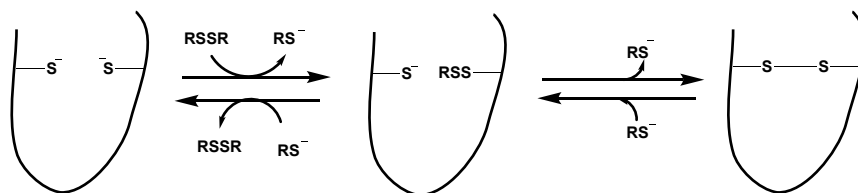


Figure 1.2. Thiol-disulfide interchange reaction during renaturation of protein where RS^- is the deprotonated reduced form and RSSR is the oxidized disulfide form.

The renaturation process of disulfide containing proteins can be improved by the addition of low molecular weight additives which prevent the aggregation of wrongly folded species by suppressing intermolecular interactions.⁸ Different denaturants such as urea, GdnHCl, and detergents such as CHAPS, Triton X-100, SDS, CTAB can be added as small molecule additives.

1.1.2.2 Importance of protein folding

The protein folding process can potentially start in several different places: in the cell co-translationally during protein synthesis on the ribosomes, in the cytoplasm after the protein has been synthesized and released from the ribosome, or in a particular compartment of the cell such as the endoplasmic reticulum (ER) or mitochondria after the protein has been translocated through a membrane.¹³ The ER contains the specialized machinery used to fold intra-organellar, secretory, and transmembrane proteins.¹⁴ The highly crowded milieu (300-400 gL⁻¹ occupied mainly by proteins, polysaccharides, and lipids) of the cell increases the possibility of protein aggregation.^{15,16} To overcome the aggregation problem, molecular chaperones are present in the cell. These chaperones prevent aggregation by not allowing the nascent protein molecules to interact with other molecules in the crowded environment of the cell. The chaperones guide protein folding either in the initial stage or later stages of the process, increasing the efficiency of the folding process.^{13,17,18}

In the case of incorrect folding, the aggregation of protein results in the formation of highly ordered amyloid fibrils (Figure.1.3), which are very stable and are responsible for neurodegenerative diseases.¹⁵ They have been grouped under protein conformational disorders (PCDs). In some cases, the aggregated proteins deposit in tissues, including heart and brain, resulting in diseases such as Alzheimer's disease, Parkinson's disease, spongiform encephalopathies, and type II diabetes. The misfolded proteins, as a result of a change in conformation lose their biological activity and acquire toxicity to the cell.

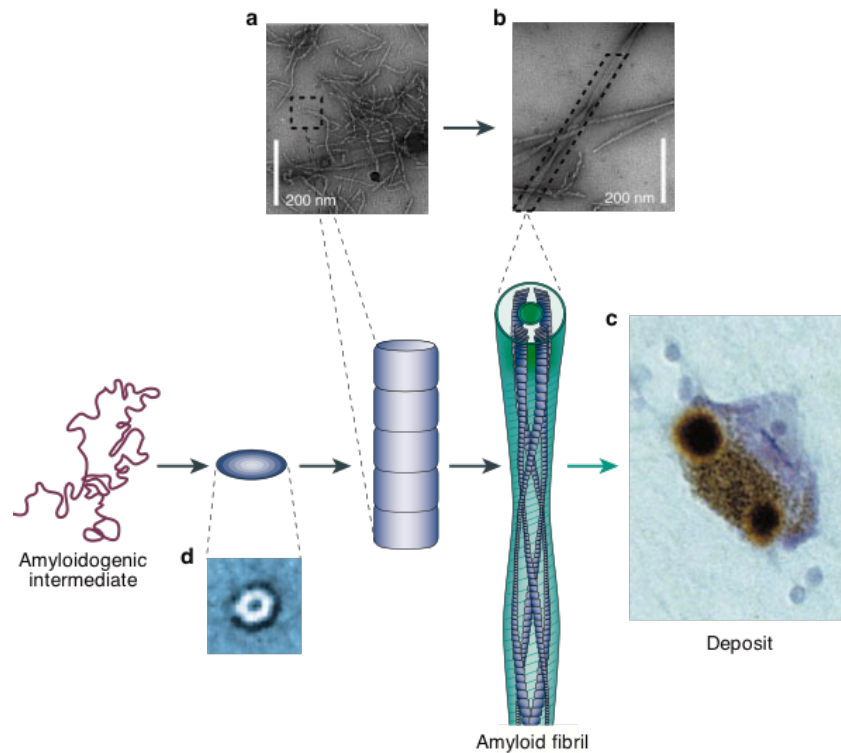


Figure 1.3. Mechanism of aggregation of amyloid fibrils (From reference 13).¹³

The misfolded proteins associated with the protein misfolding diseases have an extra stability. Therefore, during *in vitro* protein folding, it is very important to fold proteins into their correct three-dimensional shape, so as to obtain biological function, and not toxic activity.

The *in vitro* oxidative protein folding of disulfide containing proteins is done in the presence of a redox buffer containing both oxidizing and reducing equivalents. The progress of the folding process is studied by analyzing the intermediates formed, which can be isolated after quenching the reaction mixture after a certain amount of time.¹⁹ Oxidative protein folding method is applicable solely for the folding of disulfide containing proteins. Oxidative protein folding method has some advantages over the conformational protein folding process,

which is used to fold all types of proteins. These benefits include the use of a protein with clearly defined disulfide bonds, and the ease of trapping, isolation, and characterization of folding intermediates, as well as evaluation of the kinetics of the folding pathway, and control of kinetics by changing the redox reagents.¹⁹

1.1.3 Folding of disulfide containing proteins

Disulfide bond formation in secretory proteins is an essential process for their stability and biological activity as it decreases the entropy of the reduced form and thus increases the relative stability of the native form. However, in comparison with other proteins, the process of folding disulfide containing proteins is very slow and requires a redox environment.²⁰ Oxidative protein folding *in vivo* is an assisted process which takes place in the ER of the cell. The ER contains protein disulfide isomerase (PDI), a protein involved in the rearrangement of mismatched disulfide bonds and oxidation-reduction of disulfide bonds. The ER has an oxidative environment compared to the cytosol as a result of the presence of different redox enzymes and small molecule oxidants, and also because of the secretion and uptake of thiols and disulfides, respectively.²¹

1.1.4 Folding with Protein Disulfide Isomerase (PDI)

1.1.4.1 General information

The enzyme PDI belongs to the thiol-disulfide oxidoreductase family and is located in the endoplasmic reticulum (ER) of the cell²² It was first isolated and characterized by Anfinsen and co-workers.²³ Protein disulfide isomerase (PDI) is a 55 kDa, multifunctional protein found abundantly in the lumen of ER and

primarily takes part in the formation of correct disulfide bonds via isomerization of disulfide bonds.²⁴ The structure of PDI contains two active thioredoxin domains (*a* and *a'*), two inactive thioredoxin domains (*b* and *b'*) and an acidic C-terminal tail resulting in a “U” shaped structure (Figure 1.4).²⁴ The active domains (*a* and *a'*) each contain one catalytically active C-G-H-C motif located near the N terminus in the *a* domain and near the C terminus in the *a'* domain. The two C-G-H-C motifs face each other and are separated by 20 Å (distance between sulfur of C61-C406).^{24,25} The cysteines in each active site can be either in the disulfide form (oxidized PDI), because of an intramolecular bond formation, or in the dithiol form (reduced PDI). In reduced PDI, one thiol in each active site is exposed to the solvent and the other thiol is buried in the hydrophobic core. The solvent exposed thiol is responsible for the reactivity of PDI (pKa = 6.7) with other disulfide bonds. Oxidized PDI contains one disulfide bond in a cyclic 14-membered ring form (Figure 1.5) and is unstable as compared to other disulfides as a result of a lower redox potential ($E'_0 = -180$ mV).²⁶ Thus, thiol-disulfide interchange reactions take place rapidly with oxidized and reduced PDI, making PDI a model for designing small molecule thiols and disulfides.

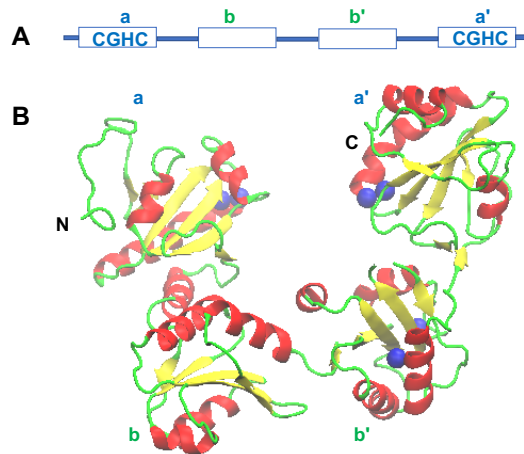


Figure 1.4 Structure of human PDI(PDB ID 4EKZ).²²

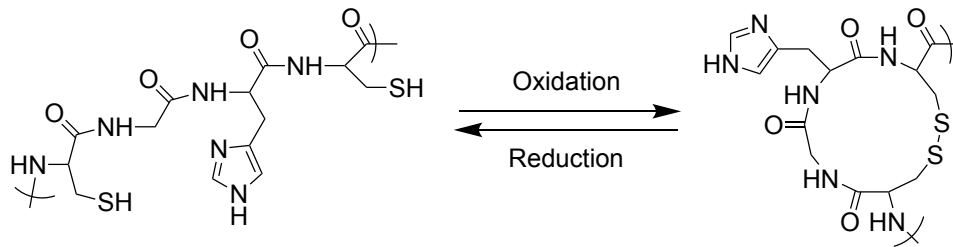


Figure 1.5 Open and closed CXXC motif of PDI.

1.1.4.2 Oxidative protein folding with PDI

1.1.4.2.1 Oxidative *in vivo* protein folding with PDI

Once the polypeptides are formed, these nascent structures containing cysteines in the reduced thiol form are translocated to the ER with the help of signal recognition particles as well as receptors.²⁷ In the ER, the conditions are much more oxidizing than in the cytosol ($[GSH]/[GSSG] = 1:1$ to $1:3$ in ER, $100:1$ in the cytosol), which is thermodynamically favorable for disulfide bond formation in proteins and hence PDI is present mostly in the oxidized form.^{25,28,29} The protein disulfide bond is formed due to the transfer of oxidizing equivalents from Ero1p to PDI²⁹ (Figure 1.6).

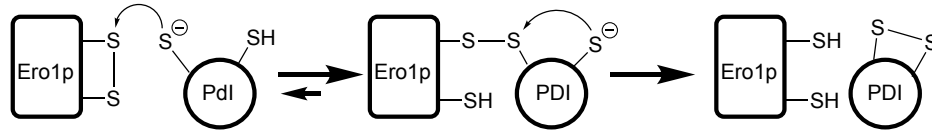


Figure 1.6 Proposed mechanism of thiol-disulfide exchange between Ero1p and a thioresoxin-like domain of PDI.²⁹

The PDI itself acts as a chaperone thereby preventing proteins from forming an aggregation. The reduced proteins form disulfide bonds with the help of oxidized PDI as oxidized PDI act as an electron acceptor whereas mismatched disulfide bonds within proteins are isomerized to native disulfide bonds with the help of reduced PDI which acts as an electron donor. The isomerization of the mismatched disulfide bond is started by the attack of the solvent-exposed thiolate of PDI on disulfide bond of the substrate protein forming a mixed disulfide bond between the protein and PDI (Figure 1.7). Then, the resulting thiol of the substrate protein can attack another disulfide bond. A series of thiol-disulfide reaction results in the formation of native disulfide bonds in the substrate protein.³⁰ The regaining of oxidized PDI will take place via the series of reactions involving Ero1p and its cofactor Flavin Adenine Dinucleotide (FAD), and molecular oxygen.

1.1.4.3 Oxidative *in vitro* protein folding with PDI

In vitro oxidative protein folding can be aided by the addition of PDI, which also catalyzes *in vivo* protein folding in the ER of the cell via a series of thiol-disulfide interchange reactions.³¹ For *in vitro* protein folding, PDI is mixed with a redox buffer which improves protein folding by preventing the unfolded proteins

from aggregating and increasing the rate of thiol-disulfide interchange reaction.^{32,33} The use of PDI for *in vitro* protein folding is not efficient as a consequence of its high cost of production, low catalytic activity, and instability.^{32,34} However, *in vivo* in the ER, the concentration of PDI is high.

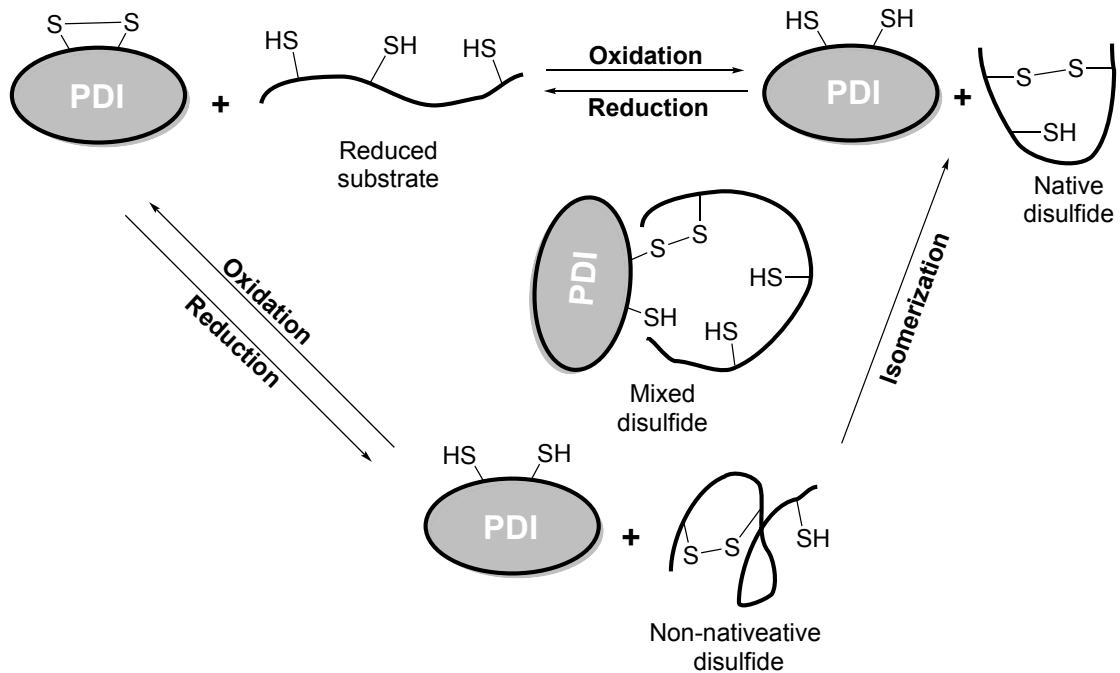


Figure 1.7 Oxidative protein folding mechanism *in vivo*.³⁵

1.1.4.4 Folding with small molecules

Oxidative *in vitro* protein folding of disulfide containing proteins is conventionally done using a redox buffer prepared with a small molecule aliphatic thiol and/or the corresponding disulfide.^{36,37} As these small molecules contain either a thiol or a disulfide group in their structure; they can react with protein thiols/disulfides in multiple steps until the native protein is formed. The native protein is a kinetically stable protein structure having only native type disulfide

bonds. Some of the traditional small molecule thiols and disulfides include glutathione (GSH) and glutathione disulfide (GSSG), reduced dithiothreitol (DTT^{red}) and oxidized dithiothreitol (DTT^{ox}), reduced and oxidized β -mercaptoethanol (BME), reduced and oxidized cysteine, reduced and oxidized (\pm) trans-1,2-bis(mercaptoacetamido)cyclohexane (BMC), reduced and oxidized cystamine^{38,39} (Figure 1.8). In general, the reduced and oxidized forms of the small molecules are mixed to prepare the redox buffer.^{40,41} Out of the above-mentioned redox systems, only two of them have been studied extensively for their effect on protein folding: DTT^{ox}/DTT^{red} and GSSG/GSH.⁴²

The GSSG/GSH system is found *in vivo*, where folding of disulfide containing proteins take place. Therefore, the GSSG/GSH redox system is the one most commonly used for oxidative protein folding experiments especially for proteins like BPTI, RNase A, and lysozyme.⁴³ The optimal conditions to fold these proteins are: 0.2 mM GSSG and 1 mM GSH for RNase A,⁴⁴ 2 mM GSSG and 7 mM GSH for lysozyme,^{45,46} and 2 mM GSSG and 2 mM GSH or 5 mM GSSG and 5 mM GSH for BPTI.⁴²

Dithiothreitol (DTT) has a reduction potential (E°) of -0.327 V; therefore, it is a weak oxidizing agent.⁴⁷ Even in the case of high molar concentration of oxidized DTT, the refolding rate of RNase A is very slow as compared to GSSG at much lower concentrations.³⁶ The advantage of using DTT is that DTT catalyzes protein folding without the formation of stable mixed disulfide intermediates; hence, the characterization of the folding pathway becomes easier.³⁶

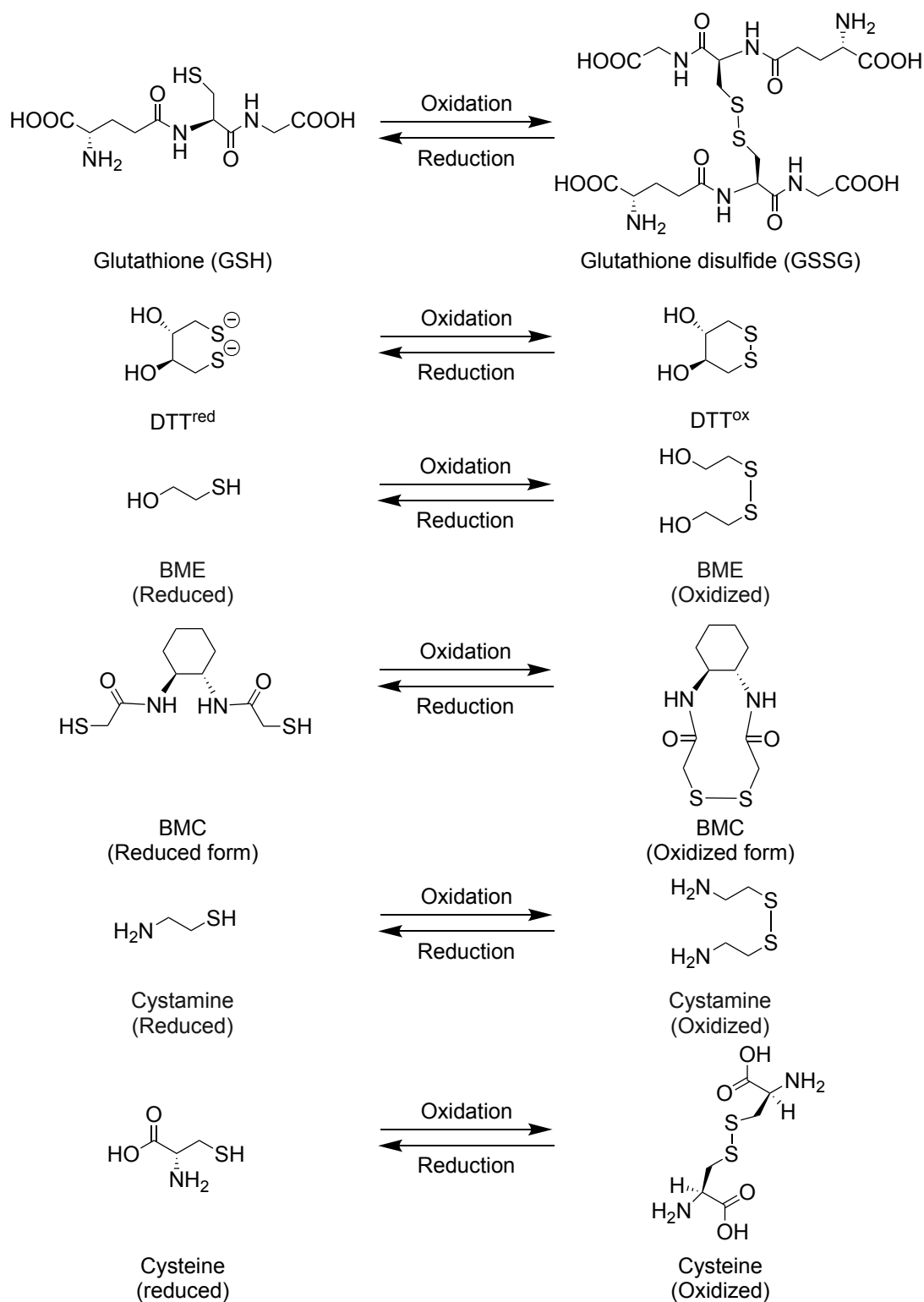


Figure 1.8 Some traditional small molecule thiols and disulfides.⁴³

For the large-scale production of proteins, less expensive oxidative folding agents are desired. Therefore, cysteine, cystamine, and β -mercaptoethanol are applicable as these compounds are cheaper than glutathione. Cystamine has a lower thiol pKa than glutathione and has a net positive charge at pH 7; hence, it is more advantageous for basic proteins like BPTI.⁴³

An aliphatic dithiol (\pm)-*trans*-1,2-bis(2-mercaptoacetamido)cyclohexane (BMC) has two thiol groups in close proximity and upon oxidation can form a comparatively less stable cyclic disulfide. The yield of protein folding can be increased significantly with BMC³¹ as demonstrated by Raines *et al.* during the folding of RNase A. When 1 mM BMC was added to a folding mixture containing 1 mM GSH and 0.5 mM GSSG, the yield of protein was two-fold as compared to folding yield with *N*-methylmercaptoacetamide (NMA),³⁶ which is the monothiol analog of BMC. The additional thiol group present in BMC helps increase the folding yield of proteins in comparison to NMA. Therefore, it is desirable to add an even low concentration of BMC to the folding mixture whether *in vivo* or *in vitro* to increase the yield.

Aromatic thiols and their corresponding disulfides (Figure 1.9) can be utilized more efficiently as a redox buffer to fold disulfide containing proteins because of their enhanced reactivity at physiological pH and lower thiol pKa values (4-7) as compared to their aliphatic counterparts. In addition, the thiol pKa is similar to that of the solvent exposed thiol of protein disulfide isomerase (PDI).⁴⁸ The enhanced reactivity is primarily dependent upon the better leaving group ability of the thiolate ion due to the higher stability of the thiolate anion as a

result of the lower pKa values of the corresponding thiols. Hence, small molecule aromatic thiols and disulfides enhance the thiol disulfide interchange reactions occurring during folding experiments.

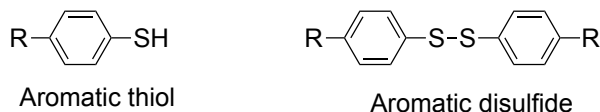


Figure 1.9 Generic structures of aromatic thiol and disulfide.

The folding rates of reduced RNase A and lysozyme were increased multiple folds with aromatic thiols in comparison to GSH. For example, folding of reduced RNase A was increased by the factor of 23 at pH 6, by the factor of 12 at pH 7 and by a factor of 8 at pH 7.7 relative to GSH.^{38,49} Similarly, folding experiments on reduced lysozyme showed that the folding rate was increased by the factor of 11 and yield by 40% with aromatic thiols and the corresponding disulfides relative to GSH and GSSG at pH 7.⁵⁰ Aromatic thiols with thiol pKa values 1-2 units lower than the pH of the folding mixture were found to be the best in terms of the reactivity. Therefore, we sought to synthesize aromatic thiols with expected thiol pKa values 5.5-6.5 as we are running folding experiments at pH 7.3 to mimic physiological conditions. I expect to dramatically increase in the folding rate of reduced protein with aromatic thiols and corresponding disulfides.

1.2 Folding of bovine pancreatic trypsin inhibitor (BPTI)

1.2.1 Introduction of BPTI

Bovine pancreatic trypsin inhibitor (BPTI) with 58 amino acid residues is one of the smallest globular proteins known, and its sole function is to bind to and inhibit serine proteases such as trypsin. The sequence of amino acids in BPTI is

RPDFC LEPPY TGPKK ARIIR YFYNA KAGLC QTFVY GGCRA KRNNF KSAED
CMRTC GGA.⁵¹ With 10 positively charged lysine (K) and arginine (R) residues
and 4 negatively charged aspartate (D) and glutamates (E) residues, the protein
is strongly basic at neutral pH and is sometimes called basic pancreatic trypsin
inhibitor. However, as the usual source for BPTI is bovine pancreas, the protein
is primarily referred to as bovine pancreatic trypsin inhibitor. Residue 15 of BPTI,
which is lysine, has a long basic side chain on an exposed loop of the structure.
Lysine is responsible for binding the specificity pocket in the active site of trypsin
hence inhibiting its enzymatic activity. Trypsin inhibitors usually have conserved
cysteine residues that participate in forming disulfide bonds. BPTI has α -helical
and β -sheet regions as well as three disulfide bonds between Cys5-Cys55,
Cys14-Cys38, and Cys30-Cys51, which stabilize the protein's tertiary structure⁵²
(Figure 1.10). Three disulfide bonds in 58 residues make BPTI one of the most
stable proteins known. BPTI was first isolated as a trypsin inhibitor from bovine
pancreas in 1936.⁵³ The crystal structure was solved by Robert Huber in 1970.⁵⁴
The first NMR structure was determined by Kurt Wuthrich at ETH in Zurich in
1980.⁵⁵ BPTI was the first protein to be studied computationally using molecular
dynamics.⁵⁶ BPTI is also the most-studied disulfide containing protein in terms of
folding pathway.

BPTI is quite inert to denaturants like urea at below 100°C but denatures
in very acidic solutions; the midpoint for reversible denaturation is 81°C at pH 2.1
(Figure 1.11).⁵⁷ If only one of the disulfide bonds, that formed between cysteine
residues 14 and 38, is reduced and then carboxymethylated, the midpoint

decreases to 59°C, hence denaturation becomes more facile than without carboxymethylation (Figure 1.11).

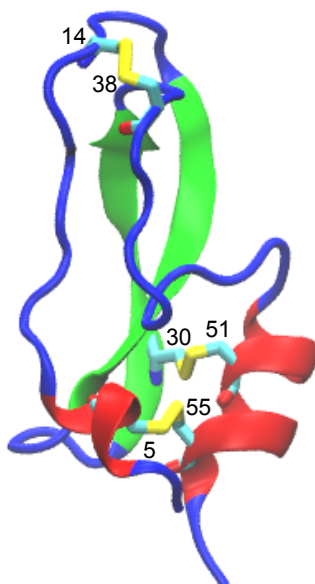


Figure 1.10. Structure of BPTI.⁵⁸

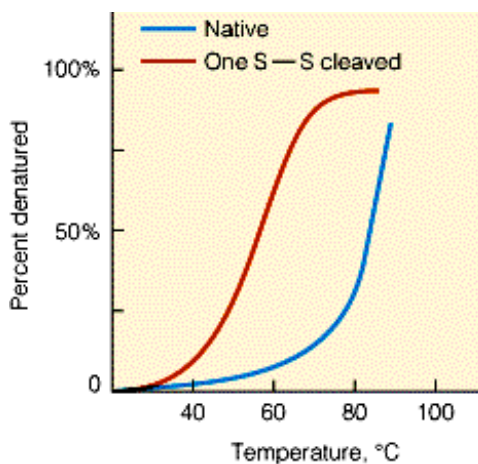


Figure 1.11. Thermal denaturation of BPTI at pH 2.1 (From reference 59).⁵⁹

When all three disulfide bonds of BPTI are reduced at room temperature, the protein unfolds. Upon oxidation under suitable conditions, native BPTI with its unique set of three disulfide bonds is formed. If BPTI were reduced to yield six cysteine residues and randomly re-oxidized, it would produce about 7% native

protein (1/15), as there are 15 possible combinations of BPTI with three disulfide bonds (Table 1.1). The first SH group to pick a partner will have five choices, the second SH group three partners, and the last SH group one partner. Therefore there are $5 \times 3 \times 1$, or 15, possible combinations.^{60,61}

Table 1.1: 15 possible combinations of six cysteine residues in BPTI

Combinations	1 st Disulfide bond	2 nd Disulfide bond	3 rd Disulfide bond
1	5-14	30-38	51-55
2	5-14	30-51	38-55
3	5-14	30-55	38-51
4	5-30	14-38	51-55
5	5-30	14-51	38-55
6	5-30	14-55	38-51
7	5-38	14-30	51-55
8	5-38	14-51	30-55
9	5-38	14-55	30-51
10	5-51	14-30	38-55
11	5-51	14-38	30-55
12	5-51	14-55	30-38
13	5-55	14-30	38-51
14*	5-55	14-38	30-51
15	5-55	14-51	30-38

*native BPTI

Previous studies of BPTI and other proteins containing disulfide bonds indicated that correct pairing of cysteines is achieved if appropriate conditions are selected and sufficient time is allowed.⁶⁰ The meaning of the finding is that the folding path of the protein places the SH groups in position for correct pairing. The corollary of this statement is that the S-S bridges are not essential for proper refolding. But, the formation of S-S bond contributes to the extra stability of the protein structure once the protein is folded. A protein containing S-S bridges has a smaller number of conformations available in the unfolded form than does a comparable protein without the bridges. Consequently, it shows a lower entropy gain on unfolding and is therefore stabilized.^{60,62}

1.2.2 Traditional *in vitro* oxidative folding of BPTI

The *in vitro* oxidative folding of fully reduced BPTI was traditionally carried out in the presence of DTT^{ox} and GSSG. The folding pathways were determined from the study of trapped intermediates. The folding study of BPTI was originally examined by Creighton who refolded reduced BPTI (**R**) at pH 8.7 in the presence of DTT^{ox} followed by the trapping of folding intermediates chemically using iodoacetamide to alkylate free thiols.^{63,64} These intermediates were separated via ion-exchange chromatography followed by analysis using two-dimensional paper electrophoresis. The study identified two main 1SS (contains one disulfide bond) intermediates, five main 2SS (contains two disulfide bonds), intermediates and only one 3SS (contains three disulfide bonds) protein structures (Figure **1.12**). Out of the two 1SS intermediates only one is native like (contains [30-51] disulfide bond), out of the five 2SS intermediates, three are native like, **N'** [30-51;

14-38], \mathbf{N}^* [5-55; 14-38], and \mathbf{N}^{SH} [30-51; 5-55], and the one 3SS containing structure is the native protein \mathbf{N} [30-51; 5-55; and 14-38]. The disulfide bond found in the most abundant one disulfide intermediate, [30-51], is present in all two-disulfide intermediates identified except in \mathbf{N}^* . Two of the 2SS intermediates containing non-native disulfide bonds, [30-51; 5-14] and [30-51; 5-38], were highly populated in Creighton's study.

From Creighton's work, it was revealed that the two well populated 2SS non-native intermediates have an important role in guiding the folding pathway to the native structure. These two 2SS intermediates which contain (30-51) as one of the two disulfide bonds have similar kinetic behavior and did not form substantially during the folding process but rearranged to another disulfide intermediate \mathbf{N}^{SH} [30-51; 5-55] which further rearranges rapidly to native BPTI \mathbf{N} [30-51; 5-55; and 14-38]. The native like 2SS intermediate \mathbf{N}^* [5-55; 14-38] was found to be very stable kinetically and only very slowly rearranged to \mathbf{N}^{SH} [30-51; 5-55], so the intermediate was called non-productive. The folding pathway of BPTI goes through two well populated non-native 2SS intermediates, [30-51; 5-14] and [30-51; 5-38] and the route is favored kinetically.

Later, the oxidative folding study of reduced BPTI was studied extensively by Kim and his team using a modified separation technique. The folding reaction was quenched at certain time points using an acid to stop further thiol-disulfide interchange reactions. Acid quenching has the advantage over the conventional method in that the process is reversible and the trapped and purified intermediates can be used for further folding experiments so that the folding

disulfide bond easily. As \mathbf{N}^* has buried Cys30 and Cys51 in its interior, the thiols of Cys30 and Cys51 are inaccessible to oxidizing agents and hence \mathbf{N}^* cannot undergo either oxidation or rearrangement on the experimental time scale; therefore, the route that forms \mathbf{N}^* is regarded as nonproductive.⁶⁶ On the other hand, the pathway via \mathbf{N}' , which also has two buried thiols, Cys5 and Cys55, is productive because this intermediate can rearrange to the more stable intermediates \mathbf{N}^* and \mathbf{N}^{SH} . The transition to \mathbf{N}^{SH} does not depend upon the concentration of oxidizing agents, which means that the transition is via an intramolecular thiol-disulfide interchange reaction.^{63,66} Conversion of \mathbf{N}' to \mathbf{N}^{SH} is the rate determining step in protein folding.^{65,67} In the final step leading to the formation of native BPTI, oxidation of Cys14 and Cys38 takes place forming the (14-38) bond.

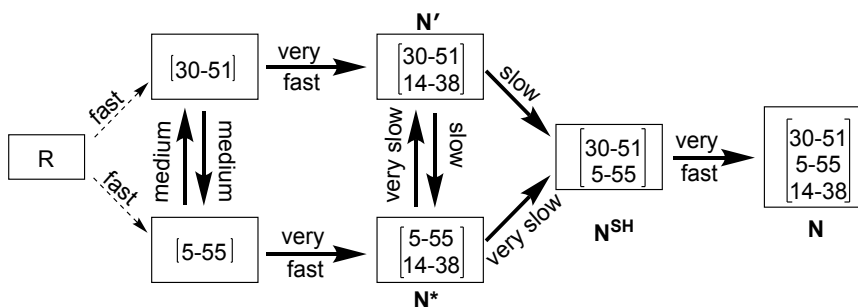


Figure 1.13 The folding pathway of BPTI proposed by Kim.^{64,65} **R** is reduced form and **N** is the native form of BPTI. The numbers inside the box separated by a dash are disulfide bonds. **N'**, **N***, and **N^{SH}** are native like 2SS intermediates. Very fast means the process can be finished within milliseconds and very slow means it could take months.⁶⁵

Subsequent studies by Kim *et al.* of the oxidative folding of reduced BPTI using GSSG concluded that the slow rate of direct oxidation of **N'** to **N** is because of the native-like structure of **N'** which slows down the intermolecular reaction

with GSSG to form a mixed disulfide as well as the subsequent intramolecular reaction leading to **N**.⁶⁸ The formation of **N** by direct oxidation requires high concentration of GSSG which also leads to the formation of a dead-end doubly mixed disulfide intermediate; therefore, folding via direct oxidation of **N'** does not form **N** in considerable amounts. During oxidative folding, two reactions were seen in competition. One is the formation of **N** from the singly mixed disulfide **N'(SG)**, and the other is the formation of **N'(SG)₂** from **N'(SG)**. The formation of singly mixed disulfide **N'(SG)** is from the oxidation of one of the free thiols of Cys5 or Cys55. At modest GSSG concentration, the formation of singly mixed disulfide **N'(SG)** is slower than the rearrangement of **N'** to **N^{SH}**. As the rate of formation of **N** from **N^{SH}** is 150 times faster than the rate of formation of singly mixed disulfide **N'(SG)** from **N'**, the formation of **N** takes place via intramolecular rearrangement. At high GSSG concentrations (> 500 μ M), formation of doubly mixed disulfide **N'(SG)₂** from singly mixed disulfide **N'(SG)** is 30 times faster than the formation of **N'(SG)** from **N'**; therefore, the process does not allow the formation of a considerable amount of **N**. The conclusion is that complete unfolding of native like intermediates **N'** and **N*** as seen in BPTI folding, is common to all disulfide containing proteins.⁶⁸

1.2.3 Updated folding pathway of BPTI

Recent investigation by Yingsong and Lees on the folding of reduced BPTI via a growth type pathway and updated the BPTI folding pathway (Figure 1.14).⁶⁹ A growth type pathway is a protein folding model where the rate determining step(s) in the folding reaction is the nucleation of native-like conformation

followed by the smooth formation of conformation with native disulfide bonds,⁷⁰ The folding condition optimized previously by Kibria and Lees with GSH and GSSG were 5 mM GSH and 5 mM GSSG to fold reduced BPTI to 93% native protein in 48 h.⁴² Conformational kinetic trap N^* and oxidative kinetic trap $N'(SG)_2$ which is also called doubly mixed disulfide, were observed in the reaction and were balanced under optimal conditions. The formation of protein doubly mixed disulfide with 5 mM GSH and 5 mM GSSG suggested that growth type pathways were needed to efficiently fold reduced BPTI. Wang *et al.* determined the rate constants for many of the steps that occur during the folding of reduced BPTI. On the basis of these rate constants, the best folding conditions for BPTI were predicted assuming only two changes to the redox buffer of GSH/GSSG were made during the folding process. The conversion took place via the formation of $N'(SG)$. The folding of reduced BPTI was initiated with 2 mM GSSG and 5 mM GSH to convert all reduced BPTI to disulfide intermediates, N' and N^* were formed as primary intermediates occupying 50% of the total concentration. Then, 30 mM GSH was added after 15 min, total GSH concentration was 35 mM, to reduce the rest of the intermediates like N' , $N'(SG)$, $N'(SG)_2$. The reduced proteins were converted to the thermodynamically more stable intermediate N^* as these intermediates react with GSSG. After 1 h, 50 mM GSSG was added and the reaction continued for 12 h to produce 93% N. N^* was previously regarded as a dead-end kinetic trap. The finding was helpful to increase the yield of native protein because folding via the productive route: N' to N^{SH} to N or N' to $N'(SG)$ to N was limited by the formation of doubly mixed disulfide $N'(SG)_2$.

25% at pH 7 and 8 respectively.⁵⁰ Additionally, the rate of folding for RNase A was also found to be enhanced up to 23 times at pH 6, up to 12 times at pH 7, and up to 8 times at pH 7.7 with aromatic thiols as compared to glutathione.³⁷ Therefore, replacing glutathione with aromatic thiols in the redox system can expedite the rate of folding of disulfide containing proteins at neutral pH and a further increase in relative rate can be achieved by decreasing the pH of the redox buffer.⁴⁶

1.3.2 Construction of the structure of small molecule aromatic thiols

The structure of aromatic thiols should have the following characteristics: these small molecule thiols should have charged side chain so that the thiols are soluble in buffer, the thiol group should have a pKa value very close to neutral pH, and the molecules should be easily separated from protein after the folding assay is completed so that it will not hamper the analysis. The charged groups are either negatively charged like sulfonic acid and phosphoric acid, or positively charged like quaternary ammonium salt. These groups are installed in the structure during their synthesis. The thiol pKa values can be calculated from the σ_p^- a value of the substituent. The Hammett plot has a slope of -1.6, $\rho = -1.6 \pm 0.1$.⁴⁸

The formation of disulfide bonds takes place via a nucleophilic substitution mechanism. A thiolate ion (R_1S^-) attacks the disulfide bond (R_2SSR_3) and substitutes (R_3S^-), as a result, a new disulfide bond (R_1SSR_2) is formed as shown in scheme 1.1. In the reaction, R_1S^- acts as a nucleophile, R_3S^- serves as a leaving group, and R_2S^- serves as the center of attack.^{34,39} The rate of the thiol-

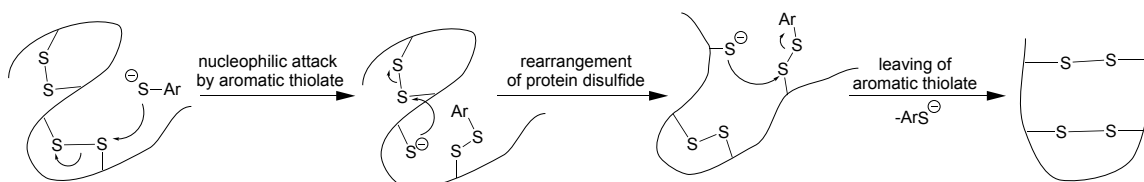
disulfide interchange reaction is dependent upon several factors including the stability of the leaving group and the nucleophilicity of the attacking group.

Scheme 1.1 Nucleophilic substitution in thiol-disulfide interchange reaction

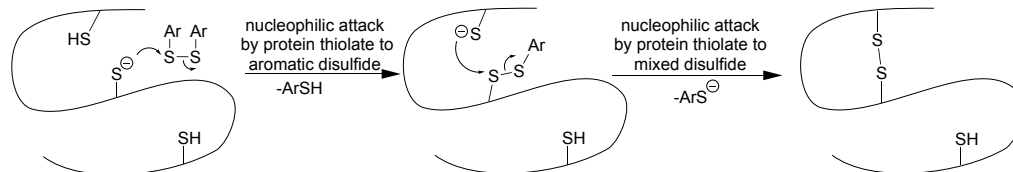


Therefore, the basis for the design of small molecule aromatic thiols for protein folding is to enhance the rate of thiol-disulfide interchange reactions which take place between the small molecules and proteins during oxidative *in vitro* protein folding. The rate of rearrangement of protein disulfide bonds found in the folding intermediates can be a slow process, as I have observed in the folding of reduced BPTI; hence, aromatic thiolate ions will expedite the process (Scheme 1.2). Native disulfide bonds formation with aromatic thiols involve reduction of non-native disulfides to thiols and rearrangement of non-native disulfide bonds to native disulfide bonds. Aromatic disulfides also help in increasing the rate of formation of protein disulfide bonds (Scheme 1.3) because aromatic thiolates are stable leaving groups. Our aim to fold BPTI faster is highly dependent upon the rate of formation and rearrangement of protein disulfides with the aid of aromatic thiols and their corresponding disulfides.

Scheme 1.2 Rearrangement of protein disulfide with aromatic thiolate ion



Scheme 1.3 Formation of protein disulfide with aromatic disulfide



1.4 Molecular dynamics (MD) simulation study of BPTI

1.4.1 Importance of MD simulation

Molecular dynamics (MD) simulation is a computational method which is regarded as a primary method for the theoretical study of the biomolecules at their atomistic levels to insight into their structure, function, and dynamics. Atoms and molecules are interacted for the fixed time providing a view of the details of the interactions of the system. The method of MD simulation has its application in wide range of science including physics, chemistry, biochemistry, biophysics, and structural biology. Growing advancement of methodology and computer power is helping to study the larger systems and variety of conformational changes utilizing the longer time of simulation to find the details of a process going on inside the body which is not possible from experiments.⁷¹ The three-dimensional structure of proteins is predicted via the MD simulation of folding of a random coil of that particular proteins.

1.4.2 Protein folding and MD simulation

The knowledge of a folding process of a newly synthesized protein helps to understand the basic principle of life at its atomistic levels.⁷² The field of medicine can take the advantages of the molecular dynamics (MD) simulation of protein folding process as the study can facilitate the development of the

treatment methods of diseases associated with protein misfolding.⁷³ The study of protein folding helps the field of nanotechnology because the investigation can reveal the principle behind the folding.⁷³ Both the experimental⁷⁴ and computational⁷⁵ methods have been advancing to elucidate the process of conformational changes of proteins. MD simulation has been improvised and coupled with the ultrafast, inexpensive computers to study the unfolding and folding of proteins in their atomistic levels.⁷⁶

1.4.3 Molecular dynamics (MD) simulation of BPTI

Bovine pancreatic trypsin inhibitor (BPTI) is the first protein which was tested with molecular dynamics (MD) simulations in *vacuo*.⁵⁶ After eleven years, MD simulation of BPTI done in water at the same time was reported stating that the simulation was run for higher time scales and improved the results giving better RMSD value and reducing the number of incorrect hydrogen atoms as opposed to the simulation run in *vacuo*.⁷⁷ The presence of water molecules in simulation provides more realistic motion of protein and structure will attain very close to the crystal structure.⁷⁷ Later on, simulation on BPTI has been performed in different laboratories.⁷⁸⁻⁸²

Bovine pancreatic trypsin inhibitor (BPTI), as it contains three disulfide bonds, has an extra stability in its native form. During simulation, if the disulfide bonds are included as constraints, can reduce the conformational space. Saito and coworkers were the first to study the protein folding/unfolding of disulfide containing proteins assuming that folding starts with the formation of secondary structure (α -helices and β -sheets) followed by the attaining the tertiary

structure.^{83,84} The simulation on finding the role of disulfide bonds in protein folding revealed that folding of disulfide containing proteins undergoes with different pathways to the native form via the formation of native-like intermediates only, but the process is mediated by the formation of non-native intermediates.⁸⁵ The results were in agreement with both the conflicting experimental results by Creighton,⁸⁶ and Weissman and Kim.⁶⁵ Another study on disulfide bonds and protein folding by Scheraga and coworkers⁸⁷ concluded that the conformational folding and the disulfide bond formation are extremely cooperative process as well as the development and breaking of disulfide bonds in the disulfide containing proteins takes place when certain conditions such as closeness of cysteine residues, orientation, and easiness of thiols to oxidizing agents are fulfilled. Lately, MD simulation works on BPTI revealed that the initially formed specifically collapsed structure of protein similar to native form guides the formation of disulfide bonds.⁸⁸ Herein, the importance of conformations of intermediates during folding in the formation of disulfide bonds is described, taking BPTI as a model protein, and using targeted molecular dynamics (TMD)⁸⁹ simulation. Targeted MD is a great computational tool to study the conformational changes of starting structure to an assigned target structure with the application of time-dependent geometrical constraint, usually run at ordinary temperature.⁹⁰ As the process of conformational folding and disulfide bond formation are coupled to each other, the TMD simulation study on BPTI would give an opportunity to understand the mechanism of conformational changes and disulfide bond formation visually.

CHAPTER 2

Objectives

The aims of my dissertation research are to synthesize aromatic thiols and their corresponding disulfides, and to investigate the folding of reduced BPTI using these compounds.

2.1 Synthesis of different aromatic thiols and their corresponding disulfides for the study of folding of reduced BPTI

Four different QAS thiols and their corresponding disulfides as well as one sulfonic acid thiol and its disulfide will be prepared with the expectation that they will improve the efficiency and folding rate of reduced BPTI.

2.2 Folding of reduced BPTI faster using different aromatic thiols and their corresponding disulfides

Three different aromatic thiols (PA, SA, and QAS) are used to fold reduced BPTI at physiological pH selecting different concentrations of the thiols and the corresponding disulfides to prepare the redox buffer. The best thiol in our folding study as well as the best condition will be determined and the results compared with the traditional folding buffer GSSG/GSH.

2.3 Molecular dynamics (MD) simulation study of BPTI intermediates to understand the folding of BPTI at a molecular level

The molecular mechanism of the conformational changes at an atomistic level will be modeled. The software NAMD will be used for the simulation study and the software VMD will be used for visualization of the simulation.

CHAPTER 3

Synthesis of aromatic thiols and corresponding disulfides

3.1 Abstract

The use of redox buffers containing an aromatic thiol and its corresponding disulfide were found to increase the *in vitro* folding rate of disulfide containing proteins compared to buffers composed of an aliphatic thiol and its corresponding disulfide. The increased folding rate with aromatic thiols at physiological pH, 7.3, is attributed to their lower thiol pKa values (4-7), greater nucleophilicity at neutral pH, and enhanced leaving group ability. Oxidative protein folding in the endoplasmic reticulum (ER) of a cell is aided by protein disulfide isomerase (PDI). The enzyme PDI contains two active sites each with a CXXC motif where one of the cysteine is buried and the other is solvent exposed and has a thiol pKa of 6.7. I synthesized five different aromatic thiols and their corresponding disulfides with expected pKa values close to the pKa of the solvent exposed thiol of PDI: Four positively charged quaternary ammonium salt thiols and their corresponding disulfides, and one negatively charged sulfonic acid thiol and its corresponding disulfide. The folding of reduced bovine pancreatic trypsin inhibitor (BPTI) was performed with a redox buffer composed of one positively charged thiol and its disulfide, and one negatively charged thiol and its disulfide. The results showed that the positively charged thiol folded reduced BPTI faster as compared to the traditional redox buffer composed of aliphatic thiol, glutathione (GSH), and its disulfide glutathione disulfide (GSSG). Although the negatively charged aromatic thiol and its disulfide were found to fold

reduced BPTI rapidly, the protein also precipitated. It is expected that the other positively charged thiols and their corresponding disulfides will also fold reduced BPTI more efficiently.

3.2 Introduction

The number, importance, and use of protein-based drugs are expected to increase dramatically over the next five years.⁹¹ The total number of protein based drugs approved worldwide is around 650.⁹² Out of these 650, about 400 of them are produced using recombinant DNA technology. An additional 1300 drugs are being developed.⁹² Almost all of these drugs contain disulfide bonds and a third of them are produced in *E. coli*. Overexpression of proteins in *E. coli* is efficient as large amounts of protein are rapidly produced. However, overexpressed disulfide-containing proteins tend to misfold and aggregate as inclusion bodies inside *E. coli*. The aggregated protein is then resolubilized and folded oxidatively *in vitro* to obtain active protein.⁸ Oxidative protein folding *in vitro* as well as *in vivo* involves the conformational folding of proteins combined with the oxidation of protein thiols to disulfides, and the reduction and rearrangement of protein disulfides. During rearrangement non-native disulfide bonds are rearranged to native disulfide bonds.⁴²

Oxidative protein folding has traditionally been performed with a redox buffer of glutathione (GSH) and glutathione disulfide (GSSG), as these aliphatic small molecules are found in the endoplasmic reticulum (ER) of eukaryotes where *in vivo* oxidative protein folding takes place.⁹³ The slow step(s) in oxidative protein folding *in vitro* involve(s) thiol-disulfide interchange reactions. The thiol-

disulfide interchange reactions during protein folding occur between protein thiol/disulfide and small molecule thiol/disulfide, where thiolate ion, deprotected thiol, attacks a disulfide. As the reaction goes through the nucleophilic substitution mechanism, the rate of the reaction depends on the concentration of the thiolate ion in the solution, which ultimately depends on the thiol pKa and the pH of a solution.^{38,94} In eukaryotic cells, thiol-disulfide interchange reactions are catalyzed by protein disulfide isomerase (PDI).³¹ One of the properties of PDI that is believed to be important for catalysis is a nucleophilic low pKa thiol in the active site. The PDI is effective but is expensive for *in vitro* oxidative protein folding since it needs to be added in almost stoichiometric amounts.^{32,44}

To improve *in vitro* protein folding, I sought to prepare small molecules with nucleophilic low pKa thiols similar to PDI. Aromatic thiols have thiol pKa values (pKa = 4-7) comparable to PDI and lower than those of aliphatic thiols, such as GSH (pKa = 8.7).^{48,95} In addition, aromatic thiols are more nucleophilic than aliphatic thiols with similar pKa values.⁹⁶ Gough *et al.* demonstrated that a redox buffer composed of aromatic thiols and disulfides increased the folding rate of ribonuclease A 10 times in comparison to a redox buffer composed of GSH and GSSG.⁴⁹ These redox buffers composed of small molecule disulfides and corresponding thiols, in variable concentrations, oxidize protein thiols to disulfides as well as rearrange mismatched non-native disulfide bonds within protein to native disulfide bonds.⁴⁹

Herein, four different quaternary ammonium salt (QAS) thiols **1-4** and their corresponding disulfides **5-8** (Figure **3.1**), and the sulfonic acid (SA) thiol **9** and

its disulfide **10** (Figure 3.2) were synthesized. Compounds **1**, **5**, **9**, and **10** were synthesized using previously reported methods^{50,97-99} and utilized for the folding of BPTI. The redox buffer, composed of QAS thiol **1** and its disulfide **5**, folded reduced BPTI to about 90% completion within one hour without any indication of protein precipitation. The redox buffer, composed of SA thiol **9** and its disulfide **10**, folded reduced BPTI faster, but was found to be less suitable to be used as a redox buffer since it resulted in protein precipitation. Compounds **2-4** and **6-8** were synthesized for the first time.

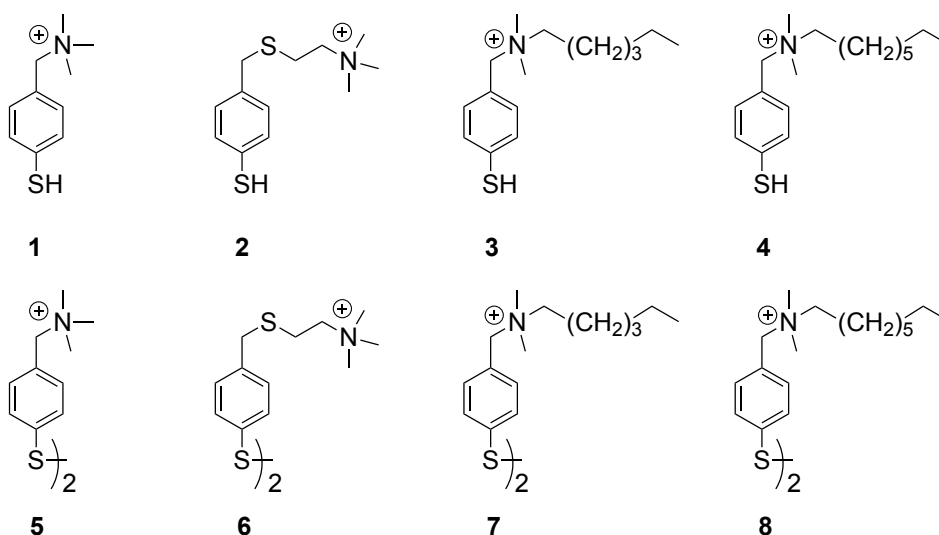


Figure 3.1. Quaternary ammonium salt (QAS) thiols **1-4** and their corresponding disulfides **5-8**.

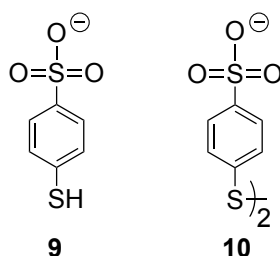


Figure 3.2. Sulfonic acid thiol **9** and its disulfide **10**.

3.3 Results and discussion

Four different quaternary ammonium thiols (**1-4**) and their corresponding disulfides (**5-8**), and one sulfonic acid thiol (**9**) and its disulfide (**10**) were synthesized. Disulfides were synthesized by dissolving the corresponding thiols in water and stirring in the presence of air until the disulfides were formed. The completion of disulfide formation was confirmed using Ellman's reagent. Quaternary ammonium salt thiols with increased number of carbons in the side chain were selected, as thiol **1** had shown significant improvement in protein folding rates and yields.^{34,46} Increasing the hydrophobic side chain may result in thiols more likely to enter the hydrophobic core of proteins.

3.3.1 Synthesis of quaternary ammonium salt thiol **1**

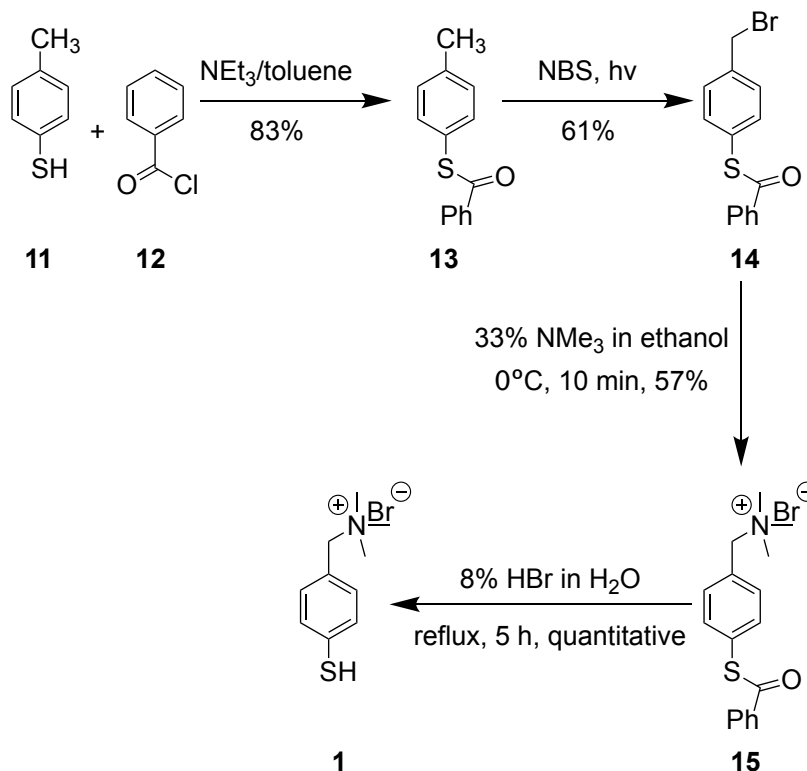
The QAS thiol **1** was synthesized as shown in scheme **3.1**. To protect the SH group *p*-toluene thiol (**11**) and benzoyl chloride (**12**) were reacted in the presence of trimethylamine to form compound **13**. The protected compound **13** was then subjected to a radical bromination reaction with *N*-bromosuccinamide in the presence of light to provide bromide **14**. Compound **14** reacted with trimethylamine to form QAS salt **15**. The benzoyl protecting group was removed from **15** by refluxing **15** with 8% HBr.

3.3.2 Synthesis of quaternary ammonium salt thiol **2**

The QAS thiol **2** was prepared following scheme **3.2**. Benzyl bromide **14** was reacted with β -mercaptoethanol in the presence of diisopropylethylamine (DIPEA) to form alcohol **16**. Compound **16** was then reacted with carbon tetrachloride and triphenylphosphine to obtain bromide **17**. Compound **17** was

reacted with trimethylamine and formed QAS salt **18**. The benzoyl protecting group was removed from **18** by refluxing **18** with 8% HBr.

Scheme 3.1. Synthesis of quaternary ammonium thiol **1**



There were lots of challenges during the synthesis of **2**. The first step was the formation of an alcohol. Initially, it was challenging to find the correct base that would initiate the reaction. Bases tried were potassium carbonate, potassium hydroxide, sodium carbonate, cesium carbonate, silver carbonate, sodium hydroxide, and DIPEA. Only potassium carbonate and DIPEA gave positive results, however DIPEA was selected as it gave the highest yield and was easy to dissolve. As the reaction should go through a S_N2 mechanism, the polar aprotic solvent DMF was selected. There was also a regioselective issue. The thiolate from β -mercaptoethanol could attack either the benzylic carbon or the

carbonyl carbon forming two different products. The best ratio obtained was 1:1. Two different side products along with 42% of product were observed in the ^1H NMR spectra of the crude mixture. The proposed the following side products (Figure 3.3) based on the NMR.

Scheme 3.2. Synthesis of elongated quaternary ammonium thiol **2**

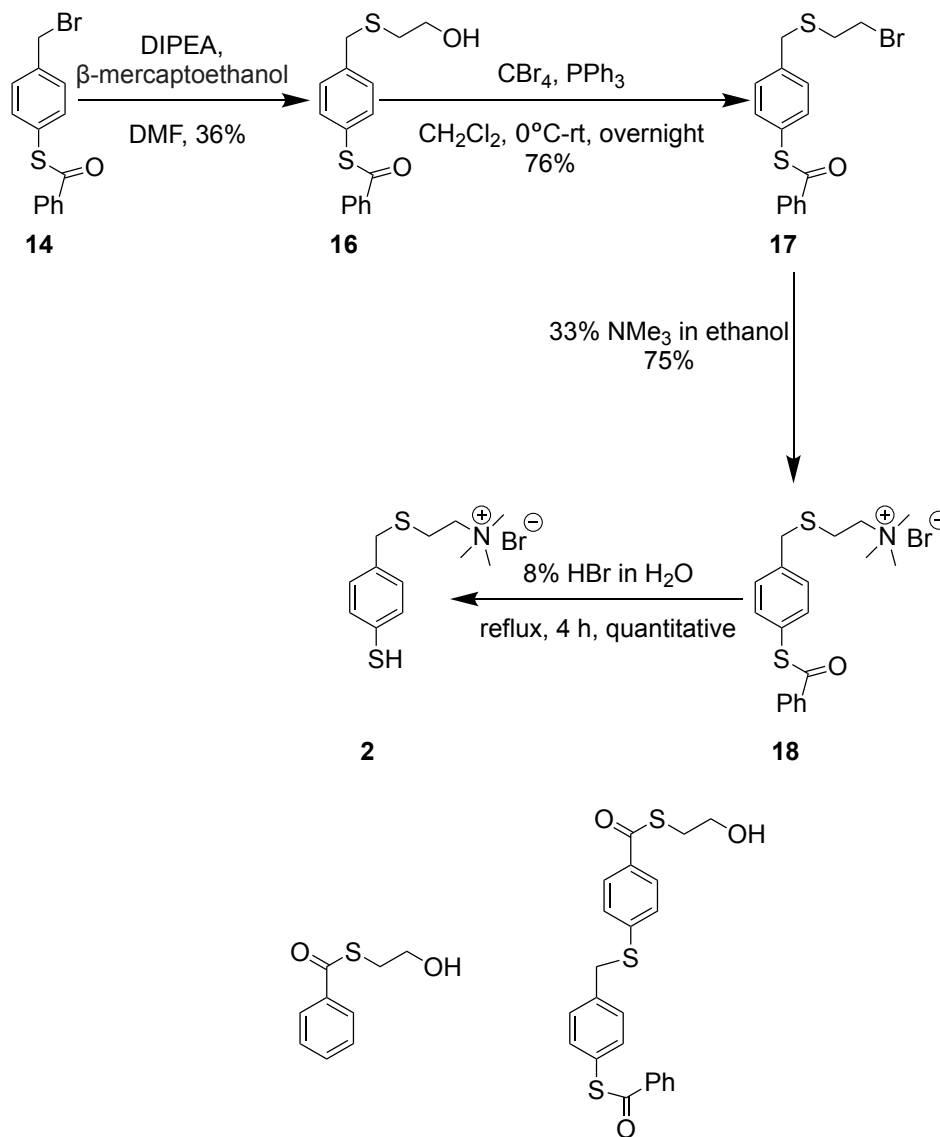
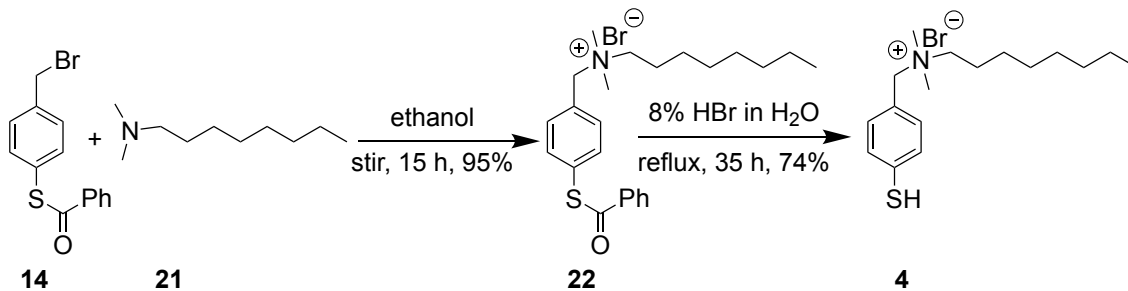


Figure 3.3. Side products of the first step in the preparation of compound **16**.

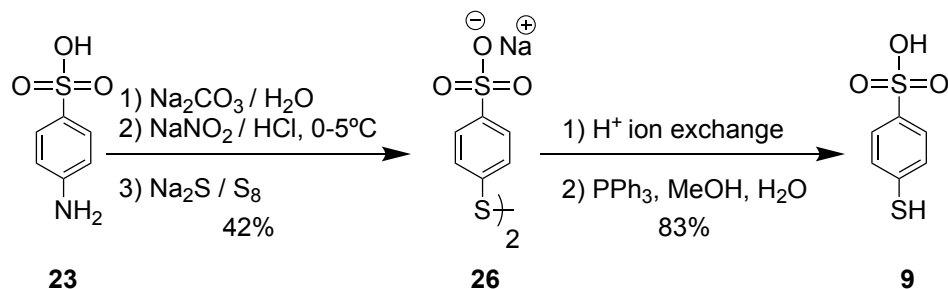
Scheme 3.4. Synthesis of octyl QAS thiol **4**



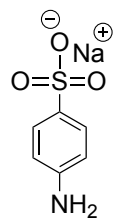
3.3.5 Synthesis of sulfonic acid thiol **9**

Preparation of sulfonic acid thiol **9** is shown in scheme 3.5. The reaction was started by treating *p*-aminobenzenesulfonic acid (**23**) with diluted sodium carbonate. The resulting sodium salt of *p*-aminobenzenesulfonic acid (**24**) was treated with nitrous acid at low temperature forming diazonium salt (**25**). Compound **25** was then reacted with disodium disulfide which resulted in sodium-4,4'-dithiobis(benzenesulfonate) (**26**). Compound **26** was run through an H⁺ ion exchange column to form the disulfide of sulfonic acid thiol (**10**). Compound **10** on treatment with triphenylphosphine in the presence of water provided sulfonic acid thiol **9**.

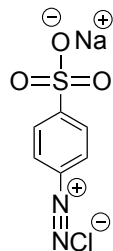
Scheme 3.5. Synthesis of sulfonic acid thiol **9**



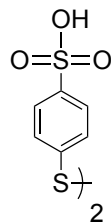
The following intermediates were not isolated but were formed during the synthetic pathway. Intermediate **10** was formed in between **26** and **9**.



24



25



10

3.4 Experimental section

3.4.1 Synthesis of 1-(4-(mercaptophenyl)-*N,N,N*-trimethylmethanaminium bromide (1)

3.4.1.1 Synthesis of *S-p*-tolyl benzothiophenol (13)⁹⁷

In the 500-mL round bottom flask, 11.5 mL of benzoyl chloride (13.91 g, 102.6 mmol), 2.39 g of *p*-toluene thiol (99.7 mmol), and 100 mL of ether were mixed. The mixture was stirred and cooled in an ice-water bath. Then 18 mL of triethylamine (13.07 g, 128.2 mmol) was added to an equal volume of ether (18 mL) and the resulting solution was added dropwise to the above mixture via a dropping funnel over 30 min. The reaction mixture was subsequently left in the ice-water bath for 1.5 h and then allowed to warm to room temperature. The mixture was filtered and the solid washed with ether. The ether fractions were combined and dried with MgSO₄. After rotary evaporation of the solvent, 19.00 g (83%) of the benzoyl derivative was obtained. ¹H NMR (CDCl₃, 400 MHz) δ 8.03 (dd, *J* = 8.4, 1.2 Hz, 2H), 7.62 (tt, *J* = 7.6, 1.2 Hz, 1H), 7.50 – 7.46 (m, 2H), 7.42 – 7.39 (m, 2H), 7.27 (d *J* = 8.0 Hz, 2H), 2.41 (s, 3H).

3.4.1.2 Synthesis of S-4-(bromomethyl)phenyl benzothiophenol (14)

S-*p*-tolylbenzothiophenol (**13**) (10.16 g, 44.5 mmol) and *N*-bromosuccinimide (7.97 g, 44.7 mmol) were mixed with deoxygenated benzene (63.5 mL). The reaction mixture was irradiated with a 250W GE heat lamp, which provided sufficient light energy to start reflux. After 30 min at reflux, the mixture was cooled to 0°C, filtered and concentrated under reduced pressure. The residue was partitioned between 300 mL of CH₂Cl₂ and 150 mL of water. The aqueous layer was washed with 125 mL of CH₂Cl₂. The combined organic layers were dried with MgSO₄, filtered and concentrated. The solid was then recrystallized from hexanes to obtain 8.36 g (61%) of product. The product also contained 5% of S-4-(dibromomethyl)phenyl benzothiophenol. ¹H NMR (CDCl₃, 400 MHz) δ 8.01 (dd, *J* = 8.4, 1.2 Hz, 2H), 7.66 – 7.60 (t, 1H), 7.54 – 7.46 (m, 6H), 4.52 (s, 2H)

3.4.1.3 Synthesis of 1-(4-(benzoylthio)phenyl)-*N,N,N*-trimethylmethanaminium bromide (**15**)⁹⁷

Benzyl bromide (**14**) (25.0 g, 81.4 mmol) was added in a round-bottomed flask and cooled to 0°C. Trimethylamine (38.30 ml of a 33% solution in ethanol, 213.8 mmol) was then quickly added to the round-bottomed flask and the resulting mixture was stirred for 10 min. The mixture was then concentrated under reduced pressure, and the residue was recrystallized from EtOAc/EtOH (95:5) to provide 17.1 g of quaternary ammonium salt (**15**), 57% yield. ¹H NMR (CDCl₃, 400 MHz) δ 7.97 (d, *J* = 7.6 Hz, 2H), 7.81 (d, *J* = 8.0 Hz, 2H), 7.64 – 7.57 (m, 3H), 7.48 (t, *J* = 8.0 Hz, 2H), 5.19 (s, 2H), 3.41 (s, 9H).

3.4.1.4 Synthesis of 1-(4-(mercaptophenyl)-*N,N,N*-trimethylmethanaminium bromide (1)^{50,97}

Quaternary ammonium salt (**15**) (1.86 g, 5.08 mmol) was dissolved in 6 mL of HBr (48% w/v in water) and 30 mL of water. The mixture was then refluxed for 5 h. After cooling to 0°C, the mixture was filtered. The aqueous fraction was lyophilized several times by redissolving the residue in 10 mL of water each time. The quaternary ammonium salt thiol (**1**) was obtained quantitatively. ¹H NMR (CD₃OD, 400 MHz) δ 7.43 (s, 4H), 4.50 (s, 2H), 3.10 (s, 9H).

3.4.2 Synthesis of 2-*S*-(4-mercapto)benzyl)-*N,N,N*-trimethylethanaminium bromide [extended QAS thiol] (**2**)

3.4.2.1 Synthesis of 2-*S*-(4-(benzoylthio)benzyl)ethanol (**16**)

Benzyl bromide (**14**) (0.77 g, 2.5 mmol), *N,N*-diisopropylethylamine (0.32 g, 2.5 mmol), 2-mercaptoethanol (0.198 g, 2.5 mmol), and 10 mL of DMF were mixed in round-bottomed flask and stirred for 15 min. Next, 1 N HCl (100 mL) was added and the mixture was extracted with ethyl acetate (3 x 20 mL). The organic layers were combined, dried with MgSO₄ and concentrated in vacuo. The residue was purified twice via silica gel chromatography using CH₂Cl₂: EtOAc (10:1) and then hexane: EtOAc: CH₂Cl₂ (3:1:1) as the eluent to provide alcohol (**16**) as a white solid, yield 0.282 g, 36%. ¹H NMR (CDCl₃, 400 MHz) δ 8.02 (dd, *J* = 8.0, 0.8 Hz, 2H), 7.61 (t, *J* = 7.6 Hz, 1H), 7.51 – 7.46 (m, 4H), 7.42 (d, *J* = 8.0 Hz, 2H), 3.77 (s, 2H), 3.70 (t, *J* = 6.0 Hz, 2H), 2.66 (t, *J* = 6.0 Hz, 2H), 2.05 (brs, 1H); ¹³C NMR (CDCl₃, 100 MHz) δ 190.3, 139.9, 136.7, 135.4, 133.8, 129.9, 128.9, 127.6, 126.2, 60.4, 35.5, 34.4.

3.4.2.2 Synthesis of 2-S-(4-(benzoylthio)benzyl)-1-bromoethane (**17**)¹⁰⁰

A mixture of an alcohol (**16**) (0.304 g, 1.0 mmol) and CBr₄ (0.365 g, 1.1 mmol) in CH₂Cl₂ (2 mL) was prepared in a 25-mL flask and cooled to 0°C. Triphenyl phosphine (0.289 g, 1.1 mmol) was added via a powder funnel in portions with vigorous stirring. Then, the mixture was stirred for 15 h at room temperature. The mixture was then concentrated *in vacuo* and the residue purified via silica gel chromatography with a mobile phase of hexane: EtOAc (3:1) to provide 0.28 g of bromide (**17**) as a white solid, yield 76%. ¹H NMR (CD₃COCD₃, 400 MHz) δ 8.03 (dd, *J* = 8.4, 1.2 Hz, 2H), 7.73 (t, *J* = 7.6 Hz, 1H), 7.60 (t, *J* = 8.0 Hz, 2H), 7.54 - 7.49 (m, 4H), 3.95 (s, 2H), 3.57 (t, *J* = 8.0 Hz, 2H), 2.92 (t, *J* = 8.0 Hz, 2H); ¹³C NMR (CD₃COCD₃, 100 MHz), δ 189.8, 141.4, 137.5, 136.1, 134.9, 130.7, 130.0, 128.1, 126.8, 35.8, 34.1, 31.6.

3.4.2.3 Synthesis of 2-S-(4-(benzoylthio)benzyl)-*N,N,N*-trimethylethanaminium bromide (**18**)

Bromide **17** (0.28 g, 0.76 mmol) and 33% trimethyl amine in ethanol (0.41 mL, 2.29 mmol) were mixed in a 25-mL flask. After 2 d at room temperature, the mixture was concentrated *in vacuo* and the residue was recrystallized from EtOAc: EtOH (95:1) to provide 0.246 g of crystals of elongated QAS salt (**18**), yield 75%. ¹H NMR (CDCl₃, 400 MHz) δ 7.98 (dd, *J* = 8.0, 0.8 Hz, 2H), 7.64 – 7.59 (m, 3H), 7.51- 7.45 (m, 4H), 3.97 (s, 2H), 3.53 – 3.48 (m, 2H), 3.34 (s, 9H), 2.89 – 2.85 (m, 2H); ¹³C NMR (CDCl₃, 100 MHz) δ 189.9, 138.7, 135.2, 134.8, 133.0, 129.4, 127.9, 126.5, 125.5, 64.6, 52.4, 34.9, 22.8.

3.4.2.4 Synthesis of 2-S-(4-mercapto)benzyl)-N,N,N-trimethylethanaminium bromide (2)

The quaternary ammonium salt (**18**) (1.08 g, 2.54 mmol) was dissolved in 3 mL of 48% HBr and 15 mL of water. The mixture was refluxed for 4 h and then cooled to 0°C and filtered. The filtrate was then extracted with EtOAc (2 X 30 mL). The aqueous fraction was lyophilized several times by redissolving the residue in 10 mL of water each time. The pure extended QAS thiol (**2**) was obtained quantitatively. ¹H NMR (D₂O, 400 MHz) δ 7.34 (dd, *J* = 15.2, 8.0 Hz, 4H), 3.78 (s, 2H), 3.32-3.28 (m, 2H), 3.01 (s, 9H), 2.80-2.76 (m, 2H); ¹³C NMR (D₂O, 100 MHz) δ 130.0, 129.9, 129.2, 128.5, 65.2, 52.8, 34.7, 22.7.

3.4.2.5 Synthesis of 1,1'-(4,4'-disulfanediyl)bis(1,4-phenylene)bis(2-S-N,N,N-trimethylethanaminium) bromide [Disulfide of extended QAS thiol] (6)

The elongated QAS thiol (**2**) (0.0053 g, 0.016 mmol) was dissolved in 40 mL of water and stirred rapidly in the presence of air. After a week, the solution was lyophilized to obtain the disulfide of elongated QAS thiol (**6**) quantitatively. ¹H NMR (D₂O, 400 MHz) δ 7.57 (d, *J* = 8.0 Hz, 2H), 7.36 (d, *J* = 8.0 Hz, 2H), 3.80 (s, 2H), 3.26-3.22 (m, 2H), 2.94 (s, 9H), 2.79-2.75 (m, 2H); ¹³C NMR (D₂O, 100 MHz) δ 137.4, 135.5, 13.0, 126.3, 65.2, 52.7, 34.9, 23.2.

3.4.3 Synthesis of hexyl QAS thiol

3.4.3.1 Synthesis of 1-(4-(benzoylthio)phenyl)-N,N-dimethyl-N-hexylmethanaminium bromide (20)

Benzyl bromide **14** (2.72 g, 8.87 mmol) and *N,N*-dimethylhexylamine (**19**) (1.54 mL, 8.84 mmol) were dissolved in 9 mL of ethanol and stirred for 6 h at

room temperature. The solvent was removed under reduced pressure and the residue was washed with EtOAc (2 X 20 mL) to provide 2.75 g (71%) of product. ^1H NMR (CDCl_3 , 400 MHz) δ 8.01 (dd, $J = 8.4, 1.2$ Hz, 2H), 7.79 (d, $J = 8.0$ Hz, 2H), 7.66-7.60 (m, 3H), 7.50 (t, $J = 8.0$ Hz, 2H), 5.20 (s, 2H), 3.57-3.53 (m, 2H), 3.31 (s, 6H), 1.82 (brs, 2H), 1.34-1.28 (m, 6H), 0.89 (t, $J = 7.2$ Hz, 3H); ^{13}C NMR (CDCl_3 , 100 MHz) δ 189.2, 136.2, 135.5, 134.0, 133.9, 131.2, 128.8, 128.4, 127.5, 66.7, 64.1, 49.7, 31.3, 25.9, 22.9, 22.4, 13.8.

3.4.3.2 Synthesis of 1-(4-mercaptophenyl)-*N,N*-dimethyl-*N*-hexylmethanaminium bromide (3)

The quaternary ammonium salt **20** (2.75 g, 6.3 mmol) was mixed with 6 mL of 48% HBr and 30 mL of water. The mixture was then refluxed for 35 h. The contents were cooled to room temperature. The mixture was then extracted with EtOAc (2 X 30 mL). The aqueous layer was then lyophilized. The resulting residue was then repeatedly dissolved in water (10 mL) and lyophilized to provide 2.03 g of QAS thiol **3** as a white solid, 97% yield. ^1H NMR (CD_3OD , 400 MHz) δ 7.42 (s, 4H), 4.49 (s, 2H), 3.33-3.29 (m, 2H), 3.01 (s, 6H), 1.87 (brs, 2H), 1.39-1.37 (m, 6H), 0.96-0.92 (m, 3H); ^{13}C NMR (CD_3OD , 100 MHz) δ 138.2, 134.6, 129.9, 125.3, 68.4, 65.8, 50.3, 32.4, 27.1, 23.6, 23.5, 14.3.

3.4.4 Synthesis of octyl QAS thiol

3.4.4.1 Synthesis of 1-(4-(benzoylthio)phenyl)-*N,N*-dimethyl-*N*-octylmethanaminium bromide (22)

Benzyl bromide **14** (2.73 g, 8.88 mmol) and *N,N*-dimethyloctylamine (**21**) (1.83 mL, 8.88 mmol) were dissolved in 9 mL of ethanol and stirred for 17 h at

room temperature. The solvent was removed in *vacuo*. The residue was washed with EtOAc (2 X 10 mL) to remove unreacted starting materials and provide 3.91 g (95%) of product. ^1H NMR (CDCl_3 , 400 MHz) δ 7.99 (d, J = 7.6 Hz, 2H), 7.79 (d, J = 8.4 Hz, 2H), 7.65-7.57 (m, 3H), 7.49 (t, J = 8.0 Hz, 2H), 5.23 (s, 2H), 3.57-3.53 (m, 2H), 3.31 (s, 6H), 1.81 (brs, 2H), 1.35-1.24 (m, 10H), 0.87 (t, J = 6.8 Hz, 3H); ^{13}C NMR (CDCl_3 , 100 MHz) δ 189.1, 136.2, 135.5, 134.0, 133.9, 131.2, 128.8, 128.4, 127.5, 66.7, 64.1, 49.7, 31.6, 29.2, 29.0, 26.3, 22.9, 22.5, 14.0.

3.4.4.2 Synthesis of 1-(4-mercaptophenyl)-*N,N*-dimethyl-*N*-octylmethanaminium bromide (4)

The quaternary ammonium salt **22** (3.24 g, 6.97 mmol) was mixed with 7.2 mL of 48% HBr and 37.5 mL of water. The mixture was then refluxed for 35 h. The contents were cooled to room temperature. The mixture was then transferred to a separatory funnel and extracted successively with EtOAc (3 X 40 mL). The EtOAc layers were then back extracted with 20 mL of H_2O . The combined aqueous layers were then lyophilized. Lyophilization was repeated several times by dissolving the residue in 10 mL of water each time. The QAS thiol (**4**) was obtained as a white solid producing 1.86 g, 74% yield. ^1H NMR (CD_3OD , 400 MHz) δ 7.42 (s, 4H), 4.49 (s, 2H), 3.33-3.28 (m, 2H), 3.01 (s, 6H), 1.87 (brs, 2H), 1.40-1.32 (m, 10H), 0.93-0.89 (m, 3H); ^{13}C NMR (CD_3OD , 100 MHz) δ 138.2, 134.6, 129.9, 125.3, 68.4, 65.8, 50.3, 32.9, 30.22, 30.21, 27.4, 23.7, 23.6, 14.4.

3.4.5 Synthesis of 4-mercaptobenzene sulfonic acid (9)

3.4.5.1 Preparation of sodium-4,4'-dithiobis(benzenesulfonate) (26)⁹⁹

p-Aminobenzenesulfonic acid (**23**) (47.5 g, 0.250 mol) and anhydrous Na₃CO₃ (13.25 g, 0.130 mol) were dissolved in water (500 mL) by warming. The solution was then cooled to 15°C. A solution of sodium nitrite (5 M) was prepared by adding NaNO₂ (18.5 g, 0.250 mol) in water (50 mL) and added to the solution above. The mixture was then slowly added to a mixture of conc HCl (52.5 mL, 0.640 mol) and 300 g of crushed ice. A suspension of diazo compound **25** was formed and then stirred for 15 min in an ice bath.

Sodium sulfide nonahydrate (65.2 g, 0.270 mol) and powdered sulfur (8.50 g, 0.270 mol) were dissolved in water (75 mL) by heating on a hot plate at 100°C. Then a 10% NaOH solution (10.0 g NaOH in 100 mL H₂O) was added and the mixture was cooled to 0°C in an ice bath. Sodium disulfide was formed. The diazo solution was added to the disulfide solution over a period of 30 min, along with 50 g of ice to maintain the temperature below 5°C. After the addition was completed, the vessel was removed from the ice bath and allowed to come to room temperature. Once the evolution of nitrogen gas ceased, which took 2 h, the reaction mixture was acidified to pH 2 with conc HCl. The precipitated sulfur was removed by filtration and the filtrate was heated to remove hydrogen sulfide. The heating was continued until the volume reached ca. 500 mL. The solution was then cooled to room temperature and neutralized with 10% NaOH. The volume was concentrated to 400 mL. The precipitate was filtered off and the filtrate was kept overnight to provide crystallized sodium-4,4'-

dithiobis(benzenesulfonate) (**26**). The crystallized product was separated by filtration and recrystallized from 80% ethanol (650 mL) to provide 21.73 g of **26**, yield 42%. ^1H NMR (D_2O , 400 MHz) δ 7.73 (d, $J = 8.0$ Hz, 4H), 7.64 (d, $J = 8.4$ Hz, 4H)

3.4.5.2 Synthesis of 4-mercaptobenzene sulfonic acid (**9**)⁹⁹

Sodium-4,4'-dithiobis(benzenesulfonate) (**26**) (4.22 g, 10 mmol) was dissolved in water and subjected to ion-exchange column chromatography (20 mL of Dowex 50WX2-200 mesh, H-form) with water as eluent. The eluted acidic fractions (150 mL) were evaporated to 35 mL and freeze dried to provide sulfonic acid disulfide (**10**). The residue was dissolved in methanol (100 mL), and then triphenylphosphine (6.1 g, 23.3 mmol) and 2 mL of water were added. The mixture was stirred overnight at room temperature. The solution was then evaporated under reduced pressure. The residue was dissolved in CH_2Cl_2 (60 mL) and extracted twice with water (100 mL then 50 mL). The aqueous layers were combined and washed with CH_2Cl_2 (4 X 50 mL). The aqueous layer was then freeze dried and the residue was recrystallized from benzene to give 1.56 g of 4-mercaptobenzenesulfonic acid (**9**) as pale yellow crystals, yield 83%. ^1H NMR (D_2O , 400 MHz) δ 7.62 (d, $J = 8.0$ Hz, 2H), 7.39 (d, $J = 8.4$ Hz, 2H)

3.5 Conclusion

We have developed and implemented efficient methods to successfully synthesize thiols **2-4** and their corresponding disulfides **6-8**. The difficult step was the reaction of β -mercaptoethanol with benzyl bromide **14**. During the preparation

of thiol **2**, three products were formed which needed to be separated carefully using silica gel column chromatography. In addition, the thiols needed to be kept in the cold to prevent air oxidation, as this can occur easily if the thiols are dissolved in water and left at room temperature. The successful preparation of these thiols and disulfides will provide new opportunities for folding disulfide containing proteins.

CHAPTER 4

Dramatic increase in the folding rate of Bovine Pancreatic Trypsin Inhibitor (BPTI) with the buffer composed of positively charged aromatic thiol and its corresponding disulfide.

4.1 Abstract

Many of the most important pharmaceuticals on the market today are proteins. A significant fraction of these proteins are produced in *E. coli* and need to be oxidatively folded *in vitro* to obtain active protein, as they contain disulfide bonds. The drawbacks of traditional oxidative protein folding *in vitro* are that it is slow and low yielding, due to protein precipitation. *In vitro* oxidative protein folding traditionally involves the use of a small molecule aliphatic thiol and disulfide, such as glutathione (GSH) and glutathione disulfide (GSSG), as a redox buffer to produce the active form of the protein. To improve oxidative protein folding, small molecule thiols and disulfides were proposed that mimic the nucleophilic low pKa thiol of protein disulfide isomerase (PDI) to fold proteins. PDI catalyzes the folding of disulfide containing proteins in the endoplasmic reticulum (ER) of eukaryotic cells. I demonstrated that aromatic thiols with positively charged groups improved the folding rate of a reduced protein relative to GSH/GSSG. The folding of BPTI was followed by reverse phase HPLC of samples obtained by quenching folding reactions at specific times with formic acid. More than 90% of native protein was obtained in an hour instead of the two days taken with GSH and GSSG.

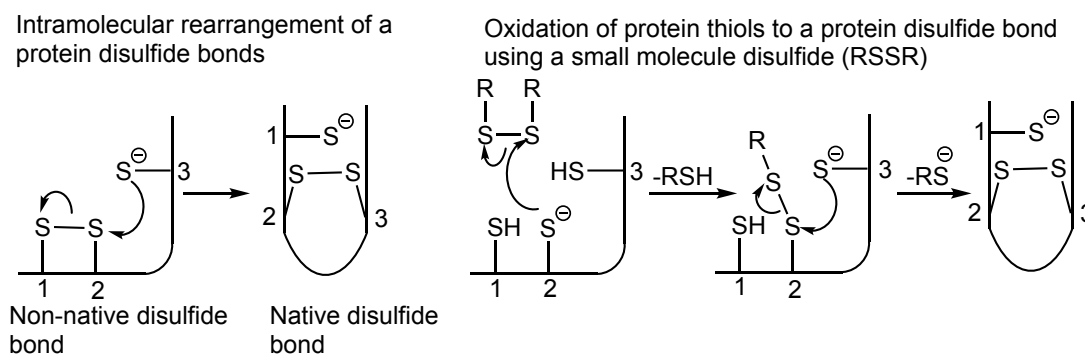
4.2 Introduction

Disulfide bonds play a vital role in stabilizing the biologically active form of numerous extracellular proteins and almost all pharmaceutically relevant proteins. Many of these proteins can be produced efficiently in bacteria; however, the proteins often aggregate as inactive inclusion bodies inside the cells. The advantage of expression of a protein in inclusion bodies is that they can be produced in large amounts, are easy to separate and are protected from proteolytic degradation.⁸ Formation of inclusion bodies may also be the best method of protein production if the protein of interest is toxic to the bacteria or host cell. To produce active protein, the protein within the inclusion bodies is re-solubilized and then oxidized *in vitro*. The disadvantage of the formation of inclusion bodies is the need to refold the aggregated protein *in vitro*. Oxidative *in vitro* protein folding involves conformational folding combined with oxidation of protein thiols to native disulfide bonds. Formation of native disulfide bonds involves reduction of protein disulfides to thiols and rearrangement of non-native disulfide bonds to native disulfide bonds (Scheme 4.1).³¹ The reaction is highly important as it is also responsible during the enzymatic formation and breaking of disulfide bonds in proteins.¹⁰¹

Bovine pancreatic trypsin inhibitor (BPTI) with 58 amino acid residues is one of the smallest globular proteins known, and its sole function is to bind to and inhibit serine proteases such as trypsin. For example, BPTI can inhibit trypsin-like West Nile virus (WNV) NS2B-NS3 protease.¹⁰² Trypsin inhibitors usually have conserved cysteine residues that participate in forming disulfide bonds (Figure

1.10). Bovine pancreatic trypsin inhibitor (BPTI) has α -helical and β -sheet regions as well as three disulfide bonds between Cys5 - Cys55, Cys14 - Cys38 and Cys30 - Cys51, which stabilize the protein's tertiary structure.⁵² Three disulfide bonds in 58 residues make BPTI one of the most stable proteins known. When all three disulfide bonds of BPTI are reduced at room temperature, the protein unfolds. Upon oxidation under suitable conditions, native BPTI with its unique set of three disulfide bonds is formed.

Scheme 4.1. Intra- and intermolecular formation of disulfide bonds³¹



The folding pathway for BPTI is shown in the sketch (Figure 1.14), which is based on previous studies of BPTI folding using GSH/ GSSG. N' and N* are two disulfide-containing stable intermediates. N'(SG) and N*(SG) are singly mixed disulfide-containing intermediates formed when N' and N* react with glutathione disulfide, respectively. The intermediate N'(SG)₂ is a doubly mixed disulfide formed when the free thiol of N'(SG) reacts with GSSG. N^{SH} is a rearrangement product of N' and N* which undergoes oxidation to native protein.

In vitro protein folding can be aided by the addition of protein disulfide isomerase (PDI), which is found in the endoplasmic reticulum (ER) and catalyzes *in vivo* protein folding via a series of thiol-disulfide interchange reactions.³¹ The

use of PDI for *in vitro* protein folding is not efficient due its high cost of production, low catalytic activity and instability.³⁴ However, *in vivo* in the ER, the concentration of PDI is high. The design of small molecule thiols and disulfides that improve protein folding is based on PDI. PDI is composed of two active sites each consists of a CXXC motif required for its oxidoreductase activity where C is a cysteine residue and X is any other amino acid.^{31,49,103} In each active site, one cysteine thiol is exposed to solvent and other is buried in the hydrophobic core of PDI. The solvent exposed thiol in PDI can attack a substrate disulfide bond resulting in the formation of a mixed disulfide bond. The mixed disulfide bond can be attacked by another thiol to form a new disulfide bond with the release of PDI (Figure 4.1). The solvent exposed thiol has a low pKa value (6.7) and at neutral pH is very reactive with disulfides as compared to small molecule aliphatic thiols.⁴⁸ Therefore, the synthesis of small molecule thiols with thiol pKa values similar to that of the solvent exposed thiol in PDI is likely to increase the rate of *in vitro* folding of disulfide-containing proteins.

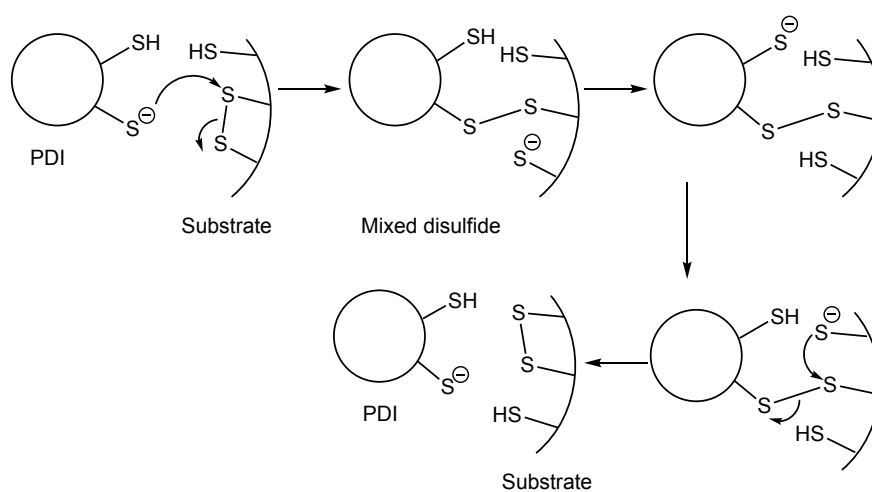


Figure 4.1. Mechanism of PDI.

A redox buffer is composed of a small molecule disulfide and its corresponding thiol in variable concentrations. During protein folding, the small molecule disulfide oxidizes protein thiols to protein disulfides and the small molecule thiol rearranges non-native protein disulfide bonds to native disulfide bonds.⁴⁹ Both processes are completed via thiol-disulfide interchange reactions between the protein and the small molecules. There are several different factors that make aromatic disulfides/thiols better redox buffer than aliphatic disulfides/thiols. Different types of aromatic thiols with corresponding disulfides are utilized to prepare a redox buffer. The thiol pKa values of aromatic thiols range from 4-7 which is close to pKa value of the solvent exposed thiol of PDI. Aromatic thiols with either electron releasing or electron withdrawing substituents at the *para* position are utilized. In addition, aromatic thiols show enhanced nucleophilicity at neutral pH and are better leaving group than aliphatic thiols. If the *para* substituent is charged, then the aromatic thiol should have improved water solubility.

Historically, aliphatic thiols/disulfides such as GSH, GSSG and oxidized dithiothreitol (DTT^{ox}) were used for the oxidative folding of proteins. *In vivo*, GSH and GSSG reduce protein disulfides and oxidize cysteine thiols to disulfides respectively.⁹³ Aliphatic thiols such as GSH, DDT^{red}, β -mercaptoethanol, (\pm) trans-1, and 2-bis(mercaptoacetamido)cyclohexane (BMC) have thiol pKa values higher than 7.¹⁰⁴ In comparison, aromatic thiols have a range of pKa values from 4 to 7 and are more reactive towards disulfides than aliphatic thiols with comparable pKa values. Therefore, the thiol pKa value and enhanced reactivity

of aromatic thiols mimic the properties of PDI.^{49,95} Therefore, selective synthesis of small molecule aromatic thiols with nearly the same thiol pKa as that of the free thiol of PDI, which are soluble in water in both the thiol and disulfide forms, should enhance the reactivity of these small molecule aromatic thiols at pH 7 relative to the traditionally used aliphatic thiol such as glutathione.

Herein, I describe the dramatic increase in folding rate of reduced BPTI with a redox buffer composed of an aromatic thiol and its corresponding disulfide relative to the traditional folding buffer GSH/GSSG. Out of three aromatic thiols investigated, quaternary ammonium salt thiol and its corresponding disulfide was the best for folding reduced BPTI in comparison with GSH/GSSG where BPTI is folded to 90% native protein in 48 h with 5 mM GSH and 5 mM GSSG.⁴² The folding intermediates that accumulated during folding with aromatic thiols and their corresponding disulfides were not the same as those observed with GSH/GSSG (N' and N*).

4.3 Results

Three different *p*-substituted aromatic thiols **27**, **9**, **1** and their corresponding disulfides **28**, **10**, **5** were chosen for the preparation of redox buffers to fold reduced BPTI^{50,97–99,105} (Figure **4.2**). These thiols and disulfides were selected as the pKa values of the thiols are charged at neutral pH to similar to the pKa value of solvent exposed thiol of PDI (6.7).¹⁰⁶ These compounds enhance water solubility. Both positively and negatively charged thiols were selected to examine the effect of charge on protein folding at physiological pH.

The protein folding experiments with aromatic thiols and their corresponding disulfides were performed at pH 7.3 using 30 μM of reduced BPTI.¹⁰⁷ Variable concentrations of disulfides and thiols were used for the preparation of the redox buffer along with 0.20 M KCl, 0.10 M bis-tris-propane, and 1 mM EDTA. The folding experiment was run at 25°C under argon.^{107,108} The reactions were quenched with formic acid at six different time points by removing 300 μL aliquots from the reaction mixture at each time point.¹⁰⁷ Each aliquot was analyzed by reverse phase HPLC.⁹³ A pH of 7.3 was selected to mimic physiological conditions of protein folding and to compare the results with previously reported work.^{67,93,109} The curve of percentage native protein formed versus refolding time was plotted for every experiment performed and compared to other conditions. The highest percentage of native protein formed in the shortest time without observed protein precipitation was considered the best condition. Finally, the result was compared to the optimal conditions of the traditional folding buffer GSSG/GSH (5 mM/5 mM).⁴²

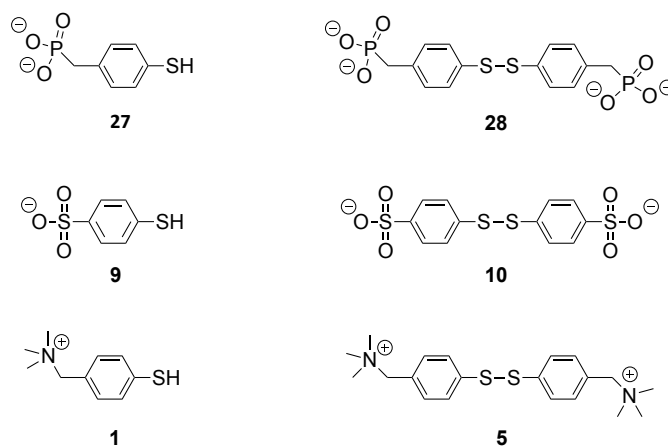


Figure 4.2. Different aromatic thiols and their corresponding disulfides. **27:** phosphonic acid thiol (PA); **28:** phosphonic acid disulfide; **9:** sulfonic acid thiol

(SA); **10**: sulfonic acid disulfide; **1**: quaternary ammonium salt thiol (QAS); **5**: quaternary ammonium salt disulfide.^{50,97–99,105}

4.3.1 Folding with negatively charged aromatic thiols and their corresponding disulfides

Two different negatively charged aromatic thiols, phosphonic acid thiol (PA) **27** and sulfonic acid thiol (SA) **9**, were selected to study the folding of reduced BPTI. Thiol **27** has two negative charges and thiol **9** has one negative charge. Initially, reaction mixtures were prepared by adding selected concentrations of thiol **27** and its disulfide **28** to the folding mixture containing reduced BPTI and bis-tris-propane buffer at pH 7.3. Two different concentrations of disulfide **28** were chosen, 0.09 and 0.25 mM. The folding experiment was first done using 0.09 mM disulfide **28** and 1 mM thiol **27**. Protein precipitation was observed almost immediately after protein folding started, as the solution became cloudy. The precipitation was worse with higher concentrations of thiols.

Next, the folding of reduced BPTI was investigated using aromatic thiol **9** and its disulfide **10**. For 0.09 mM disulfide **10** concentration, 1, 2, 5, and 10 mM thiol **9** were investigated and for 0.25 mM concentration of disulfide **10**, 1, 2, 5, and 10 mM thiol **9** were investigated. A reaction mixture containing 0.25 mM of disulfide **10** in combination with 1 mM of the thiol **9** folded BPTI to 82% while a reaction mixture with 2 mM thiol achieved 91% in 6 h. With 5 mM and 10 mM thiol **9**, more than 90% native protein was obtained within an hour. With thiol **9** and 0.25 mM disulfide **10**, all combinations of redox buffer precipitated protein. The concentration of disulfide **10** was reduced and used 0.125 mM to see if

protein precipitation was reduced. No precipitation was with 2 mM thiol **9** and folding was almost complete in 8 h forming 95% native BPTI. While with 5 mM thiol **9**, 92% of native BPTI was formed in 4 h; however, protein precipitation was observed at about 6 h. The 1 mM thiol was not used as folding was slower with 2 mM thiol and also the 10 mM thiol was not used as protein was precipitated with 5 mM thiol. The concentration of the disulfide **10** was further reduced to 0.09 mM and used it in combination with 1, 2, 5, and 10 mM thiol **9**. With 5 and 10 mM thiol **9** (Figure 4.3). The folding yield was higher with higher concentration of thiols and folding was faster too.

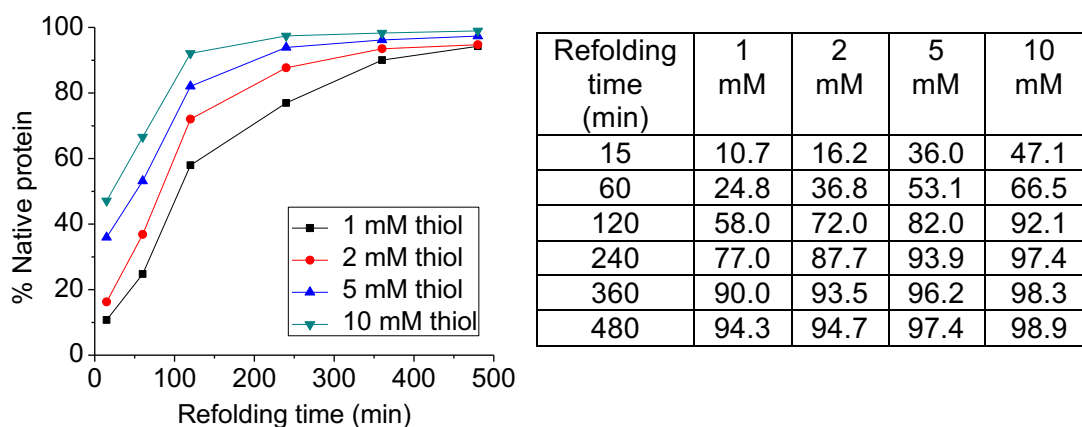


Figure 4.3. Folding of reduced BPTI with 0.09 mM disulfide **10** and different concentrations of thiol **9**.

The protein area obtained from the analysis is shown in Figure 4.4 which showed that 0.09 mM of disulfide **10** with all concentrations of thiol **9**, areas of total protein is lower than the expected. However, 0.09 mM of disulfide **10** and 1 mM of thiol **9**, area of protein is very close to expected value, as there is no observed protein precipitation. Therefore, 0.09/1 mM disulfide/thiol combination is the best condition for these sets of experiments. The overall conclusion from

these folding experiments using negatively charged aromatic thiols and their corresponding disulfides was that the protein precipitates. Therefore, to fold basic proteins like BPTI faster and to obtain higher yield at shorter time, these thiols should not be considered.

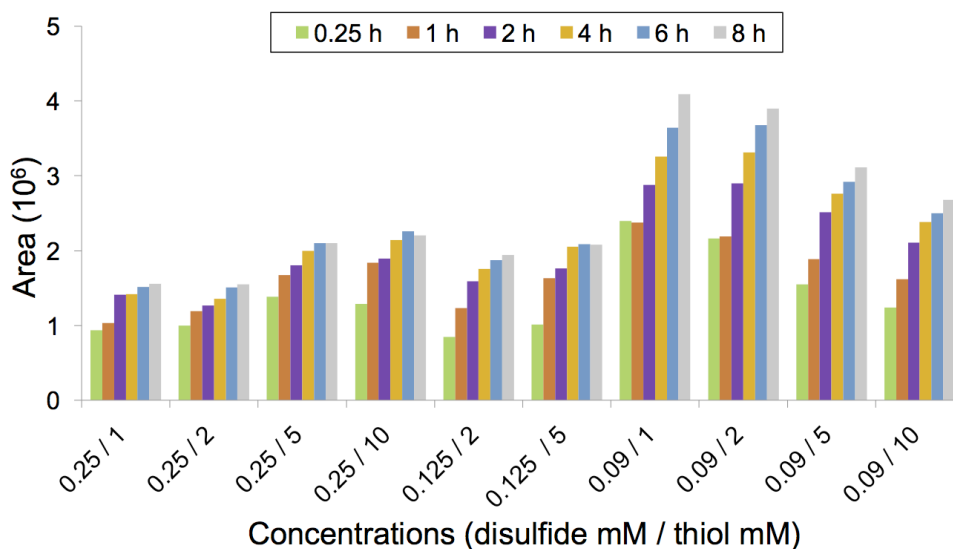
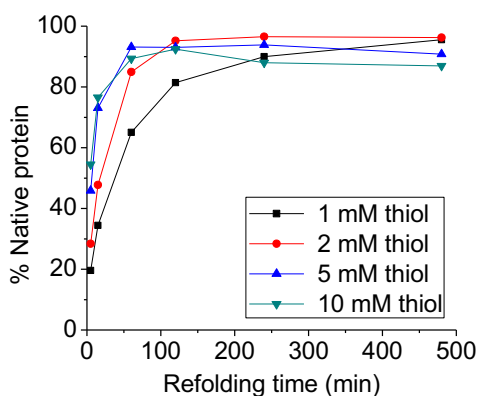


Figure 4.4. Total area of protein in different folding conditions with thiol **9** and disulfide **10**.

4.3.2 Folding with positively charged aromatic thiol **1** and its corresponding disulfide **5**

It was proposed that a positively charged small molecule thiol would increase the net positive charge in the mixed disulfide or between the positively charged protein and small molecule and thus increase solubility. With negatively charged small molecules, the net charge of the mixed disulfide between the small molecule and positively charged protein is decreased. For this purpose, quaternary ammonium salt (QAS) thiol **1** and its disulfide **5** were used. Two

different disulfide concentrations, 0.09 mM and 0.25 mM, were first selected to optimize the condition. Eight different conditions of folding buffer were prepared using 0.09 and 0.25 mM disulfide **5** concentrations with 1, 2, 5, and 10 mM thiol **1**. The results are shown in the following Figures **4.5** and **4.6**. With 1 mM thiol **1**, 90% folded protein was observed in 4 h. With 2 mM thiol **1**, 95% folded protein was observed in 2 h. With 5 mM and 10 mM thiol **1**, folding resulted in more than 90% native protein in 1 h. In all these conditions, protein precipitation was not observed. Comparing these conditions, 0.25 mM of disulfide **5** with 5 and 10 mM of thiol **1** were our best conditions for folding reduced BPTI. In these experiments, the drawbacks of folding with QAS were the decrease of native protein percentage with higher thiol concentrations (Figures **4.5** and **4.6**) and the increase in total protein area (Figure **4.7**) with higher time points. Adventitious oxidation of thiol **1** was observed to be a problem at longer time points (Figure **4.8**). I hypothesized that this was the reason for the described drawbacks. Therefore, thiol oxidation needs to be controlled for better results.



Refolding time (min)	1 mM	2 mM	5 mM	10 mM
5	19.6	28.4	45.9	54.5
15	34.4	47.7	73.0	76.5
60	65.0	84.9	93.1	89.3
120	81.4	95.2	93.0	92.4
240	90.0	96.6	93.8	88.0
480	95.6	96.2	90.7	86.9

Figure 4.5. Folding of reduced BPTI with 0.09 mM disulfide **5** and different concentrations of thiol **1**.

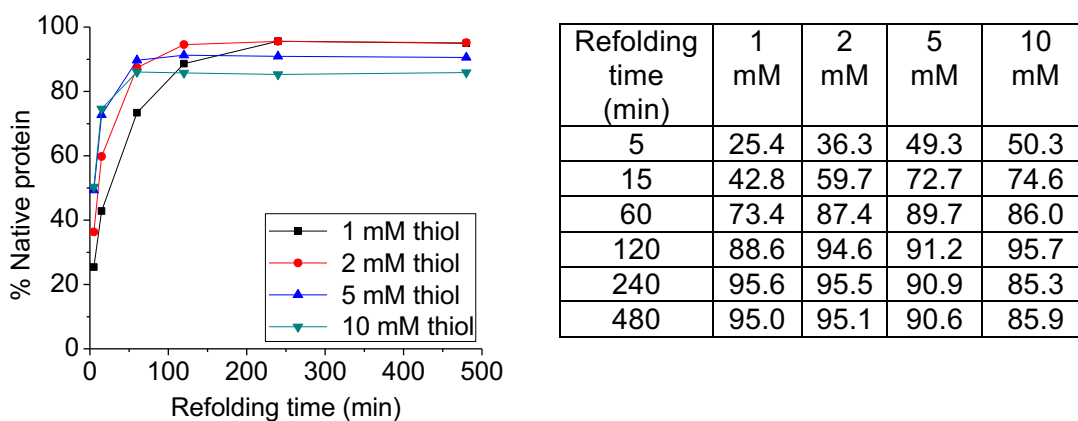


Figure 4.6. Folding of reduced BPTI with 0.25 mM disulfide **5** and different concentrations of thiol **1**.

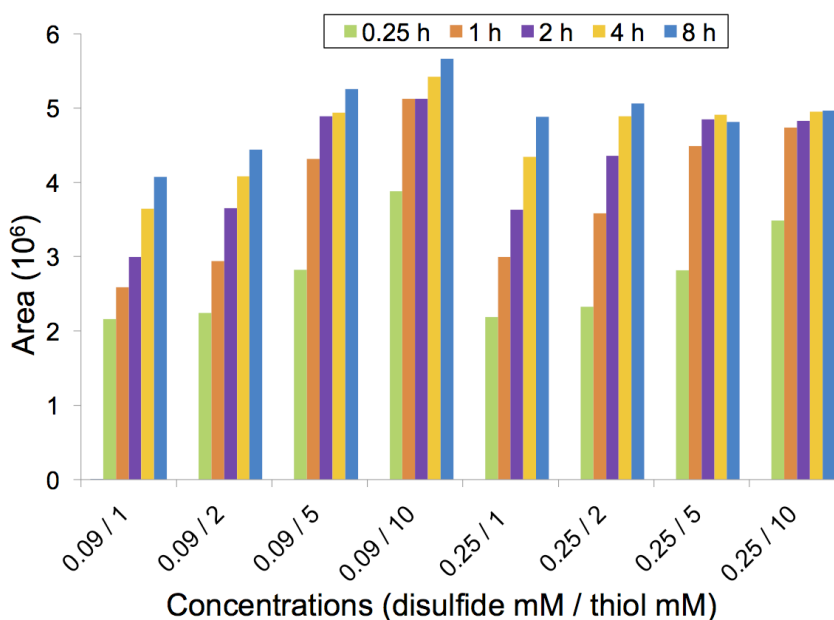


Figure 4.7. Total area of protein in different folding conditions with thiol **1** and disulfide **5**.

Two intermediates were seen during the analysis with retention times of 38 min and 42 min, the amount of these intermediates decreased with the refolding time (Figures **4.9** and **4.10**). These intermediates are promising for the determination of rate constants in the future.

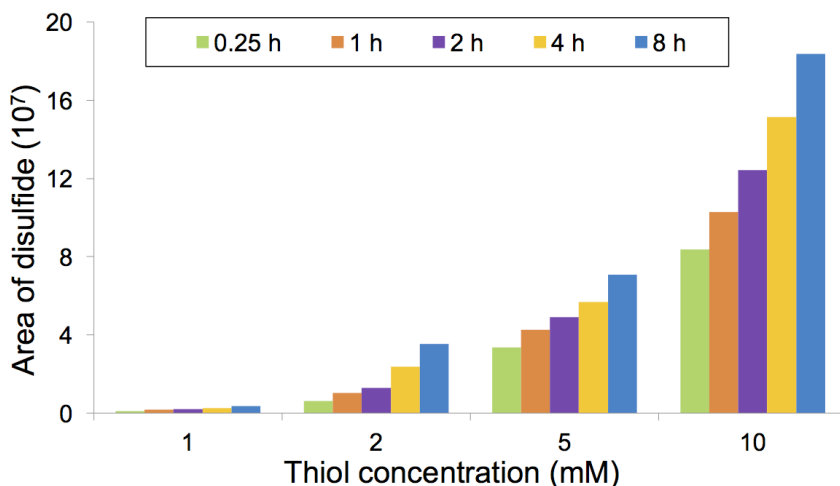


Figure 4.8. Oxidation of thiol **1** in different folding conditions with thiol **1** and disulfide **5**.

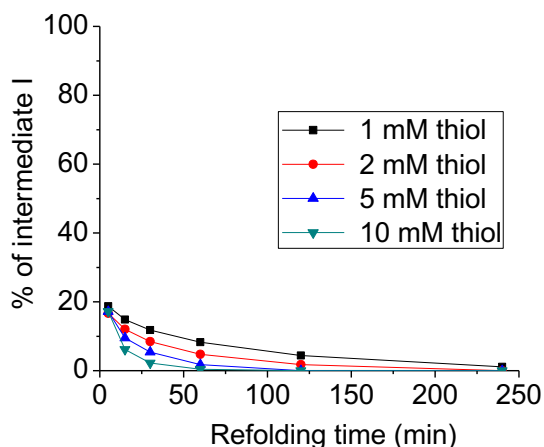


Figure 4.9. Prominent intermediate during folding of reduced BPTI with 0.25 mM disulfide **5** and thiol **1** at 38 min.

Different experiments were performed to minimize the oxidation of thiol **1** and to achieve a consistent protein area over different time points. When the reaction without protein was run, the oxidation of thiol **1** was observed, indicating poor quenching. The reaction with 5 mM thiol **1** only was also run and quenched with different concentrations of different acids and observed that 80 μL HCOOH was the best to quench the 300 μL reaction mixture (Figure 4.11).

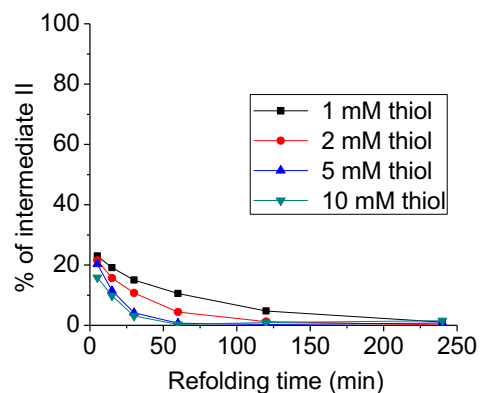


Figure 4.10. Prominent intermediate during folding of reduced BPTI with 0.25 mM disulfide **5** and thiol **1** at 42 min.

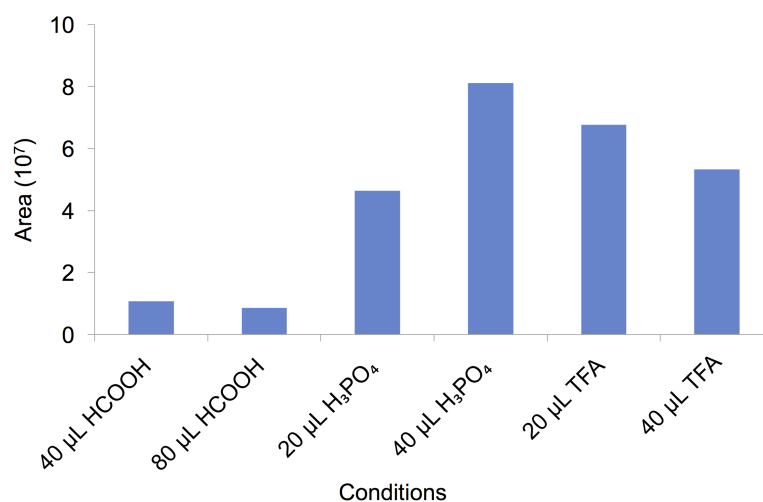
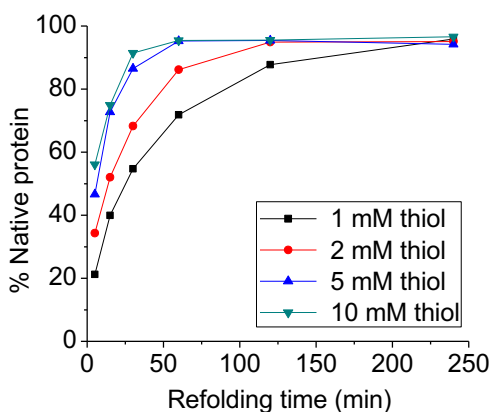


Figure 4.11. Different quenching conditions.

The experiments were performed by mixing protein, thiol, disulfide, water and buffer in different ways and found that mixing all components of folding mixture in an argon environment reduced thiol oxidation dramatically. The QAS reaction (0.25 mM disulfide **5** and different concentrations of thiol **1**) was repeated again with 4 h as the last time point. All solutions were bubbled with argon before mixing and mixing itself was done with argon gas bubbling. The result is summarized in graphical form (Figure **4.12**).



Refolding time (min)	1 mM	2 mM	5 mM	10 mM
5	21.2	34.3	46.6	56.0
15	40.0	52.0	72.7	74.9
30	54.7	68.2	86.5	91.4
60	71.8	86.1	95.2	95.4
120	87.8	94.9	95.4	95.5
240	95.9	95.1	94.1	96.6

Figure 4.12. Folding of reduced BPTI with 0.25 mM disulfide **5** and different concentrations of thiol **1**.

Although the thiol oxidation was diminished, it was still observed that the total protein area was going up with higher time points. I proposed that the waiting time before the injection in HPLC was causing the increase in the total area of protein. Therefore, reactions were quenched at 5 min utilizing three different methods: analyzed by immediate injection, injection after few hours storing in ice bath, and inject next day storing at -20°C . It was found that total protein area in all samples had a close range of total area (Figure 4.13). In the previous experiments, where samples waited in the HPLC auto sampler for a long time before injection, the total protein area increased. However, the storage time for these samples were too long due to longer analysis time of HPLC which took 110 min for one sample. To minimize the storage time, the HPLC analysis time was decreased to 40 min by changing the HPLC gradient to 90% solvent A in 0 min and 60% solvent A in 40 min. Aliquots after quenching were stored at 4°C before being injected into the HPLC. With the new program, the maximum waiting time was 2 h.

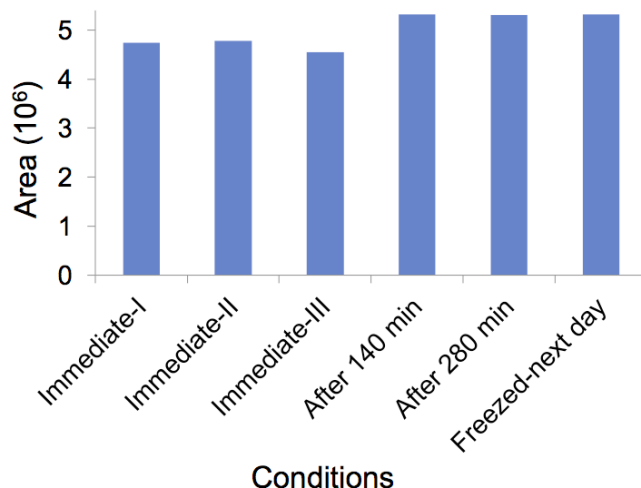


Figure 4.13. Analysis of total protein area with different storage methods.

Then, folding reactions were run containing 0.25 mM disulfide **5** and 1, 2, 5, and 10 mM thiol **1** concentrations to see the effect. It was observed that total protein area was consistent and almost no thiol oxidation was observed (Figure **4.14**). It was also observed that the native protein percentage was not going down with higher time points. It was concluded that the decrease in native protein percentage was because of the increase in total protein area with longer time points. The problem of decreasing native protein percentage was solved through the series of experiments. It was observed that reduced BPTI folds to more than 90% native BPTI within an hour (Figure **4.15**). Likewise, there was no protein precipitation with any concentrations of thiol **1** and disulfide **5**. The observation showed that the protein's total area was close to the area of native protein. It was concluded is that 0.25 mM disulfide **5** and 10 mM thiol **1** give the best results.

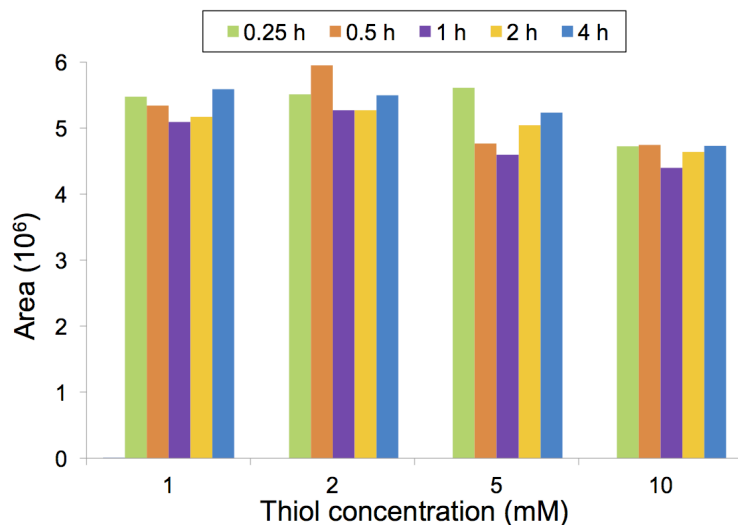


Figure 4.14. Total protein area in new HPLC method.

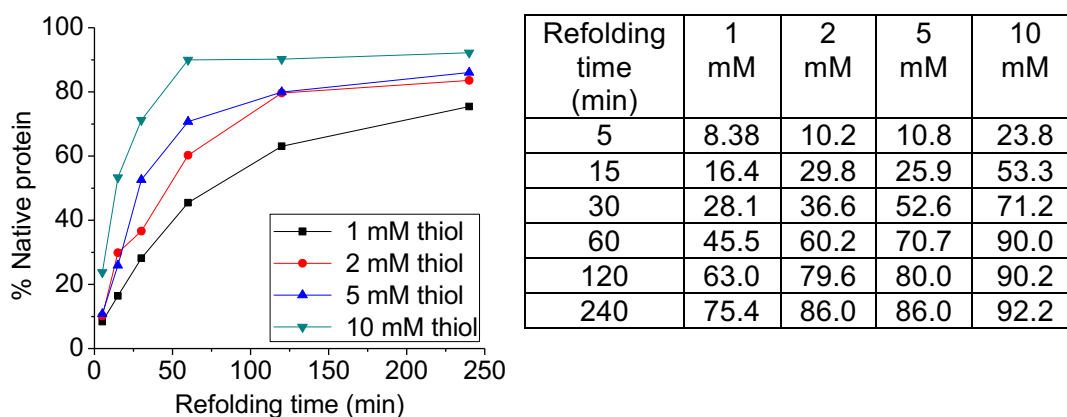


Figure 4.15. Folding of reduced BPTI with 0.25 mM disulfide **5** and different concentrations of thiol **1**.

The problem associated with new HPLC method was that the intermediate peaks were not well resolved. This did not cause any problem for the overall results because the focus was only on the folding yield of protein (Figures 4.16, 4.17, 4.18, and 4.19).

Then 10 mM thiol **1** was used and changed the disulfide **5** concentrations from 0.25 mM to 1 mM and 5 mM to see the effect. With 1 mM disulfide **5**, the

result was very close to 0.25 mM, but with 5 mM disulfide concentration, the result was worse (Figure 4.20).

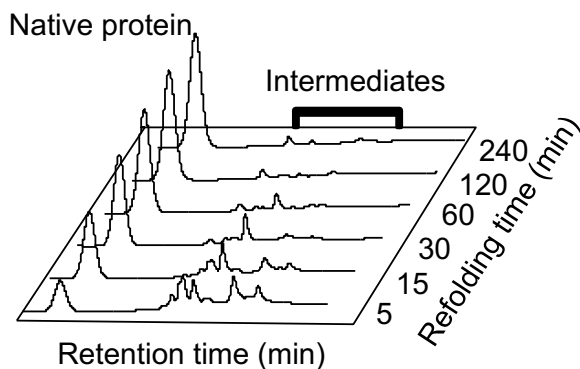


Figure 4.16. Chromatogram showing native protein and intermediates with 0.25 mM disulfide **5** and 10 mM thiol **1**.

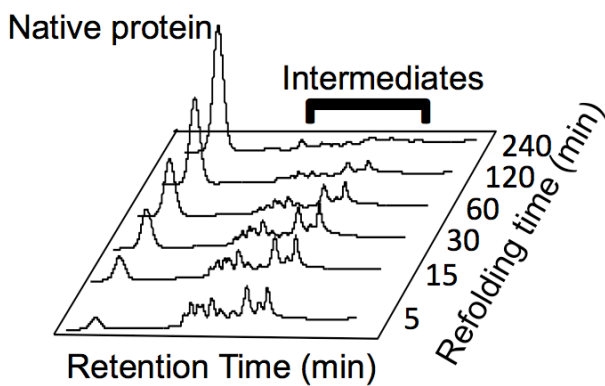


Figure 4.17. Chromatogram showing native protein and intermediates with 0.25 mM disulfide **5** and 1 mM thiol **1**.

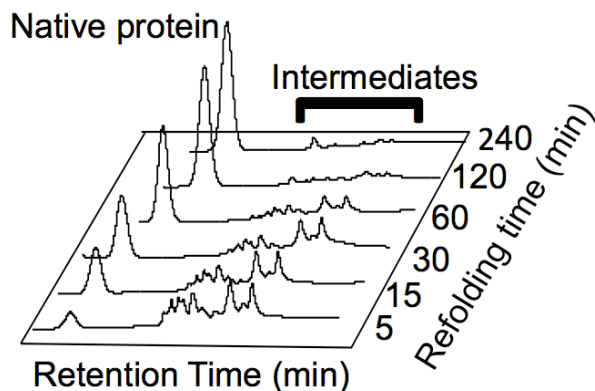


Figure 4.18. Chromatogram showing native protein and intermediates with 0.25 mM disulfide **5** and 2 mM thiol **1**.

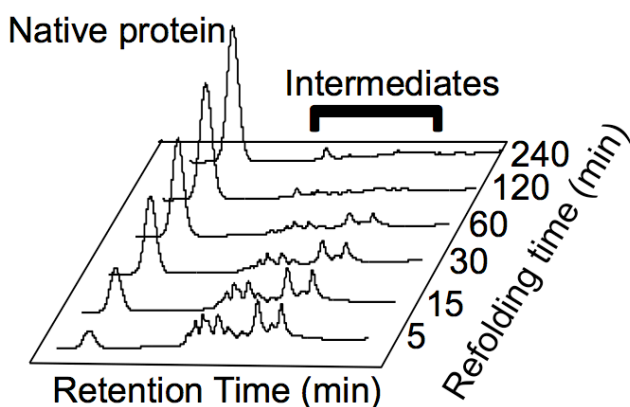


Figure 4.19. Chromatogram showing native protein and intermediates with 0.25 mM disulfide **5** and 5 mM thiol **1**.

Then the folding of BPTI was compared using QAS with that of GSSG/GSH. The results indicated that QAS is better than GSSG/GSH for folding reduced BPTI in terms of time and yield (Figure 4.21).

From the folding results with reduced BPTI and positively charged aromatic thiol, QAS, and its corresponding disulfide, it was found that 0.25 mM QAS disulfide with 5 and 10 mM of its thiol as a redox buffer were the best conditions for BPTI folding. In this condition, BPTI can fold within 1 h to over 90%. Therefore, the method improved significantly over the traditional method of

BPTI folding using GSSG/GSH, which needed 48 h to fold to 90%. To conclude, with the thiols that have negatively charged para-substituents, protein precipitation was observed resulting in the loss of protein. In addition, protein folding was slower than QAS.

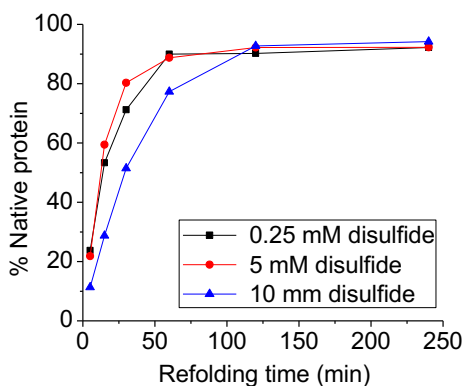


Figure 4.20. Folding of reduced BPTI with 10 mM thiol **1** and different concentrations of disulfide **5**.

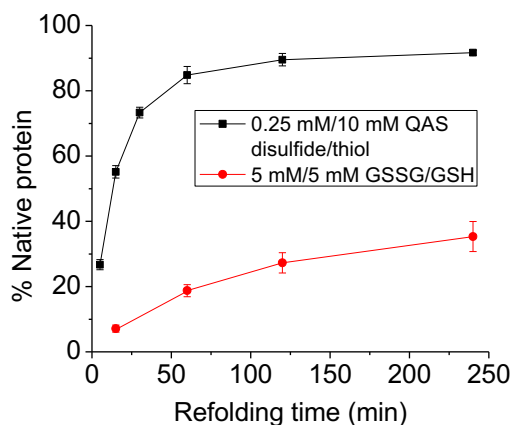


Figure 4.21. Comparison of folding of reduced BPTI with our optimal condition (10 mM thiol **1** and 0.25 mM disulfide **5**) with optimal condition of traditional buffer (5 mM GSH and 5 mM GSSG).

4.4 Discussion

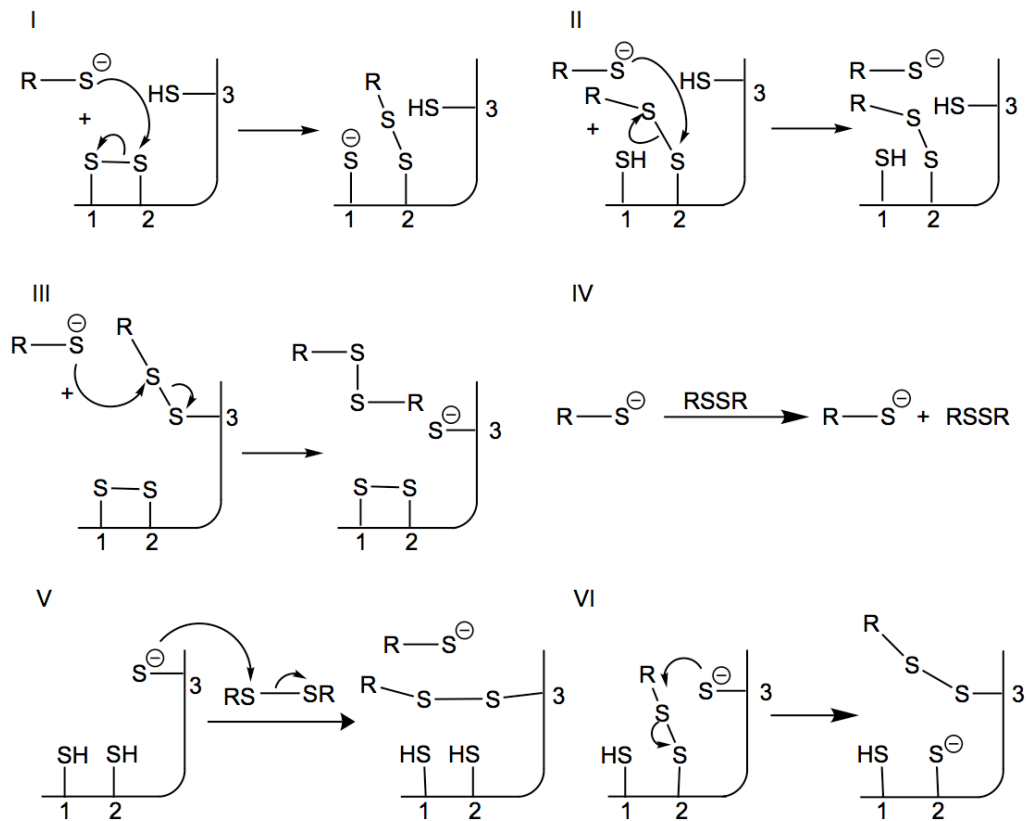
Our hypothesis was that a redox buffer composed of aromatic thiol and the corresponding disulfide would fold protein faster than a redox buffer

composed of aliphatic thiol and the corresponding disulfide. To demonstrate the dramatic increase in the folding rate of reduced BPTI with a redox buffer composed of aromatic thiols and corresponding disulfides, three different aromatic thiols and corresponding disulfides were selected. The pKa of these thiols, their structure, and pH of the solution were considered for the selection. Aromatic thiols have good nucleophilic character, and are better leaving groups than glutathione at physiological pH.^{94,110} Thiolates of aromatic thiols **27**, **9**, and **1**; and glutathione thiolate have approximately equal nucleophilic character, but at physiological pH, large proportions of glutathione (pKa = 8.7) is in its inactive thiol form while large proportions of aromatic thiols **27**, **9**, and **1** (pKa = 5.5-5.7) are in their thiolate form.⁴⁸ Previous work showed that at neutral pH, the observed rate constant of the reaction with aromatic thiol is 6 times faster than glutathione, a small molecule aliphatic thiol, and its disulfide.⁴⁹ Therefore, at pH 7.3, thiolates of thiols **27**, **9**, and **1** are expected to react faster than glutathione. The leaving group ability of any thiol is inversely proportional to its pKa values.^{48,94} Hence, thiolates of **27**, **9**, and **1** are better leaving groups than glutathione as their pKa values are lower.

During *in vitro* protein folding with a redox buffer containing small molecule aromatic thiols and disulfides, there are eight possible mechanisms of thiol-disulfide interchange reactions, six of them are shown in scheme **4.2** where **I-IV** involves small molecules as a nucleophile and **III-VI** involve the small molecules as a central thiol.^{38,49} The thiolate from an aromatic thiol can attack a protein disulfide (reaction **I**), a small molecule disulfide (reaction **IV**), or a mixed disulfide

between the small molecule and protein (reaction **II** and **III**). In reactions, **I-IV**, these thiolates act as a nucleophile whereas in reactions, **III-VI**, the small molecule thiols act as a central thiol. In reaction **V**, the aromatic thiol acts as both a leaving group and a central thiol. Reactions **I, III, V, and VI** show a net change in protein disulfide bonds. Therefore, aromatic thiols are expected to involve in rate limiting steps in reactions **I, III, V** and **VI**. The rate constants for these reactions are expected to be greater than with glutathione.

Scheme 4.2 Reactions of aromatic thiol as a nucleophile and/or central thiol in a redox buffer



Reduced BPTI was folded using redox buffers composed of one of three different aromatic thiols, QAS, PA, or SA and its corresponding disulfide. It was determined that the redox buffer composed of the positively charged aromatic

thiol, QAS thiol, and its disulfide could fold reduced BPTI faster and more efficiently than redox buffers composed of negatively charged SA thiol/disulfide or PA thiol/disulfide. The decrease in the folding yield of native BPTI from reduced BPTI with a redox buffer composed of **27** and **28** or **9** and **10** was proposed to be due to the decrease in net positive charge of unfolded BPTI as these negatively charged small molecules form mixed disulfides with reduced BPTI and decrease the net positive charge of BPTI (Figure 4.22). The result is the formation of aggregation. Therefore, to increase in the folding yield of BPTI, a decrease in aggregation is required.¹¹¹

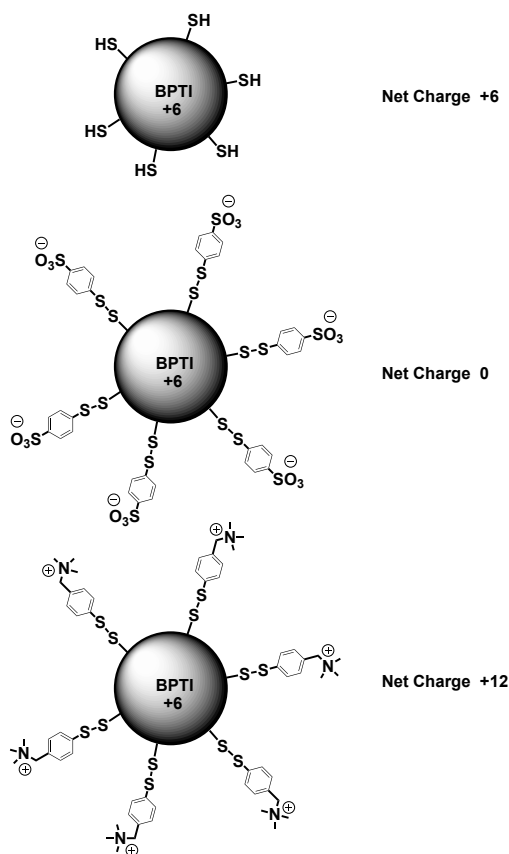


Figure 4.22. Effect of negatively and positively charged thiols on net charge of BPTI.

Positively charged quaternary ammonium thiol **1** and its disulfide **5** were used to prepare a redox buffer. The use of a positively charged thiol and disulfide will result in an increase in the net positive charge of reduced BPTI so that folding goes smoothly and rapidly. The results obtained from the folding of reduced BPTI using QAS thiol **1** and its disulfide **5** at pH 7.3 proved that a redox buffer composed of an aromatic thiol and corresponding disulfide increases the rate of folding dramatically relative to glutathione at their optimal conditions. Also, positively charged thiols and disulfides are better for BPTI folding. It is also noteworthy that thiols with lower pKa values undergo the thiol disulfide interchange reactions faster hence increasing the rate of formation of native protein at their optimal concentration. At higher thiol/disulfide concentrations, the folding rate of BPTI decreases.

To conclude, folding of reduced BPTI increased dramatically in the presence of a redox buffer composed of positively charged aromatic thiol QAS and its corresponding disulfide as compared to traditional redox buffer composed of glutathione/glutathione disulfide. The folding with QAS thiol and its disulfide took about an hour to fold reduced BPTI to 90% while glutathione/glutathione took about 48 h to fold reduced BPTI to 90%. The optimal condition of QAS thiol was 10 mM and disulfide was 0.25 mM at pH 7.3. Use of thiols/disulfides with negatively and positively charged groups allowed us to understand their effect on protein precipitation. For BPTI, use of positively charged thiols/disulfides with pKa close to that of free thiol of PDI helps to fold BPTI rapidly in high yield.

4.5 Experimental section

4.5.1 Materials

The protein used for the folding study, BPTI, was purchased from Roche Applied Science under the trade name Aprotinin and was used to prepare reduced BPTI directly. Trizma base, guanidinium chloride (GdnHCl), bis-tris propane, EDTA, potassium chloride (KCl), dithiothreitol (DTT), GSH, and GSSG were purchased from Sigma-Aldrich. SephadexTM G-25 Fine was purchased from GE Healthcare and made wet for 24 h with 0.01 N HCl before packing the chromatographic column. Trifluoroacetic acid (TFA) and acetonitrile (ACN) were HPLC grade and were purchased from Fischer Scientific. Concentrated hydrochloric acid was also purchased from Fischer scientific. Nanopure deionized water was prepared using a Branstead D3750 and was deoxygenated by bubbling argon for 30 min through it before using in each experiment. Aromatic thiols **27**, **9**, and **1** and their corresponding disulfides **28**, **10**, and **5** were prepared as described previously. The UV-Vis spectra were measured using a Cary 300 spectrophotometer. The HPLC analysis was performed on a Hitachi D-7000 system, which was connected with a L-7400 UV-Vis detector and a column oven. The pH measurements were done using a VWR symphony SB20 pH meter which was calibrated before its use. BPTI was lyophilized using a Labconco FreeZone 2.5 L Benchtop freeze dryer. The columns used for reverse phase HPLC (RP-HPLC) were an Alltech Macrosphere C18 preparative column (250 × 22 mm); a Vydac C18 semi-preparative column (250 × 10 mm); and a Vydac C18 analytical column (250 × 4.6 mm).

4.5.2 Preparation of reduced BPTI

Reduced BPTI was prepared from Aprotinin in Trizma buffer using reducing agents. The Trizma buffer was prepared by dissolving Trizma base, KCl and EDTA in deionized water. The pH of the buffer was adjusted to 8.7 using concentrated HCl. The solution was prepared on a 100 mL scale by maintaining the final concentration of Trizma as 0.01 M, KCl 0.20 M, and EDTA 1.0 mM. The reduction mixture was prepared in a 15 mL centrifuge tube using Trizma buffer in which GdnHCl and DTT were added. The volume of 10 mL was prepared by maintaining the final concentration of GdnHCl 6 M and DTT 0.05 M. The solution was equilibrated in 25°C water bath before its application. Aprotinin was added to the reduction mixture at a concentration of 6.5 mg/mL. The resulting mixture was kept at 25°C in a water bath for 1 h to reduce BPTI followed by the addition of 0.2 N HCl to adjust the pH between 2-3 and quench the reduction. The reduced BPTI was then purified by gel filtration on a sephadex G-25 ccolumn using 0.01 N HCl as the mobile phase. The fractions were analyzed by a UV-Vis spectrophotometer at 280 nm. The fractions that contain reduced BPTI were combined and then lyophilized before further purification by HPLC. The dried reduced BPTI was then dissolved in 0.01 N HCl and purified by RP-HPLC on a C18 preparative column. The mobile phase used was a mixture of solvent A (0.1% TFA in water) and solvent B (90% acetonitrile with 0.1% TFA in water). The elution gradient used was 0 min, 90% solvent A; 20 min, 65% solvent A; 100 min, 61% solvent A; 120 min, 50% solvent A with a flow rate of 5 mL/min. The fractions containing reduced BPTI were identified by absorbance at 280 nm. The

fractions were then further analyzed using a Vydac C18 analytical column by monitoring the absorbance at 229 nm. The flow rate of 1 mL/min was used with the elution gradient of 0 min, 90% solvent A; 15 min, 73% solvent A; 35 min, 71% solvent A; 50 min, 69% solvent A; 70 min, 65% solvent A. The pure reduced BPTI was then lyophilized and dissolved in 0.01 N HCl to prepare a stock solution of concentration 1 mg/mL. The stock solution was stored in -20°C before use.

4.5.3 Oxidative folding of reduced BPTI

To start a folding reaction, 1.5X folding buffer was first prepared. In 80 mL deionized water, 4.234 g of bis-tris propane, 2.236 g of potassium chloride (KCl), and 0.0558 g of EDTA were dissolved and the pH was adjusted to 7.3 with concentrated HCl. Then, deionized water was added until the volume was 100 mL in a volumetric flask. The buffer was deoxygenated by passing argon gas through it for 30 min. The thiols and their corresponding disulfides were purified using a Vydac C18 semi-preparative HPLC column heated to 50°C before using them in a folding buffer. Injection of samples was done manually, 2 mL at a time, and a flow rate of 3 mL/min was utilized. The gradient used was 0 min, 90% solvent A; 15 min, 75% solvent A; 35 min, 73% solvent A; 50 min, 72% solvent A; 100 min, 65% solvent A. The absorbance was monitored at 252 nm. Pure fractions of thiols and disulfides were collected, lyophilized, dissolved in deoxygenated buffer, and kept at -20°C before use. The final folding buffer for the reaction contains 0.10 M bis-tris propane, 0.20 M KCl, 1.0 mM EDTA, and indicated concentration of aromatic thiols and their corresponding disulfides.

Folding reactions were conducted under argon at 25°C. At each specific time, a 300 μ L aliquot was removed and quenched by the addition of formic acid. Initially 20 μ L formic acid was used but it was found from experiments done to improve folding efficiency that 80 μ L formic acid quenched better than 20 μ L, therefore, I used 80 μ L in later experiments. Each aliquot was analyzed by RP-HPLC on a Vydac C18 analytical column. A flow rate of 1 mL/min was used. For the traditional HPLC analysis method, linear gradient was used: 0 min, 90% solvent A; 15 min, 75% solvent A; 35 min, 73% solvent A; 50 min, 72% solvent A; 110 min, 70% solvent A. The absorbance was monitored at 229 nm and the column temperature was maintained at 50°C. All peak areas were summed and the total area was assigned a value of 100%. An improved HPLC analysis method was developed for the faster analysis of samples. The flow rate was 1 mL/min and elution gradient used was 0 min, 90% solvent A; 40 min 60% solvent A.

4.6 Conclusion

Folding of reduced BPTI was investigated using both negatively and positively charged aromatic thiols/disulfides. With the redox buffer composed of negatively charged thiols, phosphonic acid thiol and sulfonic acid thiol, and their corresponding disulfides BPTI was precipitated during folding. Therefore, the conclusion was that the negatively charged aromatic thiols and their corresponding disulfides are potentially poor folding agents for basic proteins. With the positively charged thiol, QAS, and its disulfide as the redox buffer, reduced BPTI was folded without precipitation and reached 90% native form within an hour. The area of native protein and total protein area were consistent

with no protein precipitation. The percentage of native protein in 1 h time point was highest with 10 mM thiol, and 0.25 mM QAS disulfide.

CHAPTER 5

Targeted Molecular Dynamics (TMD) simulation study for conformational folding from the [5-55] like conformation to the native conformation of BPTI

5.1 Abstract

Oxidative folding of extracellular proteins includes conformational folding and disulfide bond formation which are coupled to each other during the folding process until the formation of the native protein structure. Therefore, conformational changes of these secreted proteins during folding play an important role in the formation of native disulfide bond and to complete the folding process. Targeted molecular dynamics (TMD) was used to study the conformational changes and the formation of disulfide bonds in bovine pancreatic trypsin inhibitor (BPTI) as a model protein containing disulfide bonds. The initial structure was constructed with Cys5 and Cys55 close enough to form a disulfide bond but all other cysteines are far apart and not close enough to form disulfide bonds. The TMD simulations were carried out in two different ways and investigated the conformational changes during the simulation. The folding process and the formation of the native protein was studied using visual analysis, evolution of secondary structure, disulfide bond formation, RMSD calculation, radius of gyration, and hydrogen-bond formation. With the initial simulation, targeting all atoms of the initial structure, it was found that conformational changes played an important role in the formation of the disulfide bonds as seen for the decrease in distance of Cys14-Cys38 which was not observed until the last stage of the TMD. The formation of the kinetic traps N' and N* were not

observed during our initial simulations. The final native conformation was obtained once the correct antiparallel β -sheets and subsequent Cys14-Cys38 distance came closer to form disulfide bond. In the second simulation, targeting only alpha carbons and sulfur of cysteines of the starting structure to the final structure, formation of native protein was achieved via the formation of N* followed by N^{SH}. The Cys14-Cys38 distance was decreased to a value close to S-S distance value and observed increased many times until the final native structure was formed.

5.2 Introduction

Folding studies of disulfide containing proteins are significant because of the diseases associated with misfolded proteins containing disulfide bonds.¹¹² Experimentally, folding studies are performed by quenching the folding reaction at various stages and studying the formation of disulfide bonds.^{19,86} The conformational changes of these intermediates are difficult to determine with experimental procedures alone.¹¹³ Therefore, highly standardized computational methods are required to complement the experiments and understand the formation of disulfide bonds and protein folding.^{85,114}

Molecular Dynamics (MD) computational simulation is a valuable tool for investigating conformational changes of macromolecules because it can give atomic level details of conformational changes.¹¹⁵ Examples of TMD simulations used to study conformation changes include the conformational changes during the opening and closing of GroEL to unravel its ATP binding mechanism¹¹⁶, transition from open form to closed form of ion channels to understand their

function as a ion transport such as KcsA potassium ion channels^{117,118}, and structural changes of the C-terminal domain (CTD) from α -form to β -form of RfaH.¹¹⁹ Targeted molecular dynamics (TMD) is a robust simulation tool used to examine the process of transition from one conformation to another at normal temperature, reducing the distance continuously to the target confirmation by applying time dependent geometrical constraint.¹²⁰ During TMD, the root mean square distance (RMSD), which is a measure of physical distance between two structures, to the target is continuously reduced; the system forces initial state to find the path to final state; and the Cartesian distances between the conformations describes the progress of reaction.¹²¹ The RMSD between the current coordinates and the target structure is computed in every time step by aligning the target to the current coordinates. Reasons of calculating RMSD are to find out the time point when conformation changes and to define the folding procedure. The following equation is used to calculate the force on each atom.

$$U_{TMD} = [\frac{k}{2N}[rmsd(t)-RMSD(t)]^2] \dots \dots \dots (1)$$

where, $rmsd(t)$ is the instantaneous best-fit RMSD of the coordinates of simulated initial structure from the coordinates of targeted structure, and $RMSD(t)$ is the linear distance from initial RMSD at the first TMD step to the final RMSD at the last TMD step.⁸⁹ The symbol k is the spring constant which is scaled down by the number N of the targeted atoms.

Herein, the formation of disulfide bonded like intermediates along with the conformational changes was studied using bovine pancreatic trypsin inhibitor (BPTI) as a model protein, which contains 58 residues with three disulfide bonds.

Experimental work by Creighton⁸⁶ on the renaturation of reduced BPTI showed that the non-native single-disulfide like intermediates were formed closing Cys5 and Cys30, Cys30 and Cys55, and Cys5 and Cys51 in 1/4th of the total isolable intermediates. Later, Weissman and Kim reexamined the folding of the reduced BPTI⁶⁵ using improvised techniques such as acid quenching (quenching technique) and reverse phase high-performance liquid chromatography (HPLC) (separation technique) and found that only the native-like disulfide bonds were present in the isolated intermediates. Simulation study using a lattice model⁸⁵ and theoretical study using proximity rule¹²² showed that non-native type disulfide bonds were formed transiently. However, only the intermediates with native type disulfide bonds were formed during the later stages of folding.

Targeted MD was used to study to see the effect of conformational changes in disulfide bond formation starting with the [5-55] like intermediate of BPTI, which is challenging to perform experimentally. The crystal structure of native BPTI was obtained from the protein data bank (PDB ID: 4PTI). The conformation was modified with pymol¹²³ so that only the Cys5-Cys55 distance was close enough to form bond and all the other native Cys-Cys were far apart. Some important structural criteria (proximity and orientation of cysteine residues) of folding required by disulfide containing proteins were considered during the selection of the starting structure. Starting from the modified structure, TMD was performed, targeting the initial structure to the final native structure in explicit water. TMD was selected because it can provide important information on conformational changes and molecular motions that are hard to study in shorter

computational times.¹¹⁹ BPTI has been extensively used as a model system in many molecular dynamics simulation studies.^{80,124} However, to the best of our knowledge, our work represents the first investigation of the conformational changes in BPTI using TMD simulations. The conformational changes in BPTI during the folding was investigated and compared the results with previous MD simulations and experiments.

5.3 Methods

The x-ray structure of native BPTI was obtained from the crystal structure of BPTI in the protein data bank (PDB ID: 4PTI). The starting structure containing all cysteine residues but without the presence of actual disulfide bond in the structure was constructed. Cysteine 5 and 55 were close enough in the model to form disulfide bond. All atoms were used during simulation. The change in the conformation of [5-55] to native structure was first simulated in explicit solvent with CHARMM36 force fields.¹²⁵

5.3.1 Molecular dynamics (MD) setup for equilibration and TMD

The initial, [5-55] like structure for running TMD was prepared from the native structure obtained from the protein data bank (PDB ID: 4PTI). By manually adjusting some of the dihedral angles, we obtained an open form structure from the native structure which still retains the secondary structural elements. The resulting protein structure was solvated in the rectangular box of water molecules having minimum solute-wall distance of 10 Å with TIP3 water. The system was neutralized by adding chloride ions using Monte-Carlo ion placing method. I added 0.15 M KCl which generated 30 positive and 36 negative ions. CHARM-

GUI¹²⁶ web-server was used for solvation and preparation of the input files needed for simulations. The dimension of the simulation box was 80×80×80 Å³ with the total number of 34828 atoms in the system. Molecular dynamics (MD) simulations were performed with CHARM36¹²⁵ force field using NAMD.¹²⁷ The particle mesh Ewald method¹²⁸ was used to calculate long range interactions using a 12 Å nonbonded cutoff. The energy minimization was done for 20 ps. The temperature of the system was maintained at 303.15 K using Langevin dynamics with a damping coefficient of 1 ps⁻¹. The system was energy minimized for 20 ps and equilibrated for 180 ps with NPT run using 2 fs integration time step. The RATTLE and SETTLE algorithms were used to restrain protein bonds, and to maintain water geometry respectively. A 1 ns production run was performed, followed by a TMD run for 15 ns. A biasing force of force constant per atom of $k_{atom} = \frac{k}{N} = 0.589 \text{ kcal/ (mol Å}^2\text{)}$ was used for the TMD simulation.

5.4 Results and discussion

The native structure of BPTI has two α -helix, two β -strand, and three disulfide bonds as shown in Figure 5.1. The first α -helix (H1 in the figure 5.1) has one and a half turns from Asp3 to Leu6 and is close to the N terminus. The second α -helix (H2 in the figure) has three turns from Ala48 to Gly56 and is close to the C terminus. The first β -strand (B1 in the figure) lies from Ile18 to Asn24 and second β -strand (B2 in figure) lies from Leu29 to Tyr35. These two β -strands are anti-parallel to each other. Three disulfide bonds (5-55), (14-38), and (30-51) make the tertiary structure of BPTI stable by linking the secondary structures. The maximum dimension of native BPTI is 30 Å.⁵⁹

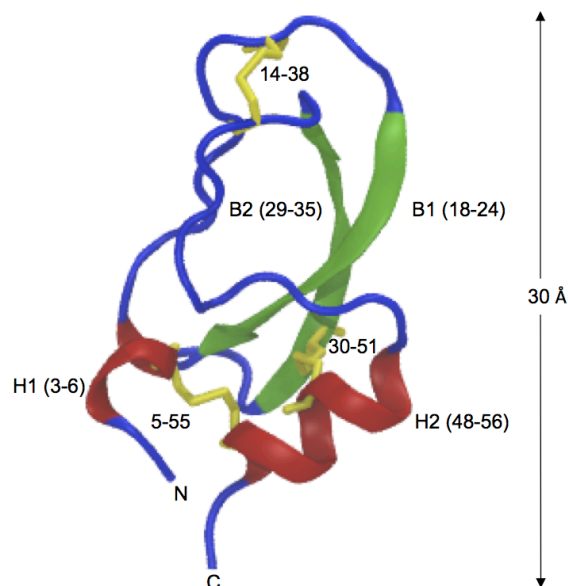


Figure 5.1 Native structure of BPTI showing α -helices (in red), β -strands (in green), disulfide bonds (in yellow), and loops and turns (in blue).^{59,88} The crystal structure is taken from protein data bank (PDB ID: 4PTI).

The topology of BPTI looks like a piece of string folded twice by itself as shown in Figure 5.2. This simplified structure indicates that the (5-55) disulfide bond joins the two terminal α -helices, the (14-38) disulfide bond joins the two β -strands near the loose end of β -hairpins. The third disulfide bond (30-51) connects the three turn α -helix (H2) with the β -sheets; therefore, the compact native structure of BPTI is formed.

5.4.1 TMD using all atoms

5.4.1.1 Changes in structural configuration of BPTI during TMD

The [5-55] like initial structure is an open form BPTI which has the rmsd of 15 Å compared to the native structure. Targeted MD simulations of 5, 10, and 15 ns length were performed and each resulted in the conversion of the [5-55] like initial structure to the native structure of BPTI. The process of conversion of the

one disulfide intermediate [5-55] to N is shown in Figure 5.3, where snapshots taken at various stages of structural transformation demonstrate the protein's conformations at respective stages.

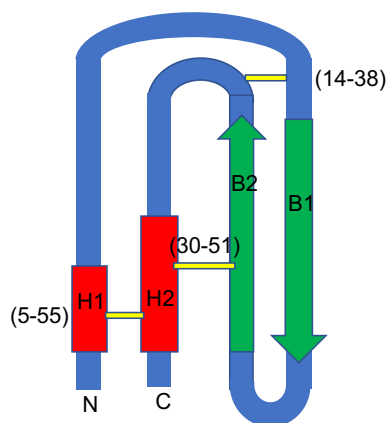


Figure 5.2 The secondary structure of BPTI with its three disulfide bonds.^{59,88}

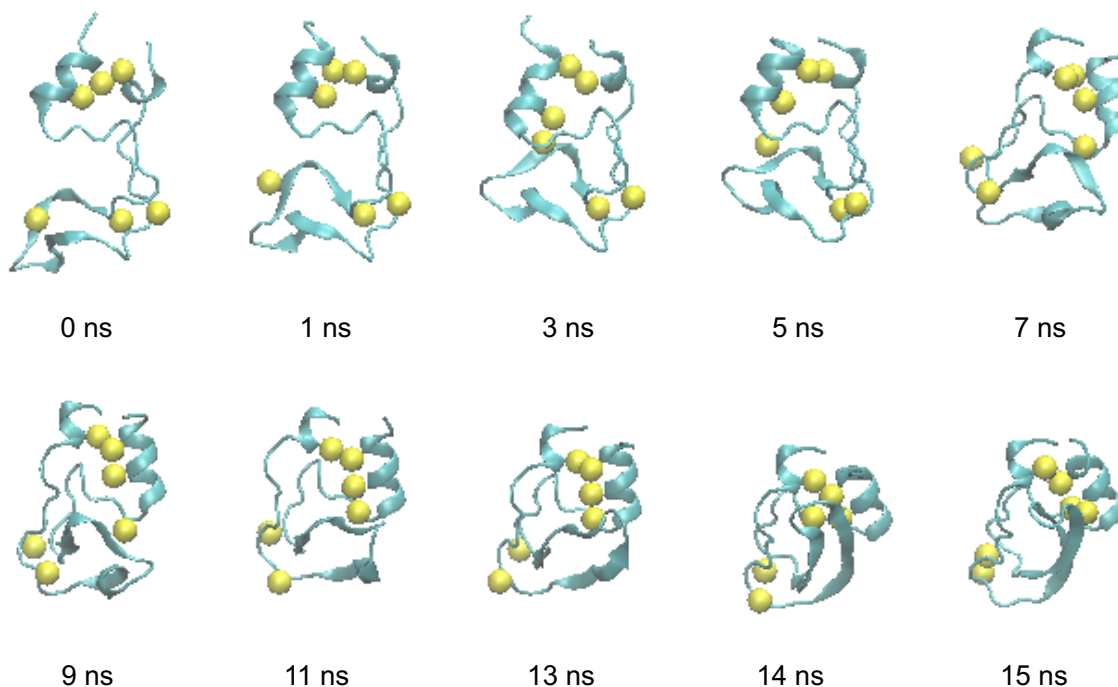


Figure 5.3 Snapshots of conformations formed at different stages of conformational changes during conformational folding of BPTI using TMD simulation. Sulfur atoms of cysteines are shown in yellow balls.

The graph of the evolution of the secondary structures as a function of time during the TMD simulation is shown below in Figure 5.4. We found that the residues 18-24 transforms from a coil/turn/loop-to a β -strand after 14 ns of simulation, which occurred after decreasing S-S distance of Cys30 and Cys51 to the value close to native bond. Similarly, for residues 28-36, and 44-46, in which turn/loop/coli-to- β -strand transitions were observed after decreasing S-S distance Cys30 and Cys51 close enough to form a bond (Figure 5.4). All other residues do not show secondary structure changes during the simulation.

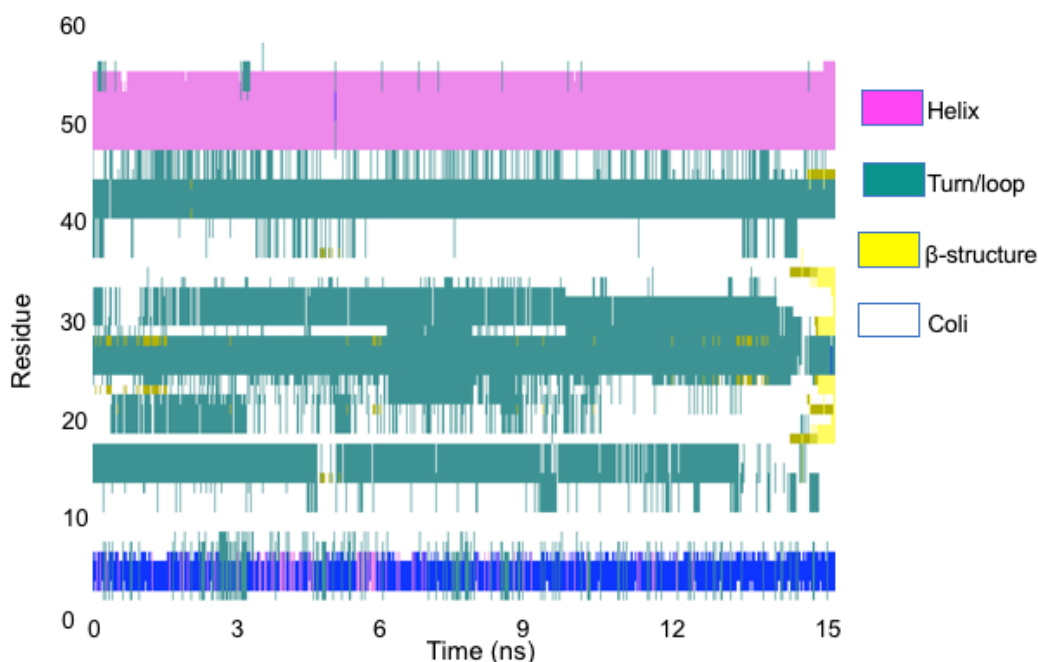


Figure 5.4 Evolution of secondary structure from TMD simulations of BPTI [(5-55) to N].

5.4.1.2 Distance between CYS residues of the native disulfide bonds

With the use of TMD, the conversion of a single disulfide containing intermediate, [5-55] to native BPTI, [5-55, 14-38, 30-51], was achieved on a 15

ns time scale. Within 2.5 ns, the Cys30-Cys51 distance was decreased to 5.3 Å with from 21.5 Å in the starting structure. On the other hand, the Cys5-Cys55 distance was increased to 11.3 Å within 2 ns from 3.73 Å in the starting structure. The Cys30-Cys51 distance was seen closing and then increasing multiple times before a compact structure of BPTI was obtained. Formation of compact native conformation was observed at the late stage of simulation. The Cys14-Cys38 distance was decreased close to real S-S bond distance after the formation of N^{SH} [5-55, 30-51] like conformation, which proved the experimental finding that N^{SH} rearranges rapidly to N (Figure 5.5).

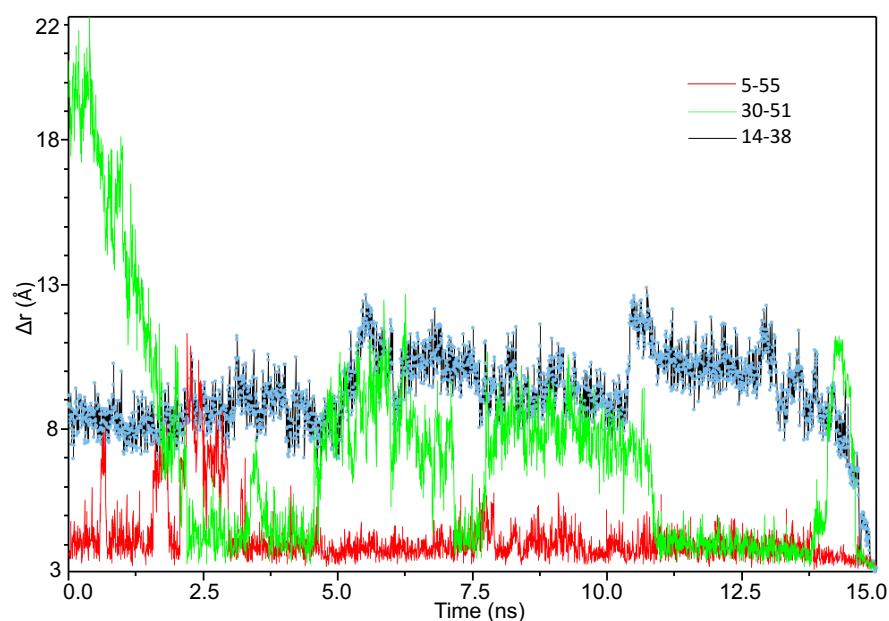


Figure 5.5 Distance between sulfur atoms in native disulfide bonds.

5.4.1.3 Root mean square deviation during TMD

The root mean square deviation (RMSD) was computed from the atomic trajectories for targeted MD run. The plot of the RMSD of all backbone and heavy

atoms in the TMD-simulated structure relative to the corresponding target structure is shown in Figure 5.6. The result showed that all backbone atoms and heavy atoms used in our TMD simulations reached the target structure within 15 ns (with the accuracy of 1 Å). The initial RMSD of 8.7 Å at first trajectory continuously decreased to 1.12 Å at 3000th trajectory forming the native structure.

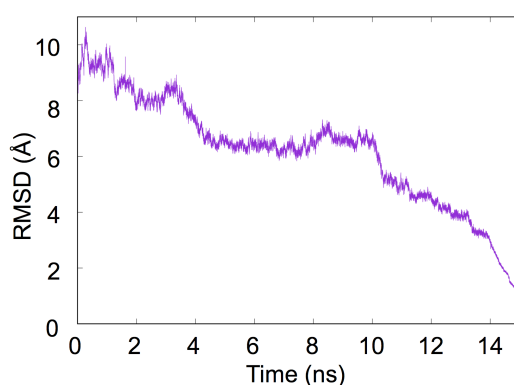


Figure 5.6 Change in RMSD during TMD of BPTI.

5.4.1.4 Analysis of intermediates with the change in radius of gyration

The relationship between the conformational changes and the folding was studied by taking and analyzing snapshots of folding trajectories as depicted in Figure 5.7. The initial structure, with Cys5 and Cys55 distance close enough to form bond, had a radius of gyration (R_g) of 14.1 Å, was targeted to native structure as targeted MD simulation was started, and observed that R_g was reduced to 11.4 Å. The β -sheets and α -helices were already present in the initial structure. The folding was proceeded by crumpling up of the β -strands and

subsequent ordering. The folding was proceeded with the rearrangement of starting structure to a non-native conformation [51-55] followed by formation of [5-51]. During the process, Cys5-Cys55 distance was decreased and then increased time and forth which promoted to decrease the distance between Cys30 and Cys51. The distance of Cys30 and Cys51 was also seen decreasing and then increasing many times rearranging to some non-native like intermediates and compacting the structure of protein. The Cys5-Cys55 distance was decreased to form bond followed by the decrease in Cys30-Cys51 distance which lead to the formation of conformation of N^{SH}. After the flipping of the Cys30 and Cys51 residues, correct antiparallel β -strands formation took place followed by rapid closeness of Cys14-Cys38 distance leading to the compact structure of BPTI was observed. The most interesting observation during our simulation was the absence of N' and N* which were key intermediates formed during oxidative folding of BPTI. Once the antiparallel β -strands were seen formed correctly during the late stage of the simulation (after the decrease in Cys30-Cys51 distance close to the bond real length), immediate decrease in the Cys14-Cys38 distance was observed that ultimately led to the native structure of BPTI. An important observation here is that the structure of N^{SH} is very close to the native form structure, and that Cys14-Cys38 distance is the last to come close enough to form a bond during the folding process of BPTI. The observations are consistent with experimental findings.

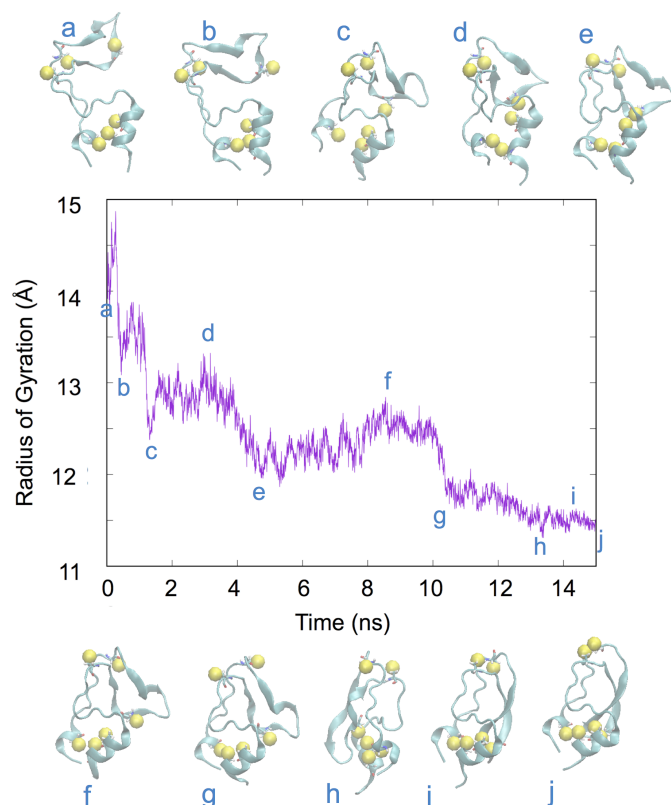


Figure 5.7 Folding trajectories demonstrating the BPTI folding pathway from [5-55] conformation to folded native state. The curve shows the decrease in the radius of gyration (R_g) with respect to folding time. Some of the conformations of trajectory (a-j) were shown to show how R_g decreases along with the progress of folding.

5.4.1.5 Analysis of the folding trajectories

In folding trajectory analysis, the complete unfolding of a conformation of single disulfide intermediate, [5-55], was found followed by the formation of single non-native intermediate [51-55]. Then, [51-55] was rearranged to another non-native like single disulfide intermediate [5-51]. The [5-51] intermediate was then rearranged to native single disulfide intermediate [30-51] which was found to be broken and formed several times. The decrease of Cys30-Cys51 distance for the last time flips one of the β -strand led the formation of native two-disulfide

intermediate N^{SH} . The N^{SH} was converted immediately to N due to the closeness of Cys14-Cys38 residues. Figure 5.8 demonstrates the transformation to target structure via the formation of different conformations.

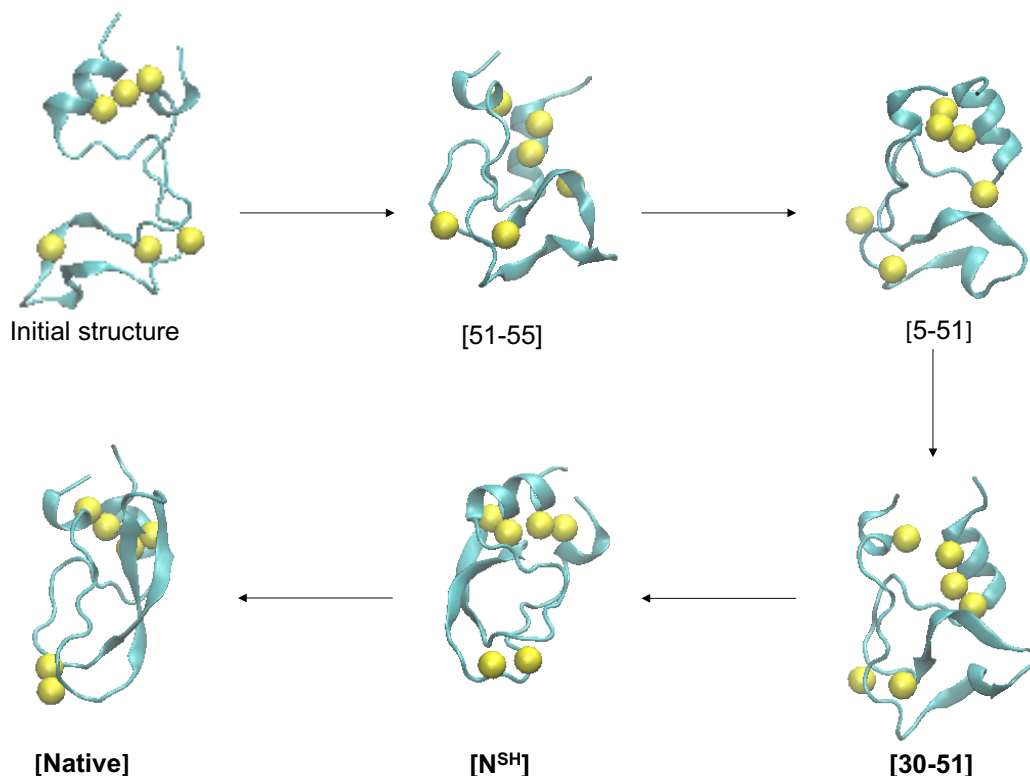


Figure 5.8 Snapshots of different conformations formed during TMD simulation of [5-55] like conformation of BPTI to native like BPTI. Sulfur atoms of cysteines are shown as yellow balls.

5.4.2 TMD using C_{α} and sulfur of cysteines (SG) only

5.4.2.1 Change in structural conformation during simulation

The change in conformation of BPTI during TMD simulation is as shown in Figure 5.9 where the snapshots taken at different time points show the progress of conformational changes from initial structure to the target structure. The 15 ns

simulation targeting only C_α and SG atoms only was performed at this time as opposed to targeting all heavy atoms in previous simulation. The transformation to the native structure was achieved at around 13 ns simulation bringing cysteines close to that distance as found in native disulfide bonds.

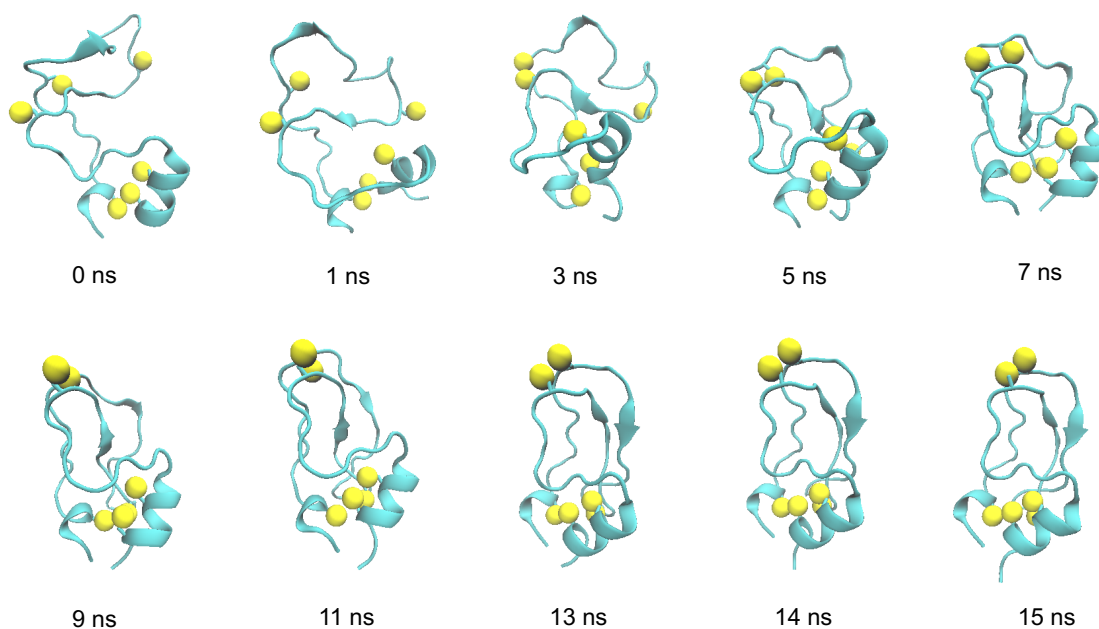


Figure 5.9 Snapshots of conformations formed at different stages of conformational changes during conformational folding of BPTI using TMD simulation. Sulfur atoms of cysteines are shown in yellow balls.

5.4.2.2 Root mean square deviation analysis

The root mean square deviation (RMSD) was computed from the atomic trajectories for TMD run. The plot of the RMSD of alpha carbons and sulfur of cysteine in the TMD-simulated structure relative to the corresponding target structure is shown in Figure 5.10. The result showed that TMD simulations reached the target structure within 15 ns. The initial RMSD of 8.70 Å at first trajectory continuously decreased to 1.17 Å at 3000th trajectory forming the native

structure which suggests that TMD successful to understand the conformational folding mechanism.

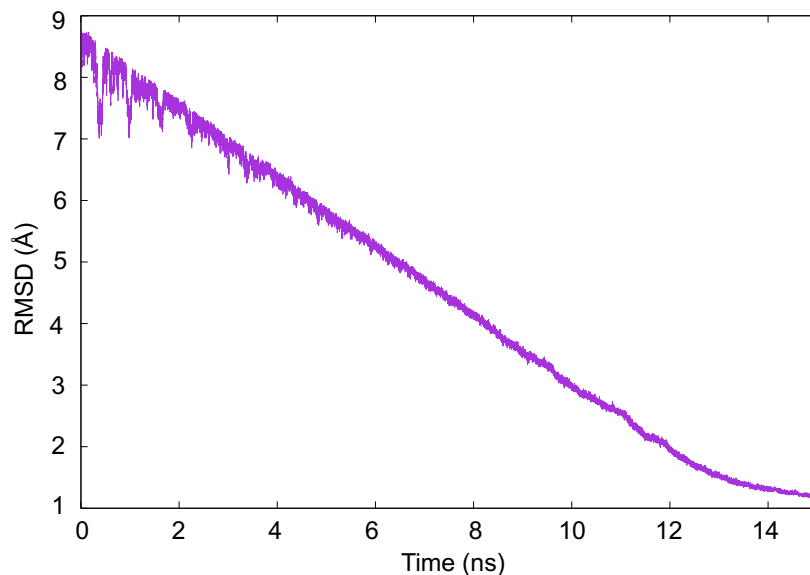


Figure 5.10 Change in RMSD during TMD.

5.4.2.3 Distance analysis of native disulfide bonds

The formation of native BPTI [5-55, 14-38, 30-51] from the starting conformation [5-55] was achieved in 15 ns time scale. The Cys14-Cys38 distance was seen closing and then increasing multiple times during simulation. Initially the Cys14-Cys38 distance was set 8.4 Å which was decreased to 3.4 Å within 2 ns. At the meantime, Cys5-Cys55 distance was increased to 12.3 Å with in 1 ns from 3.4 Å in the starting structure. The Cys30-Cys51 distance was sharply decreased to 8.4 Å from 20.1 Å of starting structure within 1.5 ns, then increased to 18.6 Å in 4 ns. It was then seen decreasing gradually. It was observed that Cys5-Cys55 and Cys14-Cys38 distances decreasing and then increasing multiple times to form a compact structure of BPTI. Formation of N^{SH}

took place transiently at 13 ns followed by the formation of N which proved the experimental finding that N^{SH} rearranges rapidly to N. Figure 5.11 shows the closing and increasing the Cys5-Cys55 and Cys14-Cys38 distances for bringing the Cys30 and Cys51 close to each other and for compacting the BPTI structure.

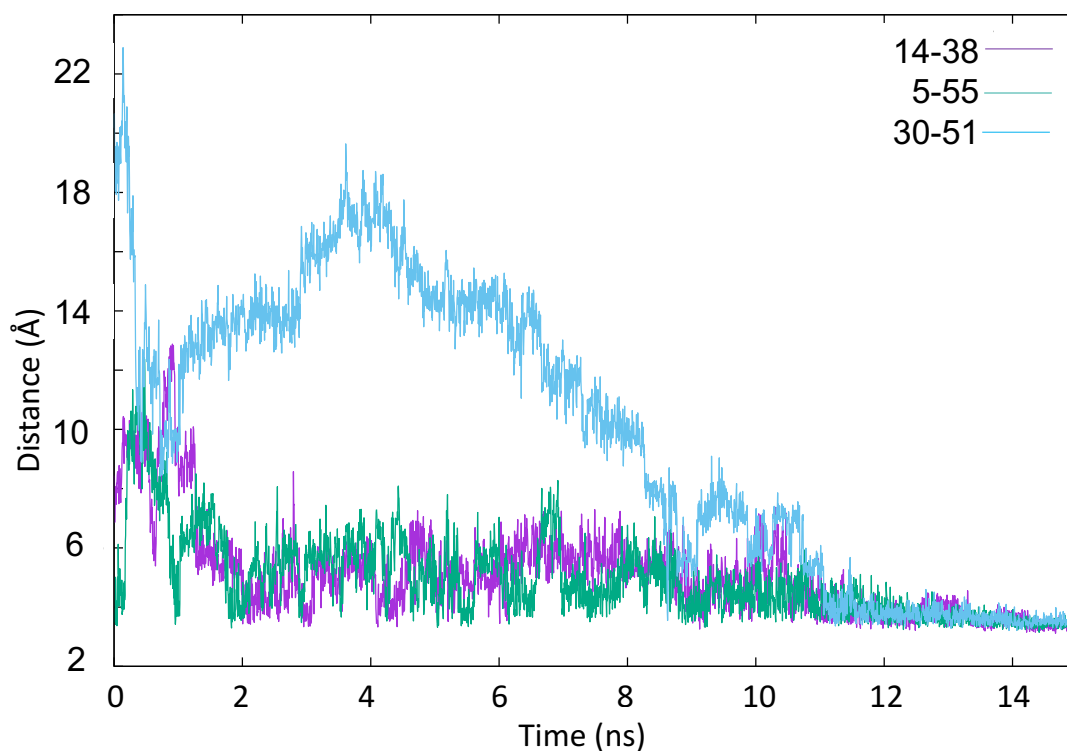


Figure 5.11 Distance between sulfur atoms in native disulfide bonds.

Formation of few non-native intermediates were also observed in our simulation as shown in Figure 5.12. The first non-native intermediate [51-55] was supposed to form as Cys51-Cys55 distance was very small enough to form a bond. At around 8.5 ns, the Cys30 and Cys55 were very close, then were Cys5 and Cys30. Rearrangement at this stage allowed formation of N^* which rearranged to N^{SH} for a very short time and immediately went to N.

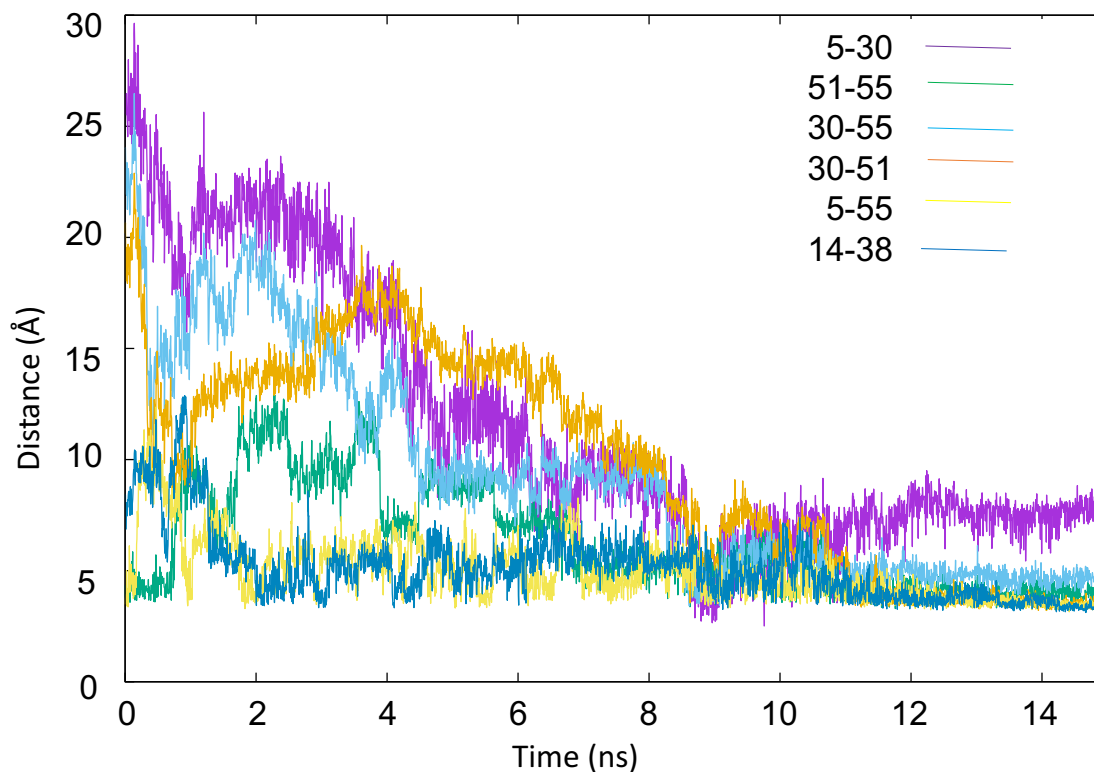


Figure 5.12 Distance between cysteines during simulation.

5.4.2.4 Analysis of intermediates with the change in radius of gyration

The figure 5.13 shows the decrease in radius of gyration with folding time. The snapshots of folding trajectories (a-j) at various steps of folding shows how the folding of BPTI is related to the formation of disulfide bonds by considering of radius of gyration. The starting structure has a radius of gyration (R_g) of 13.6 Å which on TMD simulation reached the final native structure having R_g of 10.6 Å. As folding proceeded, the collapse and subsequent ordering of β -strands was observed. The folding was proceeded with the rearrangement of starting structure to non-native conformation [51-55] followed by [5-51]. The formation of

[14-38] was observed at about 2 ns. During the process, Cys5-Cys55 and Cys14-Cys38 distances were decreased and then increased multiple times which helped to compact the structure and proceed towards the native like conformation. The Cys5 and Cys38 were seen very close at around 8.5 ns. The [5-30] non-native intermediate rearranges and compacts the structure of protein by forming native like two-disulfide intermediate N^* at about 12.5 ns which further rearranges to another native like two-disulfide intermediate N^{SH} transiently.

The very native like conformation N^{SH} has Cys5-Cys55 and Cys30-Cys51 in the close proximity. The Cys14-Cys38 distance decreased immediately leading to native structure. In the present simulation, N^* was formed and rearranged to N^{SH} . Here too, Cys14-Cys38 distance was decreased after the formation of N^{SH} which is important in the folding process of BPTI. Our finding from simulation is very close to the experimental findings.

5.4.2.5 Analysis of trajectories

The folding proceeded via the complete unfolding followed by immediate formation of non-native [51-55] intermediate which rearranged back to [5-55] but with different conformation which then rearranged to [14-38] intermediate. The Cys5-Cys55 and Cys14-Cys38 distances were decreasing and then increasing multiple times while the conformation is changing more towards the native one. Another single disulfide containing non-native intermediate [5-30] was observed which rearranged to N^* . The N^* intermediate was then rearranged to N^{SH} . The decrease in Cys14-Cys38 distance was then observed bringing the stable

conformation of native BPTI. The pathway of transformation depicted in Figure 5.14 showing the intermediate structures.

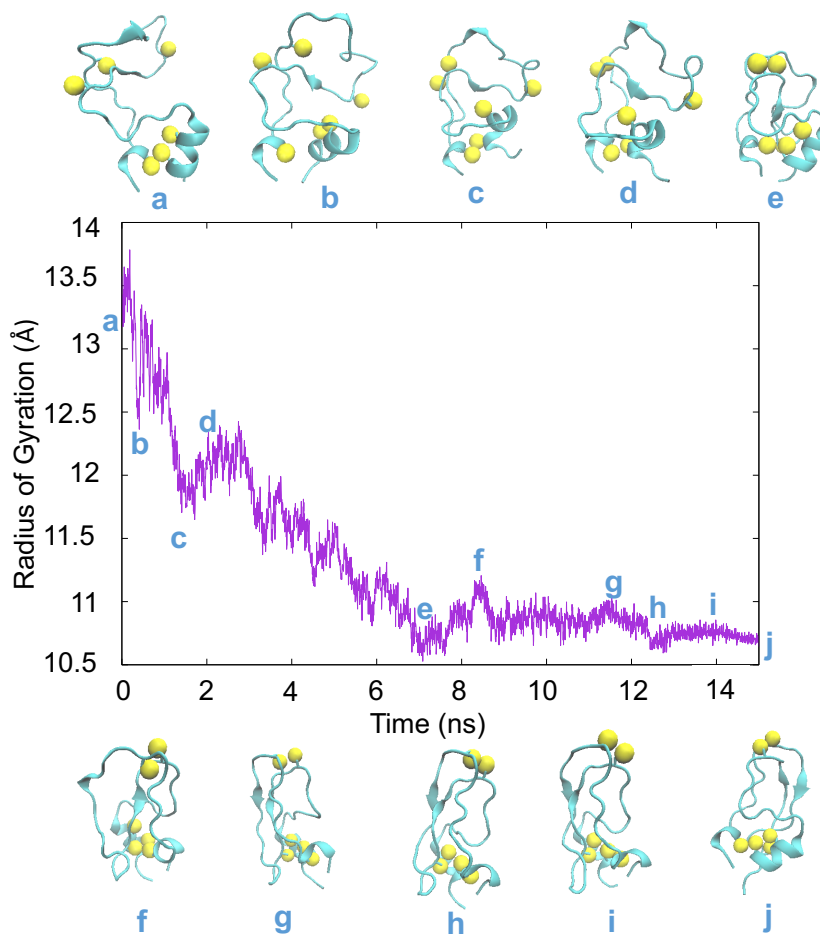


Figure 5.13 Folding trajectories demonstrating the BPTI folding pathway from [5-55] conformation to folded native state. The curve shows the decrease in the radius of gyration (R_g) with respect to folding time. Some of the conformations of trajectory (a-j) were shown to show how R_g decreases along with the progress of folding.

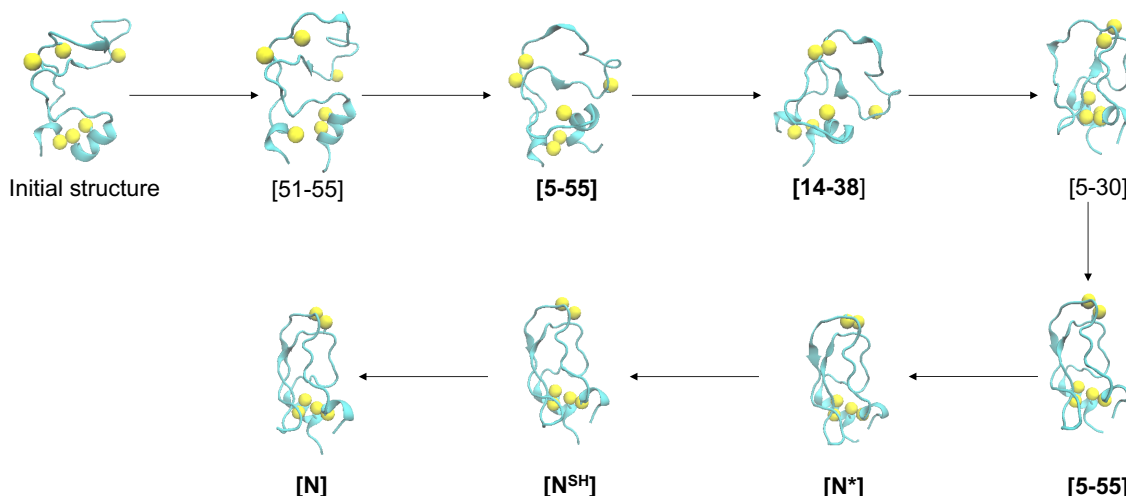


Figure 5.14 Snapshots of different conformations formed during TMD simulation of [5-55] like conformation of BPTI to native like BPTI. Sulfur atoms of cysteines are shown as yellow balls.

5.5 Conclusion

The actual disulfide bonds were made absent during the preparation of input files for simulation for targeted MD. The role of disulfide bond is very important for the folding of BPTI resulting in the much better approach for the final native structure. Targeted MD was run for single domain for 15 ns. The presented TMD simulations were focused on orientation of cysteine residue for disulfide bond formation as a result of the conformational changes during the folding process. The formation of stable native structure at the end of simulation without the involvement of actual disulfide bonds in simulation proves that our model can be used for the study of conformational folding mechanism of disulfide containing protein. The variations of the radius of gyration (R_g) along with the folding trajectories analyzed to investigate the pathway of BPTI folding.

CHAPTER 6

Conclusion

Folding of reduced BPTI was investigated oxidatively using three different aromatic thiols and their corresponding disulfides namely PA, SA, and QAS. The effect of charge(s) of the side chain group was also studied. The optimal folding condition using a redox buffer composed of QAS thiol and its disulfide was determined by plotting a graph of percentage of native protein formed versus refolding time for every condition selected and then comparing the graphs. Hence, an efficient folding method of reduced BPTI was determined and compared with the previously published results using GSH/GSSG. In best condition, the native form of BPTI was produced in over 90% yield in less than an hour while using GSH/GSSG under optimal condition, took 2 days to produce over 90% native protein.

As folding was most efficient using QAS thiol and its corresponding disulfide, it was sought to prepare different QAS thiols with more hydrophobic groups for further study. Three different QAS thiols (**2**, **3**, and **4**) and their corresponding disulfides (**6**, **7**, and **8**) were successfully prepared. The purity of these compounds was determined by nuclear magnetic spectroscopy and HPLC.

The folding of reduced BPTI was also studied by taking advantage of sophisticated computational programming methods developed to study molecular dynamics. Targeted molecular dynamics was used for our folding study. The folding process was studied in two different ways. In one method, all atoms of the initial structure were targeted to the target structure. It was seen that the correct

antiparallel β -sheets formation is required to form the (14-38) disulfide bond. The formation of N' [30-51; 14-38] and N* [5-55; 14-38] intermediates were not observed. The [5-55] intermediate rearranged to N^{SH} [5-55; 30-51] after a series of thiol-disulfide interchange process simultaneously with the conformational folding. Almost at the end of simulation, flipping of one β -sheet allowed the protein to form N^{SH} which immediately transformed to native protein as the (14-38) disulfide bond was formed. In other method, only the α -carbons and sulfur atoms of the cysteine residues (SG) were targeted to the target structure. The study showed the formation and breaking of (14-38) bonds multiple times. The formation of native intermediate N* [5-55; 14-38] was observed followed by the formation of N^{SH} [5-55; 30-51] transiently, which was transformed to native structure immediately. It was concluded from both of our studies that, conformational changes in the intermediate formed plays a crucial role to form disulfide bonds.

CHAPTER 7

Future Works

Folding of BPTI was very successful using both experimental and computational methods. To further improve the folding rate and yield, the use of redox buffer made up of more hydrophobic QAS thiols 2, 3, and 4 and their corresponding disulfides 6, 7 and 8 is proposed. As the hydrophobicity increases, the pKa value decreases. It is expected that the pKa of these QAS thiols will be close to 7 hence folding will go more smoothly forming less intermediates. It is also expected that the yield will also increase even though the folding will go at a slower rate.

The use of different computational methods is also proposed to investigate the folding process of reduced BPTI. Use of different shaped random structures of reduced BPTI and run simulations using different molecular dynamics is also suggested. One can mimic the oxidative folding conditions using computer programming so that better insight on the folding process can be found which will help experimentalists to think about setting up experiments in a different way.

References

- (1) Vickery, H. B. The Origin of the Word Protein. *Yale J. Biol. Med.* **1950**, *22*, 387–393.
- (2) Wang, Z.; Shen, W.; Kotler, D. P.; Heshka, S.; Wielopolski, L.; Aloia, J. F.; Nelson, M. E.; Pierson, R. N.; Heymsfield, S. B. Total Body Protein: A New Cellular Level Mass and Distribution Prediction Model. *Am. J. Clin. Nutr.* **2003**, *78*, 979–984.
- (3) Creighton, T. E. *Proteins : Structures and Molecular Properties*; Freeman: New York, 1996.
- (4) Protein Structure. *Part. Sci. - Drugs Dev. Serv.* **2009**, *8*, 1–2.
- (5) Misawa, S.; Kumagai, I. Refolding of Therapeutic Proteins Produced in Escherichia Coli as Inclusion Bodies. *Biopolymers* **1999**, *51*, 297–307.
- (6) Baneyx, F. Recombinant Protein Expression in Escherichia Coli. *Curr. Opin. Biotechnol.*, 1999, *10*, 411–421.
- (7) Schwartz, J. R. Advances in E. Coli Production of Therapeutic Proteins. *Curr. Opin. Biotechnol.* **2001**, *12*, 195–201.
- (8) Clark, E. D. Protein Refolding for Industrial Processes. *Curr. Opin. Biotechnol.* **2001**, *12*, 202–207.
- (9) Lilie, H.; Schwarz, E.; Rudolph, R. Advances in Refolding of Proteins Produced in E. Coli. *Curr. Opin. Biotechnol.* **1998**, *9*, 497–501.
- (10) Taylor, G.; Hoare, M.; Grey, D. R.; Gray; Marston, F. A. O. Size and Density of Protein Inclusion-Bodies. *Bio/Technology* **1986**, *4*, 553–557.
- (11) Palmer, I.; Wingfield, P. T. Preparation and Extraction of Insoluble (Inclusion-Body) Proteins from Escherichia Coli. In *Current Protocols in Protein Science*; John Wiley & Sons, Inc., 2001.
- (12) Rudolph, R.; Lilie, H. In Vitro Folding of Inclusion Body Proteins. *FASEB J.* **1996**, *10*, 49–56.
- (13) Dobson, C. M. Protein Folding and Misfolding. *Nature* **2003**, *426*, 884–890.
- (14) Kaufman, R. J.; Scheuner, D.; Schröder, M.; Shen, X.; Lee, K.; Liu, C. Y.; Arnold, S. M. The Unfolded Protein Response in Nutrient Sensing and Differentiation. *Nat. Rev. Mol. Cell Biol.* **2002**, *3*, 411–421.

- (15) Hartl, F. U.; Hayer-Hartl, M. Converging Concepts of Protein Folding in Vitro and in Vivo. *Nat. Struct. Mol. Biol.* **2009**, *16*, 574–581.
- (16) White, D. A.; Buell, A. K.; Knowles, T. P. J.; Welland, M. E.; Dobson, C. M. Protein Aggregation in Crowded Environments. *J. Am. Chem. Soc.* **2010**, *132*, 5170–5175.
- (17) Hartl, F. U.; Hayer-Hartl, M. Molecular Chaperones in the Cytosol: From Nascent Chain to Folded Protein. *Science (80-.)*. **2002**, *295*, 1852–1858.
- (18) Bukau, B.; Horwich, A. L. The Hsp70 and Hsp60 Chaperone Machines. *Cell* **1998**, *92*, 351–366.
- (19) Chang, J. Diverse Pathways of Oxidative Folding of Disulfide Proteins : Underlying Causes and Folding Models. *Biochemistry* **2011**, *50*, 3414–3431.
- (20) Tu, B. P.; Weissman, J. S. Oxidative Protein Folding in Eukaryotes: Mechanisms and Consequences. *J. Cell Biol.* **2004**, *164*, 341–346.
- (21) Frand, A. R.; Cuozzo, J. W.; Kaiser, C. A. Pathways for Protein Disulphide Bond Formation. *Trends Cell Biol.* **2000**, *10*, 203–210.
- (22) Appenzeller-Herzog, C.; Ellgaard, L. The Human PDI Family: Versatility Packed into a Single Fold. *Biochim. Biophys. Acta - Mol. Cell Res.* **2008**, *1783*, 535–548.
- (23) Goldberger, R. F.; Epstein, C. J.; Anfinsen, C. B. Acceleration of Reactivation of Reduced Bovine Pancreatic Ribonuclease by a Microsomal System from Rat Liver. *J. Biol. Chem.* **1963**, *238*, 628–635.
- (24) Tian, G.; Xiang, S.; Noiva, R.; Lennarz, W. J.; Schindelin, H. The Crystal Structure of Yeast Protein Disulfide Isomerase Suggests Cooperativity between Its Active Sites. *Cell* **2006**, *124*, 61–73.
- (25) Wilkinson, B.; Gilbert, H. F. Protein Disulfide Isomerase. *Biochim. Biophys. Acta - Proteins Proteomics* **2004**, *1699*, 35–44.
- (26) Lundström, J.; Holmgren, A. Determination of the Reduction-Oxidation Potential of the Thioredoxin-like Domains of Protein Disulfide-Isomerase from the Equilibrium with Glutathione and Thioredoxin. *Biochemistry* **1993**, *32*, 6649–6655.
- (27) Anken, E. van; Braakman, I. Versatility of the Endoplasmic Reticulum Protein Folding Factory. *Crit. Rev. Biochem. Mol. Biol.* **2005**, *40*, 191–228.

- (28) Hwang, C.; Sinskey, A. J.; Lodish, H. F. Oxidized Redox State of Glutathione in the Endoplasmic Reticulum. *Science* **1992**, *257*, 1496–1502.
- (29) Frand, A. R.; Kaiser, C. A. Ero1p Oxidizes Protein Disulfide Isomerase in a Pathway for Disulfide Bond Formation in the Endoplasmic Reticulum. *Mol. Cell* **1999**, *4*, 469–477.
- (30) Schwaller, M.; Wilkinson, B.; Gilbert, H. F. Reduction-Reoxidation Cycles Contribute to Catalysis of Disulfide Isomerization by Protein-Disulfide Isomerase. *J. Biol. Chem.* **2003**, *278*, 7154–7159.
- (31) Lees, W. J. Small-Molecule Catalysts of Oxidative Protein Folding. *Current Opinion in Chemical Biology*, 2008, *12*, 740–745.
- (32) Gilbert, H. F. Protein Disulfide Isomerase and Assisted Protein Folding. *J. Biol. Chem.* **1997**, *272*, 29399–29402.
- (33) Huthso, J. R.; Perinisq, F.; Bedowss, E.; Ruddonsv, R. W. Protein Folding and Assembly in Vitro Parallel Intracellular Folding and Assembly. *J. Biol. Chem.* **1993**, *268*, 16472–16482.
- (34) Patel, A. S.; Lees, W. J. Oxidative Folding of Lysozyme with Aromatic Dithiols, and Aliphatic and Aromatic Monothiols. *Bioorganic Med. Chem.* **2012**, *20*, 1020–1028.
- (35) Wang, L.; Wang, X.; Wang, C. C. Protein Disulfide-Isomerase, a Folding Catalyst and a Redox-Regulated Chaperone. *Free Radic. Biol. Med.* **2015**, *83*, 305–313.
- (36) Woycechowsky, K. J.; Wittrup, K. D.; Raines, R. T. A Small-Molecule Catalyst of Protein Folding in Vitro and in Vivo. *Chem. Biol.* **1999**, *6*, 871–879.
- (37) Gough, J. D.; Lees, W. J. Effects of Redox Buffer Properties on the Folding of a Disulfide-Containing Protein: Dependence upon pH, Thiol pKa, and Thiol Concentration. *J. Biotechnol.* **2005**, *115*, 279–290.
- (38) Gough, J. D.; Gargano, J. M.; Donofrio, A. E.; Lees, W. J. Aromatic Thiol pKa Effects on the Folding Rate of a Disulfide Containing Protein. *Biochemistry* **2003**, *42*, 11787–11797.
- (39) Wedemeyer, W. J.; Welker, E.; Narayan, M.; Scheraga, H. A. Disulfide Bonds and Protein Folding. *Biochemistry* **2000**, *39*, 4207–4216.
- (40) Creighton, T. E.; Zapun, A.; Darby, N. J. Mechanisms and Catalysts of Disulphide Bond Formation in Proteins. *Trends Biotechnol.* **1995**, *13*, 18–23.

- (41) Konishi, Y.; Ooi, T.; Scheraga, H. A. Regeneration of Ribonuclease A from the Reduced Protein. Isolation and Identification of Intermediates, and Equilibrium Treatment. *Biochemistry* **1981**, *20*, 3945–3955.
- (42) Kibria, F. M.; Lees, W. J. Balancing Conformational and Oxidative Kinetic Traps during the Folding of Bovine Pancreatic Trypsin Inhibitor (BPTI) with Glutathione and Glutathione Disulfide. *J. Am. Chem. Soc.* **2008**, *130*, 796–797.
- (43) Lees, W. J. Oxidative Protein Folding with Small Molecules. In *Folding of Disulfide Proteins*; 2011; pp. 109–132.
- (44) Lyles, M. M.; Gilbert, H. F. Catalysis of the Oxidative Folding of Ribonuclease A by Protein Disulfide Isomerase: Dependence of the Rate on the Composition of the Redox Buffer. *Biochemistry* **1991**, *30*, 613–619.
- (45) Hevehan, D. L.; De Bernardez Clark, E. Oxidative Renaturation of Lysozyme at High Concentrations. *Biotechnol. Bioeng.* **1997**, *54*, 221–230.
- (46) Gurbhele-Tupkar, M. C.; Perez, L. R.; Silva, Y.; Lees, W. J. Rate Enhancement of the Oxidative Folding of Lysozyme by the Use of Aromatic Thiol Containing Redox Buffers. *Bioorganic Med. Chem.* **2008**, *16*, 2579–2590.
- (47) Lees, W. J.; Whitesides, G. M. Equilibrium Constants for Thiol-Disulfide Interchange Reactions: A Coherent, Corrected Set. *J. Org. Chem.* **1993**, *58*, 642–647.
- (48) DeCollo, T. V.; Lees, W. J. Effects of Aromatic Thiols on Thiol-Disulfide Interchange Reactions That Occur during Protein Folding. *J. Org. Chem.* **2001**, *66*, 4244–4249.
- (49) Gough, J. D.; Williams, R. H.; Donofrio, A. E.; Lees, W. J. Folding Disulfide-Containing Proteins Faster with an Aromatic Thiol. *J. Am. Chem. Soc.* **2002**, *124*, 3885–3892.
- (50) Madar, D. J.; Patel, A. S.; Lees, W. J. Comparison of the Oxidative Folding of Lysozyme at a High Protein Concentration Using Aromatic Thiols versus Glutathione. *J. Biotechnol.* **2009**, *142*, 214–219.
- (51) Kassell, B.; Radicevic, M.; Ansfield, M.J.; Laskowski, M. S. The Basic Trypsin Inhibitor of Bovine Pancreas. IV. The Linear Sequence of the 58 Amino Acids. *Biochem. Biophys. Res. Commun.* **1965**, *18*, 255–258.
- (52) Wagner, G.; Braun, W.; Havel, T. F.; Schaumann, T.; Gö, N.; Wüthrich, K. Protein Structures in Solution by Nuclear Magnetic Resonance and Distance Geometry. *J. Mol. Biol.* **1987**, *196*, 611–639.

- (53) Kunitz, M.; John, H. N. Isolation from Beef Pancreas of Crystalline Trypsinogen, Trypsin, a Trypsin Inhibitor, and an Inhibitor-Trypsin Compound. *J. Gen. Physiol.* **1936**, *19*, 991–1007.
- (54) Huber, R.; Kukla, D.; Rühlmann, A.; Epp, O.; Formanek, H. The Basic Trypsin Inhibitor of Bovine Pancreas - I. Structure Analysis and Conformation of the Polypeptide Chain. *Naturwissenschaften* **1970**, *57*, 389–392.
- (55) Wagner, G., Wüthrich, K. Sequential Resonance Assignments in Protein ¹H Nuclear Magnetic Resonance Spectra. Basic Pancreatic Trypsin Inhibitor. *J. Mol. Biol.* **1982**, *155*, 347–366.
- (56) McCammon, J. A.; Gelin, B. R.; Karplus, M. Dynamics of Folded Proteins. *Nature* **1977**, *267*, 585–590.
- (57) Pan, H.; Barbar, E.; Barany, G.; Woodward, C. Extensive Nonrandom Structure in Reduced and Unfolded Bovine Pancreatic Trypsin Inhibitor. *Biochemistry* **1995**, *34*, 13974–13981.
- (58) Humphrey, W.; Dalke, A.; Schulten, K. VMD-Visual Molecular Dynamics. *J. Mol. Graph.* **1996**, *14*, 33–38.
- (59) Dittrich, M.; Kanchanawarin, C. *Case Study: BPTI*; 2006; pp. 1–19.
- (60) Berndt, K. D.; Güntert, P.; Orbons, L. P. M.; Wüthrich, K. Determination of a High-Quality Nuclear Magnetic Resonance Solution Structure of the Bovine Pancreatic Trypsin Inhibitor and Comparison with Three Crystal Structures. *J. Mol. Biol.* **1992**, *227*, 757–775.
- (61) Conn, P. M. *Molecular Biology of Protein Folding*; Progress in Molecular Biology and Translational Science; Elsevier Science, 2009.
- (62) Vincent, J.; Chicheportiche, R.; Lazdunski, M. The Conformational Properties of the Basic Pancreatic Trypsin-Inhibitor. *Eur. J. Biochem.* **1971**, *23*, 401–411.
- (63) Creighton, T. E. Experimental Studies of Protein Folding and Unfolding. *Prog. Biophys. Mol. Biol.* **1978**, *33*, 231–297.
- (64) Creighton, T. E.; Weissman, J. S.; Kim, P. S. The Disulfide Folding Pathway of BPTI. *Science (80-)*. **1992**, *256*, 111–114.
- (65) Weissman, J. S.; Kim, P. S. Reexamination of the Predominance Intermediates. *Science (80-)*. **1991**, *253*, 1386–1393.

- (66) Weissman, J. S.; Kim, P. S. Kinetic Role of Nonnative Species in the Folding of Bovine Pancreatic Trypsin Inhibitor. *Proc. Natl. Acad. Sci. U. S. A.* **1992**, *89*, 9900–9904.
- (67) Creighton, T. E.; Goldenberg, D. P. Kinetic Role of a Meta-Stable Native-like Two-Disulphide Species in the Folding Transition of Bovine Pancreatic Trypsin Inhibitor. *J. Mol. Biol.* **1984**, *179*, 497–526.
- (68) Weissman, J.; Kim, P. A Kinetic Explanation for the Rearrangement Pathway of BPTI Folding. *Nat. Struct. Mol. Biol.* **1995**, *2*, 1123–1130.
- (69) Wang, Y. Investigating the In Vitro Oxidative Folding Pathways of Bovine Pancreatic Trypsin Inhibitor (BPTI), FIU, 2013.
- (70) Konishitu, Y.; Qoit, T.; Scheragat, H. A. Regeneration of RNase A from the Reduced Protein: Models of Regeneration Pathways (Nucleation/folding/growth-Type Model/rearrangement-Type Model). *Proc. Natl. Acad. Sci. U. S. A.* **1982**, *79*, 5734–5738.
- (71) Karplus, M.; McCammon, J. A. Molecular Dynamics Simulations of Biomolecules. *Nat. Struct. Biol.* **2002**, *9*, 646–652.
- (72) Karplus, M.; Kuriyan, J. Molecular Dynamics and Protein Function. *Proc. Natl. Acad. Sci. U. S. A.* **2005**, *102*, 6679–6685.
- (73) Swope, W. C.; Pitera, J. W. Describing Protein Folding Kinetics by Molecular Dynamics Simulations. 1. Theory. *J. Phys. Chem. B* **2004**, *108*, 6571–6581.
- (74) Mittermaier, A.; Kay, L. E. New Tools Provide New Insights in NMR Studies of Protein Dynamics. *Science (80-.)*. **2006**, *312*, 224–228.
- (75) Snow, C. D.; Nguyen, H.; Pande, V. S.; Gruebele, M. Absolute Comparison of Simulated and Experimental Protein-Folding Dynamics. *Nature* **2002**, *420*, 102–106.
- (76) Daggett, V. Protein Folding-Simulation. *Chem. Rev.* **2006**, *106*, 1898–1916.
- (77) Levitt, M.; Sharon, R. Accurate Simulation of Protein Dynamics in Solution. *Proc. Natl. Acad. Sci. U. S. A.* **1988**, *85*, 7557–7561.
- (78) Betz, S. F. Disulfide Bonds and the Stability of Globular Proteins. *Protein Sci.* **1993**, *2*, 1551–1558.
- (79) Getun, I. V.; Brown, C. K.; Tulla-Puche, J.; Ohlendorf, D.; Woodward, C.; Barany, G. Partially Folded Bovine Pancreatic Trypsin Inhibitor Analogues

Attain Fully Native Structures When Co-Crystallized with S195A Rat Trypsin. *J. Mol. Biol.* **2008**, *375*, 812–823.

- (80) Kazmirski, S. L.; Daggett, V. Simulations of the Structural and Dynamical Properties of Denatured Proteins: The “molten Coil” state of Bovine Pancreatic Trypsin Inhibitor. *J. Mol. Biol.* **1998**, *277*, 487–506.
- (81) Hao, M. H.; Pincus, M. R.; Rackovsky, S.; Scheraga, H. A. Unfolding and Refolding of the Native Structure of Bovine Pancreatic Trypsin Inhibitor Studied by Computer Simulations. *Biochemistry* **1993**, *32*, 9614–9631.
- (82) Brylinski, M.; Konieczny, L.; Roterman, I. Hydrophobic Collapse in Late-Stage Folding (in Silico) of Bovine Pancreatic Trypsin Inhibitor. *Biochimie* **2006**, *88*, 1229–1239.
- (83) Watanabe, K.; Nakamura, A.; Fukuda, Y.; Saitô, N. Mechanism of Protein Folding. *Biophys. Chem.* **1991**, *40*, 293–301.
- (84) Kobayashi, Y.; Sasabe, H.; Akutsu, T.; Saitô, N. Mechanism of Protein Folding. IV. Forming and Breaking of Disulfide Bonds in Bovine Pancreatic Tripsin Inhibitor. *Biophys. Chem.* **1992**, *44*, 113–127.
- (85) Camacho, C. J.; Thirumalai, D. Modeling the Role of Disulfide Bonds in Protein Folding: Entropic Barriers and Pathways. *Proteins Struct. Funct. Bioinforma.* **1995**, *22*, 27–40.
- (86) Creighton, T. E. The Single-Disulphide Intermediates in the Refolding of Reduced Pancreatic Trypsin Inhibitor. *J. Mol. Biol.* **1974**, *87*, 603–624.
- (87) Wedemeyer, W. J.; Welker, E.; Narayan, M.; Scheraga, H. A. Disulfide Bonds and Protein Folding. *Biochemistry* **2000**, *39*.
- (88) Qin, M.; Wang, W.; Thirumalai, D. Protein Folding Guides Disulfide Bond Formation. *Proc. Natl. Acad. Sci.* **2015**, *112*, 11241–11246.
- (89) Targeted Molecular Dynamics (TMD) (NAMD 2.10 User’s Guide).
- (90) Schlitter J, Engels M, K. P. Targeted Molecular Dynamics: A New Approach for Searching Pathways of Conformational Transitions. *J. Mol. Graph.* **1994**, *12*, 84–89.
- (91) J. D. Carroll. Top 15 Best-Selling Drugs of 2012. <http://www.fiercepharma.com/special-reports/15-best-selling-drugs>, 2012.
- (92) Sanchez-Garcia, L.; Martín, L.; Mangues, R.; Ferrer-Miralles, N.; Vázquez, E.; Villaverde, A. Recombinant Pharmaceuticals from Microbial Cells: A 2015 Update. *Microb. Cell Fact.* **2016**, *15*, 33.

- (93) Weissman, J. S.; Kim, P. S. Reexamination of the Folding of BPTI: Predominance of Native Intermediates. *Science* **1991**, *253*, 1386–1393.
- (94) Szajewski, R. P.; Whitesides, G. M. Rate Constants and Equilibrium Constants for Thiol-Disulfide Interchange Reactions Involving Oxidized Glutathione. *J. Am. Chem. Soc.* **1980**, *102*, 2011–2026.
- (95) Wilson, J. M.; Bayer, R. J.; Hupe, D. J. Structure-Reactivity Correlations for the Thiol-Disulfide Interchange Reaction. *J. Am. Chem. Soc.* **1977**, *99*, 7922–7926.
- (96) Singh, R.; Whitesides, G. M. A Reagent for Reduction of Disulfide Bonds in Proteins That Reduces Disulfide Bonds Faster Than Does Dithiothreitol. *J. Org. Chem.* **1991**, *56*, 2332–2337.
- (97) Moss, R. A.; Dix, F. M. Properties of Phenolic and Thiophenolic Surfactant Micelles. *J. Org. Chem.* **1981**, *46*, 3029–3035.
- (98) Coogan, M. P.; Harger, M. J. P. Nucleophilic Substitution in Benzylic Thiophosphinyl and Thiophosphonyl Chlorides: The Contribution of Elimination–addition Pathways with Methyleneethoxophosphorane (Thiophosphene) Intermediates. *J. Chem. Soc., Perkin Trans. 2* **1994**, *10*, 2101–2107.
- (99) Smith, H. A.; Doughty, G.; Gorin, G. Mercaptan-Disulfide Interchange Reactions III. Reaction of Cysteine with 4,4'-dithiobis(benzenesulfonic Acid). *J. Am. Chem. Soc.* **1964**, *29*, 1484–1488.
- (100) Carey, F. A.; Sundberg, R. J. *Advanced Organic Chemistry Part B: Reactions and Synthesis*; 2008.
- (101) Kolšek, K.; Aponte-Santamaría, C.; Gräter, F. Accessibility Explains Preferred Thiol-Disulfide Isomerization in a Protein Domain. *Sci. Rep.* **2017**, *7*, 1–10.
- (102) Ang, M. J. Y.; Lim, H. A.; Poulsen, A.; Wee, J. L. K.; Ng, F. M.; Joy, J.; Hill, J.; Chia, C. S. B. Miniature Bovine Pancreatic Trypsin Inhibitors (M-BPTIs) of the West Nile Virus NS2B-NS3 Protease. *J. Enzyme Inhib. Med. Chem.* **2016**, *31*, 194–200.
- (103) Li, W.; Baldus, I. B.; Gräter, F. Redox Potentials of Protein Disulfide Bonds from Free-Energy Calculations. *J. Phys. Chem. B* **2015**, *119*, 5386–5391.
- (104) Cleland, W. W. Dithiothreitol, a New Protective Reagent for SH Groups. *Biochemistry* **1964**, *3*, 480–482.

- (105) Aitken, R. A.; Drysdale, M. J.; Ferguson, G.; Lough, A. J. Flash Vacuum Pyrolysis of Stabilized Phosphorus Ylides. Part 12. Extrusion of Ph₃P from Sulfonyl Ylides and Reactivity of the Resulting Sulfonyl Carbenes. *J. Chem. Soc. - Perkin Trans. 1* **1998**, 5, 875–880.
- (106) Hawkins, H. C.; Blackburn, E. C.; Freedman, R. B. Comparison of the Activities of Protein Disulphide-Isomerase and Thioredoxin in Catalysing Disulphide Isomerization in a Protein Substrate. *Biochem. J.* **1991**, 275, 349–353.
- (107) Zhang, J. X.; Goldenberg, D. P. Mutational Analysis of the BPTI Folding Pathway: I. Effects of Aromatic→leucine Substitutions on the Distribution of Folding Intermediates. *Protein Sci.* **1997**, 6, 1549–1562.
- (108) Maxwell, K. L.; Wildes, D.; Zarrine-Afsar, A.; De Los Rios, M. A.; Brown, A. G.; Friel, C. T.; Hedberg, L.; Horng, J.-C.; Bona, D.; Miller, E. J.; *et al.* Protein Folding: Defining a “standard” Set of Experimental Conditions and a Preliminary Kinetic Data Set of Two-State Proteins. *Protein Sci.* **2005**, 14, 602–616.
- (109) Zapun, A.; Creighton, T. E. Effects of DsbA on the Disulfide Folding of Bovine Pancreatic Trypsin Inhibitor and Alpha-Lactalbumin. *Biochemistry* **1994**, 33, 5202–5211.
- (110) Whitesides, G. M.; Lilburn, J. E.; Szajewski, R. P. Rates of Thiol-Disulfide Interchange Reactions between Mono- and Dithiols and Ellman’s Reagent. *J. Org. Chem.* **1977**, 42, 332–338.
- (111) Maeda, Y.; Ueda, T.; Yamada, H.; Imoto, T. The Role of Net Charge on the Renaturation of Reduced Lysozyme by the Sulfhydryl-Disulfide Interchange Reaction. *Protein Eng.* **1994**, 7, 1249–1254.
- (112) Schröder, M.; Kaufman, R. J. The Mammalian Unfolded Protein Response. *Annu. Rev. Biochem.* **2005**, 74, 739–789.
- (113) Kosuri, P.; Alegre-Cebollada, J.; Feng, J.; Kaplan, A.; Inglés-Prieto, A.; Badilla, C. L.; Stockwell, B. R.; Sanchez-Ruiz, J. M.; Holmgren, A.; Fernández, J. M. Protein Folding Drives Disulfide Formation. *Cell* **2012**, 151, 794–806.
- (114) Czaplewski, C.; Ołdziej, S.; Liwo, A.; Scheraga, H. A. Prediction of the Structures of Proteins with the UNRES Force Field, Including Dynamic Formation and Breaking of Disulfide Bonds. *Protein Eng. Des. Sel.* **2004**, 17, 29–36.

- (115) Karplus, M.; Petsko, G. a. Molecular Dynamics Simulations in Biology. *Nature* **1990**, *347*, 631–639.
- (116) Ma, J.; Sigler, P. B.; Xu, Z.; Karplus, M. A Dynamic Model for the Allosteric Mechanism of GroEL1. *J. Mol. Biol.* **2000**, *302*, 303–313.
- (117) Mashl, R. J.; Jakobsson, E. End-Point Targeted Molecular Dynamics: Large-Scale Conformational Changes in Potassium Channels. *Biophys. J.* **2008**, *94*, 4307–4319.
- (118) Compoin, M.; Picaud, F.; Ramseyer, C.; Girardet, C. Targeted Molecular Dynamics of an Open-State KcsA Channel. *J. Chem. Phys.* **2005**, *122*.
- (119) Gc, J. B.; Gerstman, B. S.; Chapagain, P. P. The Role of the Interdomain Interactions on RfaH Dynamics and Conformational Transformation. *J. Phys. Chem. B* **2015**, *119*, 12750–12759.
- (120) Ferrara, P.; Apostolakis, J.; Caflisch, A. Targeted Molecular Dynamics Simulations of Protein Unfolding. *J. Phys. Chem.* **2000**, *104*, 4511–4518.
- (121) Apostolakis, J.; Ferrara, P.; Caflisch, A. Calculation of Conformational Transitions and Barriers in Solvated Systems: Application to the Alanine Dipeptide in Water. *J. Chem. Phys.* **1999**, *110*, 2099–2108.
- (122) Camacho, C. J.; Thirumalai, D.; Camacho, C. J. and Thirumalai, D. Theoretical Predictions of Folding Pathways by Using the Proximity Rule, with Applications to Bovine Pancreatic Trypsin Inhibitor. *Proc Natl Acad Sci U S A* **1995**, *92*, 1277–1281.
- (123) The PyMOL Molecular Graphics System, Version 1.7.4.5 Schrödinger, LLC.
- (124) Lynch, G. C.; Pettitt, B. M. Semi-Grand Canonical Molecular Dynamics Simulation of Bovine Pancreatic Trypsin Inhibitor. *Chem. Phys.* **2000**, *258*, 405–413.
- (125) K. Vanommeslaeghe, E. Hatcher, C. Acharya, S. Kundu, S. Zhong, J. Shim, E. Darian, O.; Guvench, P. Lopes, I. Vorobyov, and A. D. M. J. . CHARMM General Force Field (CGenFF): A Force Field for Drug-like Molecules Compatible with the CHARMM All-Atom Additive Biological Force Fields. *J Comput Chem.* **2010**, *31*, 671–690.
- (126) Lee, J.; Cheng, X.; Swails, J. M.; Yeom, M. S.; Eastman, P. K.; Lemkul, J. A.; Wei, S.; Buckner, J.; Jeong, J. C.; Qi, Y.; *et al.* CHARMM-GUI Input Generator for NAMD, GROMACS, AMBER, OpenMM, and CHARMM/OpenMM Simulations Using the CHARMM36 Additive Force Field. *J. Chem. Theory Comput.* **2016**, *12*, 405–413.

- (127) Phillips, J. C.; Braun, R.; Wang, W.; Gumbart, J.; Tajkhorshid, E.; Villa, E.; Chipot, C.; Skeel, R. D.; Kalé, L.; Schulten, K. Scalable Molecular Dynamics with NAMD. *J Comput Chem.* **2005**, *26*, 1781–1802.
- (128) Essmann, U.; Perera, L.; Berkowitz, M. L.; Darden, T.; Lee, H.; Pedersen, L. G. A Smooth Particle Mesh Ewald Method. *J Chem Phys* **1995**, *103*, 8577–8593.

VITA

RAM PRASAD MARAHATTA

Chhoprak-5, Gorkha, Nepal

- 1999-2004 B.SC., Chemistry
Tribhuvan University
Kathmandu, Nepal
- 2003-2005 Science Teacher
Namuna Machhindra Higher Secondary School
Lalitpur, Nepal
- 2009 M.Sc., Chemistry
Tribhuvan University
Kathmandu, Nepal
- 2009-2012 Lecturer of Chemistry
Notre Dame College
Bandipur, Nepal
- 2012-2017 Doctoral Candidate and Teaching Assistant
Florida International University
Miami, Florida
- 2016 MS in Chemistry
Florida International University
Miami, Florida

PUBLICATIONS AND PRESENTATIONS

Ram Marahatta, Na Zhang, Michelle A. Moats and Watson J. Lees* "Folding of bovine pancreatic trypsin inhibitor (BPTI) faster using aromatic thiols and their corresponding disulfides." Poster presented at 252nd ACS National Meeting. Philadelphia, PA, Aug 21-25, 2016.

Ram Marahatta, Na Zhang, Michelle A. Moats and Watson J. Lees* "Folding of bovine pancreatic trypsin inhibitor (BPTI) faster using aromatic thiols and their corresponding disulfides." Oral presentation at GSAW Scholarly forum, FIU, March 27-28, 2017.